Integrating Polyaniline: A new electrode material for Lab on a Chip applications

By

Rowan Henderson *B.Sc (Hons), B.Eco*

Submitted in fulfilment of the requirements for the Degree of

Doctor of Philosophy

UNIVERSITY
OF TASMANIA

April 2012

Declaration

This thesis contains no material which has been accepted for a degree or diploma by the University or any other institution, except by way of background information and duly acknowledged in the thesis, and to the best of my knowledge and belief no material previously published or written by another person except where due acknowledgement is made in the text of this thesis, nor does this thesis contain any material that infringes copyright.

Rowan Henderson

April 2012

This thesis may be available for loan and limited copying in accordance with the Copyright Act 1968.

Rowan Henderson

April 2012

Acknowledgments

I would like to thank the following people for all their help and support throughout the course of my PhD work.

My primary supervisor, Assoc/Prof Michael Breadmore, for his support, encouragement, patience and continued enthusiasm for good science.

My supervisors:

- Dr Trevor Lewis, for his encouragement and guidance particularly in the area of conducting polymers.
- Dr Rosanne Guijt, for her continuous support and constructive criticism.
- Prof Emily Hilder, for her continuous support and positive feedback as a supervisor along with here help as postgraduate co-ordinator.
- Prof Paul Haddad, for his guidance and experience as a separation scientist and PhD supervisor.

All the members of the Australian Centre for Research on Separation Science and the School of Chemistry from which I have gained many lasting friendships.

I would also especially like to thank the following for their help support and encouragement during various stages of my PhD work:

Ms Kara Johns, Charlie and Matilda, Mr Warwick Marshal, Dr Adam James, Mrs Katrina Munting and Dr Doug Mclean.

I would also like to thank my family for their patience and understanding over the last few years as I pursued this path.

List of Abbreviations

AC	Alternating Current
APS	Ammonium persulfate
APTS	8-Aminopyrene-1,3,6-trisulfonic acid
BGE	Background Electrolyte
CAS	Camphorsulfonic Acid
CE	Capillary Electrophoresis
CNT	Carbon Nanotube
COC	Cyclic Olefin Copolymer
C^4D	Capacitively Coupled Contactless Conductivity Detection
DC	Direct Current
DFR	Dry Film Photoresist
DNA	Deoxyribonucleic Acid
DUV	Deep Ultraviolet
EB	Emeraldine Base
EOF	Electroosmotic Flow
ES	Emeraldine Salt
FITC	Fluorescein isothiocyanate
HDMB	Hexa-dimethrine Bromide
HFG	High Frequency Generator
HIS	Histidine
HPC	Hydroxypropyl cellulose
HV	High Voltage
ICP	Intrinsically Conductive Polymer
LB	Leucoemeraldine Base
LED	Light Emitting Diode
LIF	Laser Induced Fluorescence
LOC	Lab on a Chip

LOD	Limit of Detection
LTCC	Low Temperature Co-fired Ceramic
LW	Laser Welding
MES	2-(N-morpholino)ethanesulfonic Acid
MCE	Microchip Capillary Electrophoresis
NDA	Naphthalene-2,3-dicarbaldehyde
PANI	Polyaniline
PB	Perniganiline Base
PC	Polycarbonate
PCB	Printed Circuit Board
PCR	Polymerase Chain Reaction
PDMS	Poly(dimethysiloxane)
PEDOT	Poly(3,4-ethylenedioxythiophene)
PMAS	Poly(2-methoxyaniline-5-sulfonic acid)
PMMA	Poly(methyl methacrylate)
POC	Point of Care
PolyAMPS	Poly(2-acrylamido-2-methyl-1-propanesulfonic acid)
PPE	Personal Protective Equipment
PS	Polystyrene
PSS	Poly(styrenesulfonate)
PVC	Polyvinyl chloride
PVF	Polyvinylidene fluoride
SEM	Scanning Electron Micrograph
UV	Ultraviolet
XANES	X-ray Ablation Near Edge Structure Spectroscopy
XPS	X-ray Photoelectron Spectroscopy

List of Publications

Type of publications	References
Papers in refereed journals	1-3
Posters at national and international conferences	4-6
Oral Presentations at international conferences	7-8

1. R. D. Henderson, M. C. Breadmore, L. Dennany, R. M. Guijt, P. R. Haddad, E. F. Hilder, P. C. Innis, T. W. Lewis and G. G. Wallace, ***Photolithographic patterning of conducting polyaniline films via flash welding,*** Synthetic Metals, 2010. **160**(13-14): p. 1405-1409.

2. R. D. Henderson, R. M. Guijt, P. R. Haddad, E. F. Hilder, T. W. Lewis and M. C. Breadmore, ***Manufacturing and application of a fully polymeric electrophoresis chip with integrated polyaniline electrodes,*** Lab on a Chip, 2010. **10**(14): p. 1869-1872.

3. R. D. Hendersona, R. M. Guijt, L. Andrewartha, T. W. Lewis, A. Henderson, E. F. Hilder, P. R. Haddad and M. C. Breadmore, ***Metal-Free electrophoresis polymer chip with integrated polyaniline electrode*s**, Lab on a Chip, Submitted.

4. R. D. Henderson, M. C. Breadmore, R. M. Guijt, E. F. Hilder, T. W. Lewis and P. R. Haddad, ***Revolutionising Lab on a Chip: Synthetic Electrodes,*** 15th Annual RACI Analytical and Environmental Divisions Research and Development Topics, Adelaide, Australia, 9-12th December 2007 Winner: Aquadiagnostic Prize (Most Commercialise able Research)

5. R. D. Henderson, R. M. Guijt, E. F. Hilder, M. C. Breadmore, P. R. Haddad, T. W. Lewis, G. G. Wallace, L. Dennany, and , P. C. Innis, ***Revolutionising Lab on a Chip: Synthetic Electrodes,*** ACROSS Symposium on Advances in Separation Science (ASASS), 8-10th December 2008, Hobart, Australia.

6. R. D. Henderson, O. S. Hutter, R. M. Guijt, T. W. Lewis, E. F. Hilder, P. R. Haddad, M. C. Breadmore, ***Laser welded polyaniline circuits,*** The Proceedings of The 14th International Conference on Miniaturized Systems for Chemistry and Life Sciences - μTAS 2010, 2-6th October, Groningen, The Netherlands.

7. R. D. Henderson, R. M. Guijt, O. S. Hutter, A. D. Henderson, P. R. Haddad, E. F. Hilder, T. W. Lewis and M. C. Breadmore, ***Lithographically patterned conducting polymer electrodes for microfluidics***, Chemeca, 26-29th September 2010, Adelaide, Australia.

8. M. C. Breadmore, R. M. Guijt, R. D. Henderson, L. Andrewartha and E. Candish, ***Low cost microfluidics,*** 2nd Australian and New Zealand Micro and Nanofluidics Symposium, April 28th -29th 2011, Sydney, Australia.

Abstract

The creation of disposable, single use devices capable of performing complex tasks is one of the key motivators in Lab on a Chip (LOC) research. Replication techniques allow for low-cost manufacturing of large numbers of plastic devices capable of performing a range of functionalities. Complex tasks, however, often require the integration of electrodes, significantly increasing the costs per device when integrating metal electrodes. This thesis describes the development and application of the conducting polymer, polyaniline (PANI) as a new electrode material within LOC devices. PANI is an inexpensive alternative to metal electrodes that are currently used, most commonly in LOC research.

The electrodes were fabricated in thin films of PANI, initially by flash lithography using a studio camera flash and a transparency mask. During flash welding, a conducting polymer circuit was formed from the non-exposed regions. The flash-welding process was enhanced through the use of polymeric substrates, enabling flash welding of PANI films with a thickness ranging from 5 to 14.4 μm, significantly thicker than reported previously. Scanning electron micrographs, light microscope images and conductivity measurements were used to determine the conductive properties and morphology of the PANI electrodes. Raman spectroscopy was used to determine the sharpness of the masked edges. The interface between the flash-welded and masked regions of the PANI films was typically less than 10 μm wide. The conducting regions of the PANI film were shown to be capable of carrying the high voltages of up to 2000 V required for chip electrophoresis, and were stable for up to 30 min under these conditions.

Using a structured layer of dry film photoresist for sealing, a polydimethylsiloxane substrate containing channels and reservoirs was bound to the PANI film to form an integrated microfluidic device. The PANI electrodes were used for the electrophoretic separation of three sugars labelled with 8-

aminopyrene-1,3,6-trisulfonic acid in the dry film resist – PDMS hybrid device. Highly efficient separations comparable to those achieved in similar microchips using platinum electrodes confirmed the potential of PANI as a new material suitable for high voltage electrodes in LOC devices.

When characterising the welding process, only light with a wavelength above 570 nm was found to contribute to the welding process. A 635 nm laser diode was then used successfully for welding by direct writing lithography, for the first time welding PANI nanofibers using a narrow wavelength light-source. The improved accuracy and precision of laser patterning enabled the development of fine electrode patterns that were unachievable through the flash welding process, including those required for Capacitively Coupled Contactless Conductivity Detection, (C^4D). This enabled the fabrication of the first fully polymeric LOC device with integrated electrodes employing laser-patterned electrodes to carry the Direct Current (DC) voltages required for fluid handling and electrophoretic separation, as well as the Alternating Current (AC) voltages for C^4D. This device was used for the electrophoretic separation of Li^+, Na^+ and K^+ with detection limits down to 25 μM and an efficiency of 22,000 plates/m, which is comparable with the performance of similar electrophoresis - C^4D devices with metal electrodes.

Table of Contents

1. Introduction

1.1 Microfluidic Lab-on-a-Chip Devices

It is of no surprise that in today's society where "smaller is better" the development of various microfluidic devices has become a major research focus in separation science. There have been many types of microchips produced in recent years, from glass to polymer chips and including elastomeric polymers such as poly(dimethylsiloxane) (PDMS), with the goal to develop chips that utilise the various advantages of these devices over their larger bench top counterparts. These technologies have achieved faster sample throughput with more rapid separation and analysis times. The combination of faster sample throughput and smaller instrumentation makes microchips ideal for the development of portable or handheld analytical devices. Due to their many possible applications, these miniaturised devices have promised to play an integral role in the future of clinical and forensic analysis, as first described by Verpoorte and others [1-5]. Research in microfluidic and Lab on a Chip (LOC) devices remains at the forefront of separation science and has evolved into medical and biotechnology areas [6, 7].

With the development of these smaller systems comes the need for highly sensitive detection systems for analysis of the small sample volumes and concentrations typical of clinical and forensic samples. Conductivity detection and both indirect and direct laser induced fluorescence (LIF) detection, showing detection limits reported as 10 - 1000 times lower than that of the more conventional ultra-violet (UV) absorbance detection, are amongst the detection techniques capable of meeting this demand [8]. Direct fluorescence detection has selectivity advantages because only target analytes labelled with a fluorophore or

analytes with native fluorescence are detected. Direct fluorescence detection is typically 10 - 100 times more sensitive than indirect fluorescence.

Over the past decade there has been a strong trend towards the development of highly integrated microfluidic devices to cover a wide range of applications, with the total number of publications relating to microfluidics increasing by 200 – 250 each year since 2001 [6] with this rate of publication remaining steady to the present day with around 2200 published in 2011. The decade prior to 2001 saw microfluidics grow from its infancy in 1990, where Manz *et al.* first developed the idea of a miniaturised total analytical system [9], to becoming a mainstream research field with over 200 publications referring to microfluidics published in 2001. This increasing interest in microfluidics led to the formation of the journal *Lab on a Chip* specific to the field in 2001. *Lab on a Chip* is now regarded as one of the leading journals of small-scale sciences with an impact factor of 6.260 in 2010, which indicates the intense uptake that this platform has had within the scientific community.

In the 1990s research in this field was predominantly towards the miniaturisation of bench top separation techniques, such as high performance liquid chromatography, gas chromatography and electrophoresis, with a drive towards the development of portable devices that could be used outside standard scientific laboratories. The advantage of these systems is their ability to process samples in the field, thereby avoiding the sometimes several day turnaround from sample collection to laboratory reporting. Other advantages over the larger bench top instrumentation were also realised, such as the faster analysis times achieved by using smaller column lengths and lower chemical consumption through having smaller sample sizes.

The field has now diverged across many areas of science, particularly into the biological and bio-analytical fields. The majority of current day research in lab on

a chip focuses on processes such as drug screening, immunology and the handling and analysis of cells [10-12]. One of the key driving forces behind the movement towards biological applications is the desire for point-of-care testing where biological samples could be analysed quickly and results obtained within minutes. However, during this time of continued growth in the microfluidics research sector, there have been minimal results transferred into industrial applications and onto the commercial market. Some of the current commercial applications include devices used for pregnancy testing and drug screening. These devices are relatively simple and involve two or three chemical processes to give a qualitative result [13].

Sceptics of LOC research have often criticised the failure to deliver a killer application within the first 20 years, which may be blamed on researchers creating excessive user expectations by underestimating the fabrication costs of these devices [14]. For the highly desirable application of portable systems for field analysis and point-of-care (POC) testing it is critical that the devices remain inexpensive so they can be single use and disposable. This has resulted in a widening focus to search for "better" cheaper, recyclable technologies.

1.1.1 Microfluidic Chips

Since the first miniaturised analytical system produced by Terry *et al.* in the late 1970s, which was a gas chromatographic system on a silicon wafer [15], a number of different types of analytical techniques have been miniaturised. Although biological applications, such as the study of cell cultures, have become most common in microfluidic research, the development of microfluidic chips for various types of chromatographic and electrophoretic techniques still feature heavily in the literature. These analytical techniques can be combined with cell manipulation and biological systems in an integrated device. The pioneering groups of modern miniaturised systems reported that faster, more efficient

separations and lower reagent consumption are the leading advantages for the development of miniaturised systems [16, 17].

A microfluidic chip in general consists of a planar material substrate as a base/cover material, with a second section or layer containing interconnected microchannels, leading from various sample point reservoirs. Other features, such as valves and electrodes can also be integrated into this or other layers. Typically, the base substrate is made from a relatively inert material, such as glass or various plastics, although silicon and metal have also been used. The feature containing layers can be made from glass by direct HF etching or sandblasting techniques or from plastic using imprinting replication techniques such as hot embossing using moulds. One of the most common materials used is the elastomer PDMS because of its ease of moulding and handling.

The general process of microchip fabrication is as follows. A mask is developed in a drawing program and printed on a transparent material. This mask is then used to transfer the pattern to a photoresist via photolithography. The photoresist is developed to either a template, which can be used for imprinting or casting, or to selectively expose the substrate for etching. The flat plate containing the microchannels is then sealed with a base plate. The specific fabrication process used depends on the chip substrates, which are discussed further below.

1.1.1.1 Glass Microchips

In the early years, microchips were most commonly made from glass where channels are fabricated in the surface using a chemical etching process. HF was used as the chemical etchant to dissolve channels into the glass surface. Powder blasting has also been used for the development of channels in glass. However, these channels tend to have rough surfaces which reduce separation efficiency, thus making them undesirable for electrophoretic separation [18].

HF glass etching is still a popular technique, usually a three step process. First photolithography is used to transfer a pattern of channels into the glass by using a thin coat of photoresist and exposing the photoresist through a mask that blocks the UV light from the desired areas. The masks are easily developed in computer drawing programs as shown by Duffy *et al.* [19].

Secondly, the unexposed resist is removed by a chemical developer solution leaving fine channels in the photoresist. Usually there is a chrome layer under the photoresist that is also chemically etched, giving access to the glass underneath. The photoresist/chrome channels are filled with HF etchant that dissolves away the glass at the bottom of the channels. This forms the desired channels in the glass plate, which is then covered with another glass plate forming a closed glass channel chip. This process was shown by McCreedy *et al.* who published a comprehensive protocol for the development of glass microchips in the open laboratory [20]. However, the use of extremely hazardous chemicals such as HF, or of powder blasting techniques, and the fragility of the chips are significant deterrents for making glass chips [21]. The cost of glass per cm^2 often being, significantly higher than that of many plastics has strongly encouraged the movement of research in microfluidics towards polyermer substrates.

1.1.1.2 Polymer Microchips

In more recent times the development of microchips from moulds has become prominent, allowing chips to be made from many substrates, such as thermosetting elastomers including PDMS and a range of polymers and plastics, such as Poly(methylmethacrylate) (PMMA), Poly(carbonate) (PC), Poly(styrene) (PS) and Cyclic Olefin Co-polymer (COC)). Whatever the material used, the common properties include low electrical conductivity, low permeability (especially to water), flexible surface chemistry and high transparency, allowing

the use of optical detection systems to name but a few of the advantages discussed by Ng *et al.* [22].

1.1.1.2.1 ***Casting***

Casting is a replication technique. A liquid polymerisation mixture is poured over the mould and allowed to set, this is usually accelerated at a slightly elevated temperature. PDMS is the most commonly used material for casting.

A wide range of photoresists have been developed for application to the fabrication of moulds on the surface of silicon and similar substrates [23].

Newly developed photoresists can now produce a wide range of microstructures which were not previously possible in the general laboratory [17, 24, 25]. Fine structures down to the order of 1-10 μm have been produced with photolithography. Three dimensional structures have been developed on this scale with such photoresists by Ng *et al.* and Yu *et al.* with electron beam lithography, these have been successfully used as moulds for PDMS [22, 26].

Both types of moulds, metal and photoresist, can be used for casting chips from elastomers such as PDMS, which are poured over the mould as a viscous liquid and chemically and/or thermally cured [25]. These are then cut from the mould which can be reused. To close the channels the cast is bound to another substrate, which can be glass, polymer or another layer of PDMS. PDMS can be reversibly bound to flat substrates including glass, PMMA and silicon via hydrogen bonding which allows the PDMS to be easily peeled off the slide for cleaning [27]. Stamp and stick techniques developed by Satyanarayana *et al*. can be used to form stronger semi-permanent bonds [28]. Unfortunately, positive pressure cannot be used in reversibly bound devices because the pressure may break the seal. Hence, the use of a vacuum is recommended for pressure-driven flow in these devices. Oxygen plasmas have been used for irreversible binding of PDMS allowing

higher pressures to be used. Because PDMS is an elastomer these pressures tend to deform the channels [29, 30].

1.1.1.2.2 ***Imprinting Microchips***

Metal moulds can also be used to produce chips, especially during hot embossing and injection moulding where the extra mechanical stability over silicon is required. During hot embossing, a mould is pressed into a polymer substrate while sandwiched between two platens; the platens are heated to just above the softening point of the polymer. During injection moulding, a granulated polymer is melted and pumped into a chamber containing the mould. The chamber is cooled to solidify the polymer and the patterned substrate is released from the mould. Hot embossing is a good technique for replication of small to medium sized batches (50-100), whereas injection molding is only financially attractive for batches >500 because of high start-up costs.

After replication of the microfluidic structures, the channels can be sealed to another substrate using a thermal or solvent bonding process. In contrast with PDMS devices, pressure-driven flow is well-suited to microchannels fabricated in rigid polymers.

Despite some limitations with PDMS chips they are still ideal for electrophoretic based separations and remain prominent in current day microfluidic research [31]. PDMS chips were used in this study because of several advantages, including the lower costs of manufacturing, and being able to avoid the use of the high temperature and pressures needed for rigid polymers, or use of extremely hazardous chemicals such as HF for glass. Also being able to reversibly bind PDMS to glass and other substrates, such as PMMA, allows the chips to be cleaned and reused with ease.

The low costs and possibilities of producing large numbers of disposable chips, as well as on-site manufacturing in research labs are the main attractions of microfluidic devices, particularly when using PDMS. On-site manufacturing allows for a wide range of chip geometries to be developed for specific purposes that are not always possible with expensive, commercially available microchips.

1.1.2 Microfluidic Electrodes

Metals are the predominant electrode material used in microfluidics despite the wide variety of substrate materials investigated. Only limited research has been undertaken using alternative electrode materials. Traditionally, microelectrodes are created by metal deposition, followed by a photolithographic lift-off, but most materials commonly used for LOC applications are not compatible with the solvents required to dissolve the photoresists [32]. The lift-off process is also very wasteful, as most of the deposited metal will be removed during the lift-off process. Semi-conducting films, such as Silicides and indium tin oxide (ITO) have also been used to produce micro scale electrodes [33] manufactured using a lithographic lift off approach.

Mass replication techniques such as injection moulding allow for the fast and inexpensive production of microfluidic features. Incorporation of more advanced functionality through the integration of electrodes can be achieved, but at significant financial cost. For example, it is possible to purchase >1000 polymer chips for electrophoresis for €10 each [34], but for chips of the same design with external electrodes for detection the price increases to €32.50. Microchips of the same design with integrated electrodes in direct contact with the channels for contact conductivity detection cost €125.00 each when ordering more than 30, which is 12.5 times more expensive than the simple channel-only devices. It is obvious that the high cost of integrating electrodes into microchips makes the

devices very expensive and far from disposable. To create truly disposable LOC devices with integrated electrodes, new cost-effective alternatives are required.

It is surprising that the advances in microchip technology have not extended into the area of electrodes when considering the importance of electrodes for a large number of advanced Lab on a Chip functions [35]. Some of the main applications for electrodes within microfluidics are high voltage (HV) electrodes for electrophoretic separations and for performing di-electrophoresis sorting of cells [36], heaters for performing the polymerase chain reaction (PCR) on microfluidic devices [37], droplet manipulation in digital microfluidics [38, 39] and electrochemical detection including amperometric detection and conductivity detection.

1.1.1.3 Microfluidic High Voltage Electrodes

One of the most common applications using electrodes in microfluidics is that of electrophoresis where HVs are applied through the electrodes directly into microfluidic channels. These are typically applied using external electrode interfaces connected to HV power supplies. The electro-osmotic flow (EOF) has been used in microfluidics to move bulk solutions between different areas of a microfluidic device. The most common application of HV electrodes is to apply voltage for the electrophoretic separation of analytes with this process being known as microchip capillary electrophoresis (MCE). Given the high proportion of microfluidic and LOC devices using electrophoresis and the desire for the production of more highly integrated devices, the actual integration of HV electrodes into these areas is extremely low, with only a few papers integrating electrodes for use as high voltage electrophoresis electrodes [40, 41].

1.1.1.3.1 ***Microchip Capillary Electrophoresis***

Electrophoresis is considered as the most suitable separation technique to be adapted to miniaturised separation devices such as microchips because it does not rely on the use of pumps that produce hydrodynamic flow. Electrophoresis has been used widely with microchips for the separation of various compounds [1, 3, 16, 17, 42-46]. The technique of capillary/microchip electrophoresis separates analytes by applying an electric potential through a narrow capillary/channel filled with an electrolyte solution. Analytes are separated based on their electrophoretic mobilities, which are primarily determined by their size-to-charge ratio.

If the walls of the separation channels are charged a bulk EOF is induced. When the walls of the channel are negatively charged, such as with glass, a layer of net positive charge is induced in the electrolyte near the capillary wall that will flow towards the cathode. If the channel walls are positively charged, a negatively charged layer will be formed causing an EOF towards the anode. The EOF will be suppressed if the walls carry little or no charge. For fast separations, it is favourable to have EOF in the same direction as the migration of the analytes, provided the analytes can be separated. Ghosal has reported in detail the effects of EOF in various electrophoretic systems, including capillaries and microchips [47, 48].

With multiple channel microchips, the voltages applied are used to control the flow of analytes. Only with careful use and understanding of the voltages applied to a microchip can loading of samples, injection of a small plug and finally separation be performed in a simple and reliable manner. Harrison *et al*. [49], Von Heeren *et al.* [50] and Jacobson *et al.* [51] were among the first to report the effects of voltages and how they can be used to control the flow of analytes in four channel chips. Jacobson *et al.* described in detail the requirement for

'pinching' voltages to ensure that the injection plug was as narrow as possible and how this led to high resolution separations, as well as the requirement of 'pull back' voltages to avoid bleeding into the separation channel. Von Heeren *et al.* reported similar results on pinching but extended their study to be a more in depth analysis of the peak resolution given by the level of 'pinching' applied.

1.1.1.4 Fluorescence Detection

UV absorbance detection is a widely used detection method in Capillary Electrophoresis (CE), but the dependence of its sensitivity on the pathlength makes absorption detection a less attractive option when miniaturisation is performed. Alternative detection techniques like LIF detection and conductivity detection are more attractive for incorporation in microchips. Groups including Chabinyc *et al.* [52] have produced chips incorporating optical fibres for LIF detection systems. By using low power Light Emitting Diode (LED) in place of more expensive narrow band light sources such as lasers, the cost can be dramatically reduced. The smaller size of LEDs is also more applicable to integration into small devices than larger lasers that would incur a faster power drain, decreasing the useable time of any portable device.

Because most analytes are non-fluorescent, labelling of the target analytes with a fluorescent tag is often required. Since the development of the early MCE device by Effenhauser *et al.* [53], fluorescein isothiocyanate (FITC) has become a standard dye used for analysing the performance of microfluidic fluorescence systems [54]. For deoxyribonucleic acid (DNA) analysis, intercalating dyes are used in the majority of separations [55]. For the analysis of other biological molecules, including carbohydrates, fluorescent tags such as APTS and naphthalene-2,3-dicarboxyaldehyde (NDA) have been used specifically in microchip electrophoresis (MCE) [56-59].

1.1.1.5 Detection Electrodes

One of the main uses for electrodes in microfluidics is for detection. There are two main types; electrochemical detection including amperometric detection, and conductivity detection. Both these detection techniques have been widely researched in microfluidics over the past decade. One major advantage of these detection techniques is the small size of detectors that can easily be integrated into microfluidic devices.

Because electrochemical detection requires that there is a working electrode and reference electrode in the analyte solution, fouling of these electrodes can be a major problem. However, conductivity detection can be performed in the contactless mode, thereby eliminating the problem of electrode fouling. It is also considered that a large amount of technology established in the electronics industry can be used in the manufacturing of micro scale electrodes for microfluidic LOC devices.

1.1.1.6 Capacitively Coupled Contactless Conductivity Detection

In the past decade Capacitively Coupled Contactless Conductivity Detection (C^4D) detection has become the main electrochemical detection techniques used in microfluidics. Since 2003 Kuban *et al.*, among others, have published several reviews on C^4D and its applications in electrophoresis [60-64]. C^4D was first described in electrophoretic separations by Gas *et al.* in the 1980s and was used for detection of anions in isotachophoresis [65]. An axial arrangement of the C^4D for capillaries was later developed involving tubular electrodes fitted side by side around a standard capillary by Zemann *et al.* [66] and da Silva *et al*. [67]. This design was relatively simple with a gap between the electrodes of up to several mm forming the detection volume. Unlike other electrochemical and contact conductivity techniques, which require contact to the separation channels, C^4D

avoids the difficulties involved in manufacturing detection cells required to fit in sub mm diameter separation columns. With the ease of construction of C^4D it has recently become a major detection technique used with electrophoretic separations [68]. The low power and small spatial requirements have led to C^4D becoming an established technique in microfluidics and LOC devices.

1.1.1.6.1 ***Principles of C^4D in Electrophoresis***

Microchip C^4D, is typically performed by two electrodes capacitively coupled with the electrolyte solution in a channel. By applying an Alternating Current (AC) voltage to the excitation electrode, a current can be measured at the pick-up electrode. In the electronic scheme, the capacitive coupling through the channel wall introduces capacitors in series with the measured electrical resistance of the solution in the channel. The measurement frequency needs to be optimised to ensure measuring the resistance of the solution and not the capacitance of the walls. One important consideration of the C^4D setup is to prevent direct capacitive coupling of the electrodes, as this will influence the sensitivity and linearity of the detector response [69, 70]. This coupling can be suppressed by using shielding electrodes, optimising the electrode geometries within these constraints and optimising the operating frequency.

In microfluidic devices these electrodes can be externally placed outside the microfluidic device above or below the separation channel, or integrated into the devices and separated from the separation channel by a thin insulating layer. In either case, electrodes surrounding the separation channels, such as in conventional CE, have not been developed in microfluidics. Because of these geometric constraints, the capacitive coupling is lower in microfluidc devices than in CE [71]. However, because conductivity detection is a bulk detection system, analytical signal differences are due to a change in the overall conductivity of the bulk solution. In electrophoresis, a background signal due the

conductivity of the background electrolyte (BGE) solution will always be present, hence lower conductivity BGEs are preferable.

The development of C^4D in microfluidics has generally revolved around the search for an applicable general detection technique. Most studies use standard sets of analytes, such as Li^+, Na^+ and K^+, to show the separation and detection capabilities of the devices created. Despite this, C^4D is used with many other separation techniques and has a wide range of present day applications in research and industry. These are covered in a comprehensive review by Kuban and Hauser [61].

1.1.1.6.2 *C^4D Instrumentation*

Various C^4D design geometries have been studied to optimise the configuration for microfluidic platforms. Table 1.1 shows some of the range of materials and processes used in developing C^4D with microfluidics. In particular, Kuban and Hauser studied the geometry for external C^4D electrodes finding that antiparallel electrodes set at 45^0 with minimal detection gap, but including "Faradaic" shielding between the detection electrodes, provided the highest sensitivity [72]. Another study by Mahabadi *et al.* using external electrodes, in this case on the top and bottom of a device, to increase the coupling capacitance, found that detection sensitivity could be further improved to sub µM levels [73]. Other recent studies have shown improvements in sensitivity with more complex integrated C^4D designs, often using either platinum or gold electrodes embedded into the microfluidic devices, such as that described by Fu *et al.* [74].

Dual detection systems have been also been integrated into microfluidic devices, such as a dual LIF - C^4D by Liu *et al.* and dual C^4D – amperometric detection device produced by Vázquez *et al.* that show good results and sensitivity improvements over single detector devices [75, 76]. However, the manufacturing

of these is complex, with the C^4D – amperometric device presented by Vázquez *et al* incorporating copper printed circuit board (PCB) technology for C^4D and standard lift off process to develop a platinum amperometric detection electrode.

All of these devices have used metal electrodes and where they have been integrated, this metal has been either gold, platinum or copper. Although they

Table 1.1: Recent publications in microfluidics showing the range of substrate and electrode materials currently used in microfluidic chips with C^4D detection research.

Substrate Material	Electrode Material	Electrode Manufacturing	Level of Integration	LOD	REF
PMMA	Cu	Precision Machining	External C^4D External HV	0.3 µM Na^+	[73]
PDMS / Glass	Cu	PCB	Integrated C^4D External HV	35 µM Na^+	[75]
PDMS / PET	Cu	PCB	Integrated C^4D External HV	15 µM Na^+	[77]
PMMA	Pt	Lift off Process	Integrated C^4D External HV	21 µM Na^+	[78]
LTCC	Ag	Screen Printing	Integrated C^4D External HV	4 µM Na^+	[79]

show significant improvement in sensitivity, they are less practical for mass production and for the production of disposable point of care (POC) devices.

1.1.1.6.3 ***Advances in C4D Electrode Materials***

Recently there has been more research using other electrode materials within microfluidic devices in the search for cheaper methods for electrode integration. The use of PCB has enabled cheap micro electrodes to be manufactured and has the potential for mass replication. Several electrodes have been integrated in microfluidic devices by mounting or building the microfluidics on top of printed circuit boards [77, 80, 81]. Alternative methods, including screen printing [82]

and air brushing [83], have been used, with either silver or carbon laced paints. While these can quickly produce electrode patterns, they are limited to features larger than 200 μm [84]. Electrodes have also been created from microchannels filled with molten solder [85] or gallium [86]. An alternative approach to reduce the cost of electrode integration in microfluidic devices is to use conducting polymers instead of metallic electrodes [87].

1.2 Conducting Polymers

With all of the advances in the technology and techniques used in producing microfluidics, a cheap, disposable and analytically multifunctional Lab-on-a-chip device has remained elusive. The cheapest Lab-on-a-chip devices are still ten to a hundred times the cost required for a truly disposable device. Intrinsically conducting polymers (ICP) have been shown to be cheap alternative materials to metals and other semiconductors in many applications. Since their discovery by Shirokaowa *et al*. in 1977 [88] there has been great anticipation of the many potential applications for which they could be used, from general electronics and electromechanical uses to electrochemical membranes and sensors. The use of many ICPs for such applications has been limited by the numerous drawbacks affecting the ease with which they could be manufactured and processed. Typically, they are infusible, have low levels of solubility in water and other solvents, and are inherently less conductive than metals, with the more highly conductive ICPs also being less stable.

1.2.1 Conducting Polymers in Microfluidics

Given the limitations of the majority of conducting polymers it is not surprising that few have been used in the search for more applicable technologies in LOC research. However, recently some conducting polymers have been used in LOC devices as either aids in manufacturing or integrated for specific applications. The

conducting polymer poly(3,4-ethylenedioxythiophene) (PEDOT) has been used as a chemical biosensor in polymer devices for selective detection of dopamine [89]. PEDOT blended with poly(styrenensulfonate) (PSS) has also been used within microfluidic devices to eliminate electrolyte electrolysis in a capillary electroosmotic pump device [90]. Chun *et al.* Developed a device containing poly(2-acrylamide-2-methyl-1-propanesulfonic acid) (poly AMPS) in localized positions along the channel, enabling the generation of local electric field gradients for on chip sample pre-concentration [91]. Polyaniline (PANI) has been used to enhance the chemical bonding between PMMA components of microfluidic devices. Through the absorbance of microwaves, strong flawless seals were produced in PMMA devices [92].

1.2.2 Polyaniline

Polyaniline has been touted as one of the most promising of the ICPs because of its ease of synthesis from a low cost monomer and better stability than many ICPs. Hence, PANI was chosen in this study as a new alternative electrode material for integration into microfluidics.

PANI has been researched extensively since its discovery some 35 years ago, with many possible applications identified in electrochemical and materials science [93-97]. It has been studied extensively over the last three decades [97, 98] and has been used as an alternate electrode material for electrochemical detection in various analytical systems. The stability of PANI has driven research towards application and development of electrodes [99], electrode coatings [100] and films [101], some of which can be manipulated for purposes such as actuation [102]. The integration of polymer electrodes into microfluidic devices has the potential to significantly reduce the costs of integrated devices if the processing costs are kept low. Successful integration of such electrodes would also enable

the production of the first fully polymeric Lab-on-a-Chip devices with integrated electrodes.

1.2.3 Polyaniline Synthesis

The ease and low cost of synthesising PANI are attractive reasons why it is a primary candidate for the integration into new technologies. Over the years there has been a large variety of methods used for the production of PANI, including electrochemical, sono-chemical, photo-induced plasma, and chemical polymerisation of aniline. Chemical polymerisation can also be segregated into various forms of heterophase polymerisation and solution polymerisation. All of these production processes have their advantages for specific applications and many of them can be tuned to form polymers of specific shape and size.

Typically, PANI is produced by addition of an oxidising agent, such as ammonium persulphate (APS) or hydrogen peroxide, to an acidic solution of aniline monomer in an oxidative polymerisation reaction. A range of different approaches have been undertaken to produce PANI via chemical polymerisation to achieve differing degrees of purity, size, shape and conductivity of the resulting polymers.

Heterophase emulsion polymerisation has been a common way to produce polymers for many years [103] and can be used to produce PANI on a large scale. Emulsion polymerisation can be used to produce PANI by choosing a nonpolar or weakly polar solvent that is sparingly soluble in water to form an emulsion of the essential reactants (aniline, water soluble oxidising agent such as H_2O_2, and protonic acid) and a surfactant to stabilize the formed PANI particles. The PANI Emeraldine Salt (see Section 1.2.2.1) that is formed then requires a large amount of washing to yield a clean product [104, 105]. A reverse emulsion process can also be used to produce PANI in which a solvent soluble oxidant is used in a

nonpolar solvent system that produces PANI soluble in the organic phase [106]. Both methods require acetone or similar solvent to break the final emulsion and precipitate the PANI salt that is typically nm sized PANI fibres. The size of the fibres produced can be controlled by the type of surfactant used in emulsion polymerisation, with higher molecular weight surfactants leading to larger PANI fibres. Small-scale, mini, and micro-emulsions of sub mL volumes have also been used to produce PANI that is of lower molecular weight and higher solubility because of their more stable emulsion systems and the use of co-surfactants [107, 108].

Electrochemical synthesis is attractive because it uses fewer chemicals and is therefore generally considered to produce purer PANI. Various methods can be employed to produce structurally different forms of PANI. The galvanostatic approach produces finely divided powders at the electrode which can be isolated and purified [109]. With the potentiometric approach thin or thick films can be produced that can be peeled off to give a free standing film [110]. Specific structures using templates can also be achieved with electrochemical polymerisation. Templates have been used for producing very specifically shaped PANI fibres within the pores of a dissolvable template [111, 112]. However, the use of templates requires complex, post-synthesis treatments to remove the template material and residual chemicals [113, 114].

Interfacial polymerisation has also been used to produce nanofibres typically of 30-35 nm in length with very little branching or formation of agglomerates. In this approach, PANI is synthesised at the solvent boundary between water containing the acid/oxidant mix and an immiscible solvent such as chloroform which contains the monomer. The fibres produced exhibit minimal branching because, as they form, they are in the hydrophilic doped emeraldine form and move quickly away from the interfacial boundary before branching can occur [115]. However, washing is required to purify the PANI fibres by removing un-

reacted reactants and the short chain polymeric material after polymerisation is completed. The morphology of PANI formed by this method can also be controlled by varying the acid to aniline ratio. Chen *et al.* have shown controllable production of nano-rods, spherical particles and larger agglomerates by varying the ratio of aniline to salicylic acid dopant [116].

Solution polymerisation is one of the simplest chemical polymerisation methods used to synthesise PANI. This type of polymerisation is usually performed by slowly adding oxidant, drop-wise, to a solution of aniline monomer in 1M protonic acid producing a wide distribution of large aniline fibres. This method typically produces a high level of branched PANI in large agglomerates. The branching and agglomeration can be reduced through a rapid mixing approach described by Huang *et al.* [117]. With this approach the entire reaction mixture is added at once to a rapidly stirred solution. The rapid mixing causes the oxidant and aniline to disperse throughout the solution such that during polymerisation there is less opportunity for secondary growth/branching to occur. The nanofibre lengths produced using this approach, were similar to those produced with interfacial polymerisation. Similarly, when the acidic solution of APS is added drop-wise to an aniline solution whilst being ultra-sonicated the branching and agglomeration of the PANI fibres was also minimised. The length of fibre has also been controlled in this approach by changing the ratios of the aniline to APS [118]. Solution polymerisation has the ability to produce large amounts of nano-scale, minimally branched PANI fibres with relative simplicity.

1.2.4 Properties of Polyaniline

1.1.1.7 Structure

Polyaniline is considered one of the most important conducting polymers because of its simple doping and de-doping mechanisms that enable easy control over the four primary states of the polymer [87, 98, 119, 120]. The three base states of PANI include the non-conducting fully reduced leucoemeraldine base (LB) and the fully oxidised pernigraniline base (PB), and the semiconducting half oxidised emeraldine base (EB) that are shown in Figure 1.2. The fourth state of PANI is formed via protonation of the emeraldine base, this forms the conducting emeraldine salt (ES) (see Figure 1.3).

1.1.1.8 Conductivity

Since PANI was first discovered there have been many studies into the different forms of the polymer and effects that influence its conductivity One of the first studies by Focke *et al.* [121] covered a range of effects including oxidation state, pH and counter-ion species. With the use of cyclic voltametric analysis two redox processers were identified, the first corresponding to the formation of a cation radical at the nitrogen from the amine fully reduced LB and the second redox process corresponding to the formation of the fully oxidised quinine di-imine PB. The effects of solution pH on the resistivity of PANI were also measured in this study, showing the general trend of decreasing resistivity with increasing acidity from pH 5 to pH 1. Conductivities as high as 10^3 $S.cm^{-1}$ have since been reported for the ES form of PANI, which approaches the conductivities of some metals [7]. Huang *et al.* [122] also showed significant differences between the redox properties of PANI depending on the pH with the two processers merging with increasing pH.

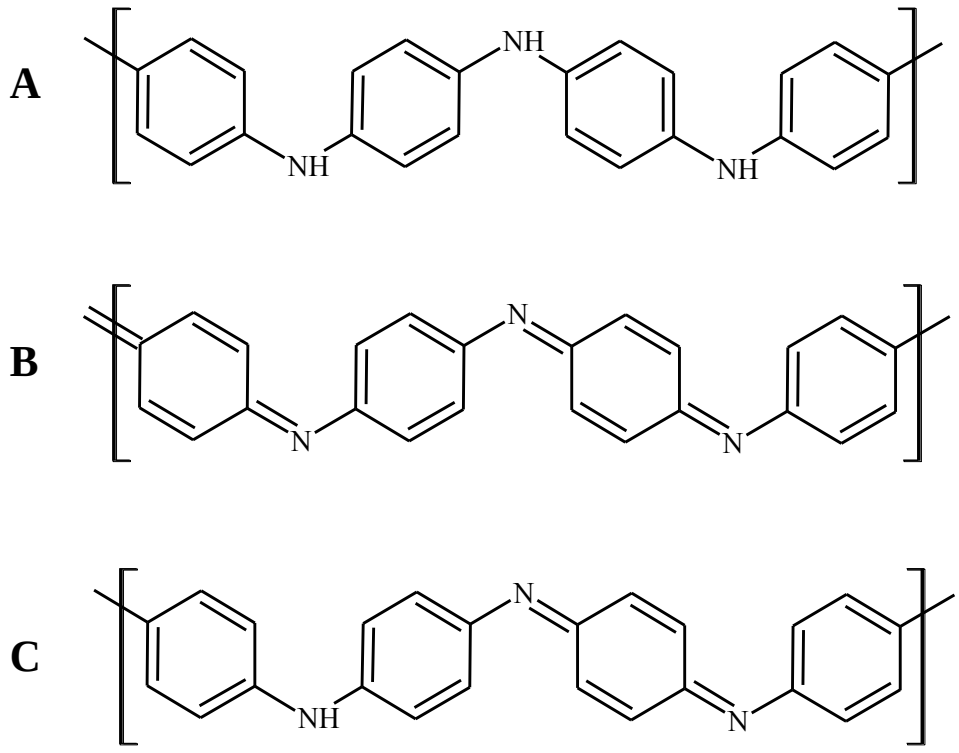

Figure 1.2: Structure of the primary forms of Polyaniline: A) fully reduced leucoemeraldine base (LB); B) fully oxidised perniganiline base (PB); C) half reduced emeraldine base (EB).

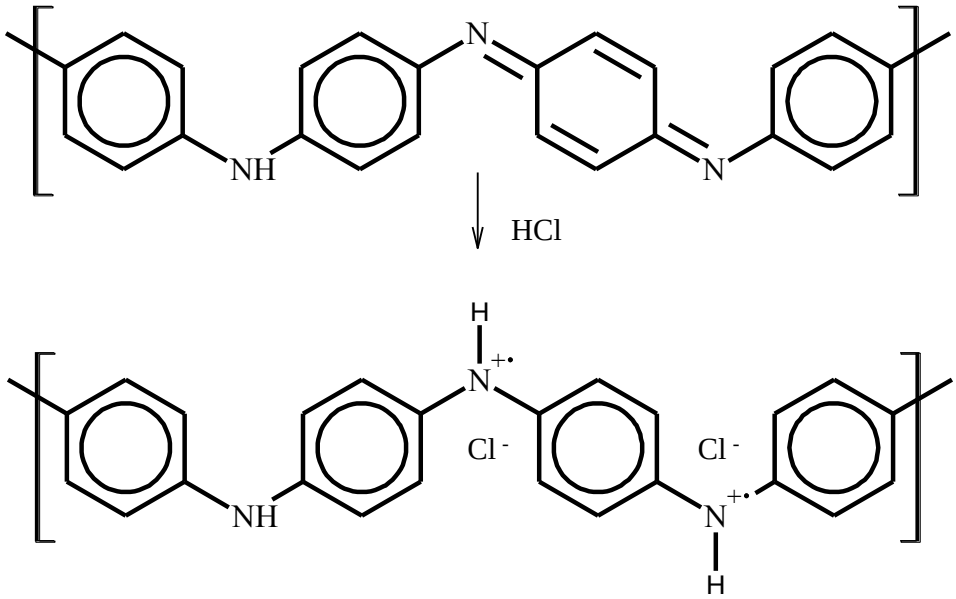

Figure 1.3: Formation of the Emeraldine Salt state of PANI via doping with HCl.

The conductivity of PANI-ES is due to the formation of polarons at the nitrogen centres when PANI-EB is doped with a protonic acid [123, 124]. Figure 1.3 shows the formation of a polaron when PANI-EB is doped with HCl. The polaron structure indicated in Figure 1.3 then dissociates to form a localised polaron lattice with cation centres on 50% of the nitrogens along the polymer backbone at maximum doping. This corresponds to the data from the results of Focke *et al.* [121], which showed that the resistivity minima was almost directly between the two redox processors shown in the cyclic voltametric experiments, suggesting the most conductive form is indeed the half oxidised half reduced form of PANI-ES

In the ES form, electrons are able to move along the chain from a neutral nitrogen centre to an adjacent charged nitrogen centre, leaving a cationic radical. This electron jumping can continue along the polymer chain in one direction while the movement of the cationic radicals is in the opposite direction, resulting in the electronic conduction along the polymer [125-127]. For the development of highly conductive PANI-ES moisture is required to facilitate the protonation/deprotenation of the nitrogen centres with dried PANI-ES typically 3 orders of magnitude less conductive than damp PANI-ES [121].

The conduction mechanism of PANI can be further described from experimental results on Hall voltages [128]. If the charge carriers were mostly negative, leading to a positive Hall voltage, PANI-ES would be an *n*-type semiconductor. However, PANI-ES is a *p*-type semiconductor with a negative Hall voltage, hence it contains a higher proportion of cationic nitrogens than neutral nitrogens along the polymer chain. Other techniques have also shown the relative abundance of cationic nitrogens along the polymer chain. It is the available π bonds along the polymer chain that allows electron movement between the nitrogen centres with the excited state π^* being responsible for conduction. As the energy difference between the π and π^* decreases, the conductivity of the polymer increases [110,

129]. Other techniques have also been used to identify the nature of the nitrogens along the polymer chain in PANI. These include X-ray photoelectron spectroscopy (XPS) and X-ray ablation near edge structure spectroscopy (XANES) both of which have been used in characterising PANI-ES along with PANI-EB and PANI-PB [130, 131].

Another feature of PANI affecting the conductivity is structural order, considered to be semi-crystalline, heterogeneous in nature with metallic conducting crystalline islands in amorphous surrounds [125, 132, 133]. Electrons move through the crystalline structures via the polaron jumping, with electronic tunnelling required to move across the amorphous regions [134]. Electronic tunnelling is also used to describe the movement of electrons between polymer chains [135]. In either case, it is considered that the higher percentage of crystalline structure in the PANI-ES macrostructure leads to a higher conductivity.

1.1.1.9 Polyaniline Doping

One aspect of PANI ES structure that leads to greater stability is that the doping is at the nitrogen centres and unlike the p doping found with other conducting polymers does not form a radical carbonium ion [122].

There has since been a large amount of research into increasing the conductivity of PANI that has evolved around the doping process. By studying a wide range of dopants and doping methods a number have been found to increase the conductivity over initial HCl doping. Typically HCl doped PANI in aqueous medium has a conductivity of 10-12 S cm^{-1} [126]. However in the past decade PANI conductivity has been measured with a wide range of dopants in different forms with conductivities ranging from 0.1 S cm^{-1} using acetic acid [136, 137] to 200 S cm^{-1} using camphor sulfonic acid (CSA) [138]. It has been found that more

basic the dopant anions result in lower conductivity [139] and that with polymeric acids the higher the molecular weight of the acid the higher the conductivity.

1.2.5 Polyaniline Processing

There have been many challenges in processing PANI including its very low solubility, hygroscopic nature, infusibility and relatively lower conductivity than metals. The lack of solubility and the hygroscopic nature of PANI restricts the post-synthesis chemical modifications that can be performed on the polymer [99]. Various modifications have been studied for generating PANI in a form that would be soluble in a range of solvents [140, 141]. However, due to the infusibility and lower conductivity in comparison to metals, it has not been considered as a general metal replacement in applications requiring reasonable conductivity and structural strength. Although, studies of the doping process with varying dopants and dopant concentrations have shown various ways to improve the conductivity of PANI after synthesis [142].

Another way used to improve the processing of PANI has been the use of composites. A number of methods have been developed for generating PANI composites, where either the PANI forms the conductive filler of an insulating polymer with good mechanical properties, or as a composite with a material such as carbon nanotubes for applications such as electro-rheological fluids or enhancing the capabilities either specificity and/or sensitivity of sensor electrodes [143, 144].

1.1.1.10 Polyaniline Films

Although there has been a high level of interest in the processing of PANI in a soluble state, most applications involve the use of PANI as a coating or film on a substrate or electrode surface. Through potentiometric electrochemical synthesis, PANI can be produced as a film on an anode material which can then be peeled

off to give a freestanding film [145]. Deposition of PANI after chemical synthesis and purification can also be used to produce films. Thin films on the nanometre scale can be made by electro-spinning a PANI solution or suspension [146] or thicker micrometre films can be produced via electrodepositing or drop casting [147]. The advantage of electro-spinning and drop casting is that the films can be formed on insulating substrates. Other techniques used for the deposition of PANI include ink jet and screen printing where PANI is deposited in a specific pattern forming a conducting polymer electrode. Despite the capability of producing basic conducting structures via ink jet or screen printing, these printing techniques are slow and require highly specialised instrumentation [148, 149].

1.1.1.11 Lithographic Processing

In 2004, Huang *et al.* demonstrated that the nanofibrous ES form of PANI possessed a unique property amongst the conductive polymers in that films could be patterned by flash-welding. During flash-welding, the film is exposed to short bursts of high intensity light, changing its conductivity, doping and spectroscopic properties [150, 151]

Flash-welding of PANI films was proposed as a photolithographic patterning technique generating conducting tracks. On glass substrates, however, the welding only penetrated about 3 µm into the PANI film, leaving the underlying part of the film in the initial conducting, fibrous form [150, 151]. This made flash welding unattractive for generating conducting tracks, but the partial welding of the films was used to develop single monolithic actuators with an actuation of up to 720° [102].

To realise patterning conducting tracks of PANI by flash welding, the welding must penetrate the entire film. This could be achieved by decreasing the thickness of the PANI film or by increasing the intensity of the flash, but both have

practical limitations. The mechanical strength and conductivity of thinner films of PANI would be insufficient to produce usable conducting tracks and the use of a higher intensity flash would result in incinerating the PANI film.

1.2.6 Applications of Polyaniline

Polyaniline has been studied for its applications in many chemical processes [107] with the most recent areas of polyaniline application discussed further below. Polyaniline lends itself to use in sensors as it aids the sensitivity and selectivity of many desired sensing applications including chemical, pH, vapour and solvent sensing. The properties enabling these types of sensors include the changing colour and conductivity of PANI on exposure to varying pH levels of gas and liquid systems including solvent systems. Some sensors have been developed using simple PANI films for nitrogen dioxide [152] and hydrogen sensing [153]. Detection of dyes has also been undertaken using PANI modified electrodes [154]. Its ability to change colour in response to changes in pH has also been reported [155]. Sensing devices have also used composite PANI films such as PANI poly(vinylidenefluoride) (PVF) for volatile organic sensing [156] and PANI poly(vinylchloride) (PVC) for toxic gases [157].

Recently, there has been a focus on the development of PANI composites with carbon nanotubes. These composites have shown positive results for the development of actuation devices [158, 159] due to the expansion and contraction of the polymer fibres upon doping and de-doping [102, 160]. High energy storage devices based on the initial high dielectric constant of PANI have also been proposed [161].

The oxidation and reduction that changes the polymer from conducting to almost insulating is usually induced by doping and de-doping, and has allowed the

production of a memory device based on PANI/gold nano-particle composites [162].

PANI in the LE or PB form has been shown to be useful as an energy capturing material for rechargeable batteries and fuel cells [163] with PANI-LB as anode material or PANI-PB as cathode. There has also been a increasing interest into the application of PANI in solar cells [164] where it has been incorporated for various capacitance and buffering processes as composites with carbon nanotubes (CNT) and other materials, or as free standing PANI coatings [165, 166].

Other applications for PANI that are beginning to be realised include the development of organic LEDs that typically emit blue light [167]. It has also been studied for anti-corrosion applications for various metals [168] and has been used extensively in the development of various conductive adhesives [169, 170]. These adhesives are often tailored for use as anti-corrosion coatings. The incorporation of PANI into ink has enabled the development of conductive inks or suspensions [171, 172]. Polyaniline has also been used directly as an ink for ink jet printing [149].

Even though PANI has been used in such a wide range of applications including many related to analytical chemistry there have been few examples of it being used as a direct replacement for traditional metal electrodes.

1.3 Project Aims

Given that the current trends in LOC research are towards the development of portable devices for in field and POC testing, many new materials have been explored in the literature for achieving these goals. One of the main challenges in this field of research is involved with integrating high levels of functionality into single devices that can be cleaned and reused with ease.

One approach to overcome the need to develop devices that can be cleaned and reused is to manufacture disposable devices. However, to achieve this, devices need to retain a high level of integration of chemical processes and remain cost-effective. Therefore, a number of considerations need to be taken into account in the manufacturing of disposable devices.

The first is to use very low cost recyclable materials for all the integrated components of the devices, with a major focus being the reduction or elimination of metals paramount. Secondly, it is essential to keep costs in the techniques for producing the devices to a minimum and to use techniques that can easily be up scaled from the production of a single device to mass production. Finally, the end products should be suitable for use by a wide range of operators not just specialists in the field. For this to be possible, the highly integrated devices produced must be easy to use with a minimal amount of operations required from the operator in generating an analysis.

This thesis examines the use of PANI for the novel application as a cheaper alternative for traditional precious metal electrodes, with the primary aim of the project being to produce a disposable lab on a chip device containing electrodes for both high voltage and detection.

1.3.1 The aims of the project were

1. To synthesise bulk PANI nano-fibres of good conductivity that could be prepared into films.

2. Development of processing techniques for generating detailed electrode patterns within the PANI films, primarily through the extension and refinement of the flash welding process

3. Integration of the developed PANI electrodes into polymeric lab-on-a-chip devices as both high voltage electrodes used for driving microchip electrophoresis and performing a separation with these using an optical detection system.

4. The development of a fully polymeric device, including both high voltage electrodes and detailed capacitively coupled contactless conductivity detection electrodes and performing several separations using such devices.

2. Polyaniline Films: Development and Processing

2.1 Introduction

Polyaniline has been touted as one of the most important conducting polymers due to its easy preparation and simple doping and de-doping mechanisms that enable easy control over the four primary states of the polymer [87, 97, 119, 120]. Conductivities as high as 10^3 S cm^{-1} have been reported for the ES form of PANI, which approaches the conductivities of some metals [119]. The stability of PANI has driven research towards the application and development of electrodes [99], electrode coatings [100] and free-standing films [101] that can be used for a variety of purposes such as actuation [102].

In 2004 Huang *et al.* and Li *et al.* demonstrated that the nanofibrous (ES form) of PANI possessed a unique property amongst the conductive polymers, specifically that films could be photolithographically patterned by flash-welding. During flash-welding, the film is exposed to short bursts of high intensity light, changing its conductivity, doping and spectroscopic properties allowing conducting circuits to be made in a simple manner [150, 151].

This chapter explores the use of PANI electrodes for applications in microfluidic devices. To enable full and complete evaluation of the flash-welding process it is necessary that films of PANI can be reliably and repeatedly produced. To overcome one of the main limitations in the study by Huang *et al.* a large studio flash was selected as the exposure source as it will provide sufficient intensity to pattern a full 10 cm silicon wafer with one exposure, rather than the multiple exposures required by Huang *et al.* It was also envisaged that the higher power provided by this flash would allow the entire film to be penetrated, not just the top 3 μm as shown by Huang *et al*. In addition, an alternative option explored here was to improve the penetration depth by improving the efficiency of the

welding process, using alternative substrates. Patterned films were characterised by a range of techniques, including conductivity measurements using the four point probe technique described by van der Pauw [173], resistivity measurements with multimeters, scanning electron microscopy, optical microscopy and Raman spectroscopy.

To overcome many of the limitations posed for developing fully penetrated flash-welded films, an alternative options were explored. One option to improve the penetration depth of flash-welding was to improve the efficiency of the welding process using alternative substrates.

SEM has previously been used as the main characterisation method to show the physical differences between flash-welded and non-flash-welded regions in a PANI film [102, 150, 151]. To gain an insight into the chemical differences between these regions Raman spectroscopy, widely used for characterisation of PANI depositions and films [102, 119, 174-177], was employed in the current work. By extracting data from both techniques valuable information has also been gained around the interfaces between the flash-welded and non-flash-welded regions of PANI films.

Conductivity measurements using the four point probe technique described by van der Pauw [173] and resistivity measurements with multi meters have also been used the current work to characterise the PANI films.

Flash-welding using a studio flash involves a wide spectrum light source. Using a series of band pass filters, the wavelengths that were most effective in the welding process were determined. Based on this study, the first report was delivered for the lithographic welding of PANI using a narrow wavelength source, a laser diode. This laser diode was used for direct writing lithography (laser-welding) of 10 μm wide features in PANI. With the use of a high precision

xy stage, laser-welding has been developed and shown here to produce extremely accurate and fine insulating regions within PANI films down to 10 µm in width.

Two other forms of patterning PANI (extrusion printing and capillary force printing) [178] were explored as further alternatives to flash and laser-welding.

2.2 Polyaniline Synthesis

2.2.1 Chemicals

For syntheses and further processing of PANI the following chemicals were used: camphorsulfonic acid (CSA) 98+% (Fluka), aniline 98+% (BDH Chemicals), ammonium persulphate 99+% (APS, Ajax Chemicals), sodium hydroxide 98+% (BDH Chemicals), Hydrochloric Acid (Ajax Chemicals, Australia). All water used was purified using a Millipore Milli-Q water purification system (Bedford, MA, USA).

2.2.2 Method and Purification

PANI nanofibres were synthesised using a rapid mixing polymerisation technique described previously [117], to yield 10 g of crude PANI nanofibres from 1 L of 1 M CSA, 10 g aniline and 5.7 g APS. The crude nanofibres were isolated from the preparation solution by centrifugation at 12 000 rpm for 10 minutes at 20^0C in a refrigerated centrifuge (Beckman Coutler Avanti™ J-30I). After the initial centrifugation the fibres were de-doped by re-suspending them in 400 mL 0.5 M NaOH. This de-doping step was followed by four more purification cycles by re-suspending the pellet in 400 mL of MilliQ water on each occasion and re-centrifuging. After the last centrifugation cycle, the pellet was resuspended in 50 mL water and ultra-sonicated for 80 min to fully re-disperse the fibres. Throughout the preparation and further handlsing of the polyaniline fibres teh appropriate personal protective equipment was worn including lab coat, nitrile

gloves and safety glasses. The synthesis reaction and decanting during the purification process was performed in a fume hood.

2.3 Polyaniline Films

2.3.1 Substrate Preparation

PANI films were produced on either glass, polyacetate (Celcast: Photocopier Film Transparency), polyvinyl chloride or acrylic substrates (Acrylic Plastic RS Australia). Each substrate was cleaned by soaking in 0.2 M NaOH for 5 min with mild agitation before rinsing with running MilliQ water followed by drying with lint-free paper towel. Directly before coating, the polymer substrates were pre-treated with an Electro Technique High Frequency Generator (HFG, BD-20ACV) that created plasma on the surface of the substrate making the surfaces more hydrophilic. This was done by holding the HFG within 1 mm of the substrate surface and moving at 5 mm s^{-1} over the entire surface for 2 min producing visible electrical arcs to the surface, this enabled the water suspended PANI nanofibres to spread evenly across the surface due to the lowered contact angle.

2.3.2 Spray Coating

Films of PANI fibres were spray coated onto glass substrates using an air pressure sprayer. 2 g L^{-1} PANI suspensions in 1 M HCl or CSA were sprayed onto glass substrates and left to dry in a fume hood before further coats were applied to produce thicker films. This process led to very a rough surface on the films of PANI as can be seen in Figure 2.1 (A)

2.3.3 Drop Casting

Drop casting was used to make PANI films. This was done by pipetting 40 $\mu L/cm^2$ of a de-doped 2 g L^{-1} PANI-EB suspension in water onto a glass or polymer substrate. These were left to dry on the open bench in a clean room at

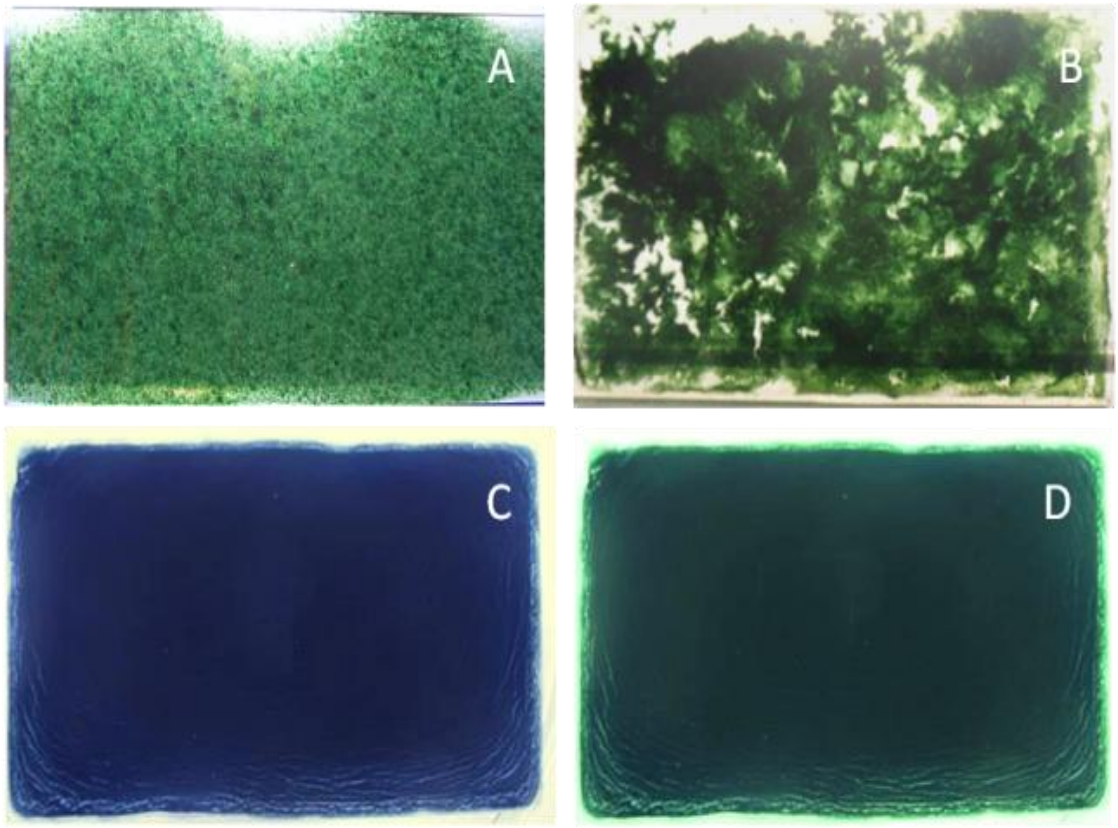

Figure 2.1: Photographs of 1.5 ml, 2 g L^{-1} PANI coated 7.5 x 5 cm glass microscope slides. A) Spray coated, B) Drop cast from 20% methanol suspension, C) Drop cast aqueous suspension pre doping, D) Drop cast aqueous suspension vapour doped using 14 M HCl.

approximately 15^0C. The time required to dry each cast was 2 hours. To decrease this drying time a number of approaches were trialled.

Attempts to dry them faster in an oven and on a hot plate at 60^0C led to cracks forming across the film. Acetonitrile, methanol and isopropanol at levels of from 10 - 50% were trialled as additives to the PANI suspensions in water. Casts done with these solvent additives were found to decrease the drying time but the PANI did not form even coatings, with large areas of substrate remaining exposed (figure 2.1(B)).

Drop casting from PANI suspensions in water was found to be the most consistent way to produce the films and hence, was used throughout. Films made by a single casting step were found to be inhomogeneous and less than 2 μm thick. Thicker, more homogeneous films were produced by repeating the casting process, allowing the PANI to dry between the castings to prevent aggregation of the fibres (Figure 2.1(C)).

After the final cast had been made and the coatings had dried the resultant films of PANI-EB were doped with acid to convert them to conducting PANI-ES. This was done through either dipping the PANI coated substrates into 1 M acid and then drying them under an air stream or placing them in a covered petri dish alongside a 1 mL drop of 14 M fuming HCl and leaving for 1 h (Figure 2.1(D)). The method of drying under an air stream made the process for doping faster but cracking formed in approximately 20% of films doped this way, thus the vapour doping with fuming HCl was used for all future doping due to higher success rates.

Scanning Electron Micrographs (SEM) were taken to determine film thickness using 8 samples of drop cast PANI on polyacetate for each thickness from 1 to 8 coats. After coating, each sample was doped forming conducting films. Samples

were prepared for SEM by cutting with a sharp blade and mounting with a cross section facing upwards using conductive silver paint to attach to the mount for the instrument. Each sample was sputter coated with a 30 nm layer of platinum. A plot of film thickness against the number of coatings is shown in Figure 2.2. For 2 coatings, the film thicknesses were measured using SEM images at eight areas of the film with a thickness of 3.16 +/- 0.12 μm recorded with some visible unevenness and a variance of 3.8%. For 7 coatings the thickness of the film was 10.94 +/- 0.20 μm which corresponds to a variation in thickness of less than 2%. Figure 2.3 shows an SEM of each of the eight film thicknesses measures.

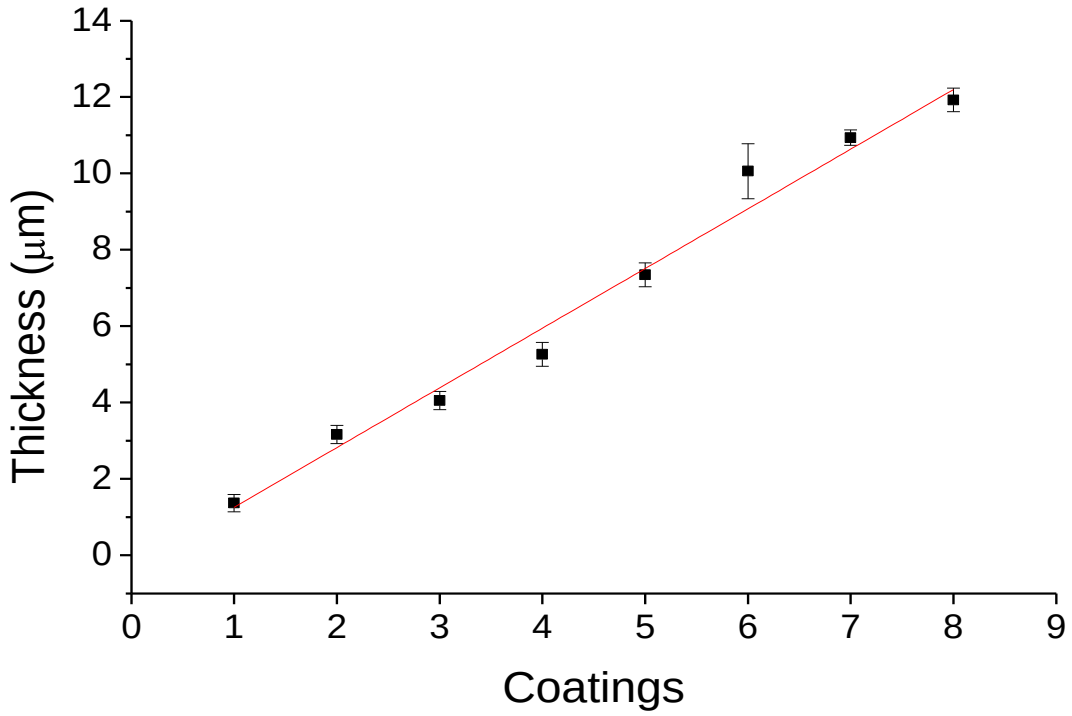

Figure 2.2: Plot of increasing film thickness with number of 1.5 ml 2 g L^{-1} coats of PANI onto 7.5 x 5 cm substrates. Cross sections were taken from 8 samples of each thickness with the standard deviation between each of them shown.

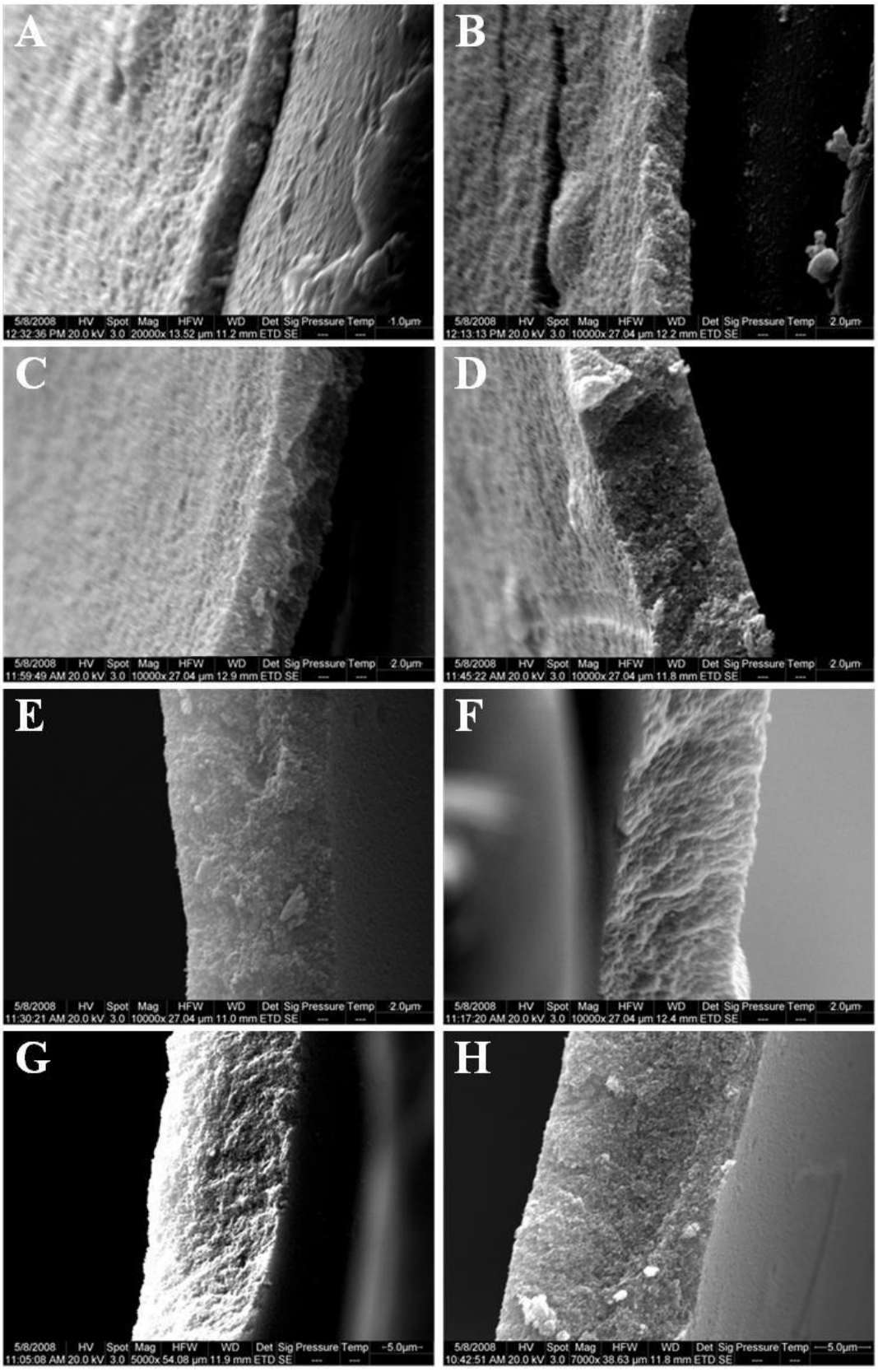

Figure 2.3: Scanning electron micrographs of doped PANI film cross-sections from A) 1 coating of dropcast PANI to H) 8 coatings of drop cast PANI.

2.4 Polyaniline Photo-processing

2.4.1 Flash Lithography

Films were first patterned using the lithography process known as flash-welding based on the original work presented by Huang and Kaner [150]. This was done using a studio flash (Elincrom 400 FX, 400 Ws) from an operating distance of 2 cm from the PANI-coated substrate. Figure 2.4 is a scheme of the flash-lithography process that shows the light from the studio flash passing through an overhead transparency mask into the PANI film on the substrate surface. With this technique basic patterns could be formed in the PANI films, an example of which is shown in figure 2.4 B.

Initial studies of the flash-welding process were carried out on PANI films of 1.8 to 14.4 μm in thickness on glass substrates. The studio flash used here was higher powered than flashes used previously for flash-welding of PANI films[150, 151]. Despite the high power output of the flash, a layer of non-cross linked fibres could be observed beneath the flash-welded fibres of films thicker than 8 μm, illustrating the limited penetration of the welding through the PANI film. When films with a thickness of less than 4 μm were used, no flash-welding was observed. This is attributed to the amount of PANI being too small, allowing thermal energy to dissipate more readily into the glass substrate and thereby reducing the energy held within the fibres to below the threshold required for welding to occur. When flash-welding was performed through the bottom side of the glass substrate, no welding was observed for film thicknesses between 1.8 and 14.4 μm, suggesting dissipation and absorbance of the energy through the glass.

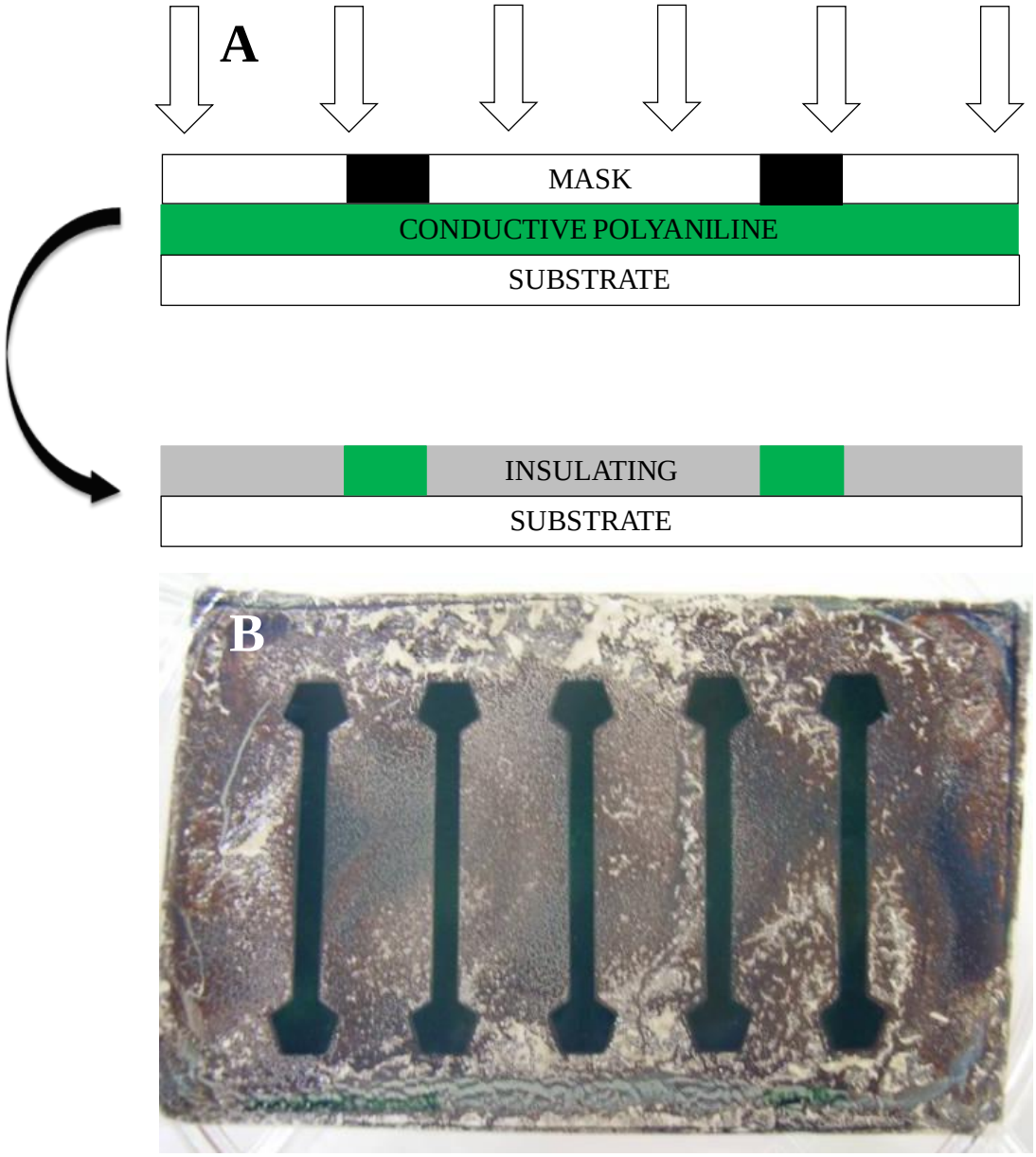

Figure 2.4: A) Scheme of the bottom side flash welding lithographic process, B) Photograph of a flash welded PANI film on a polyimide substrate through a basic mask.

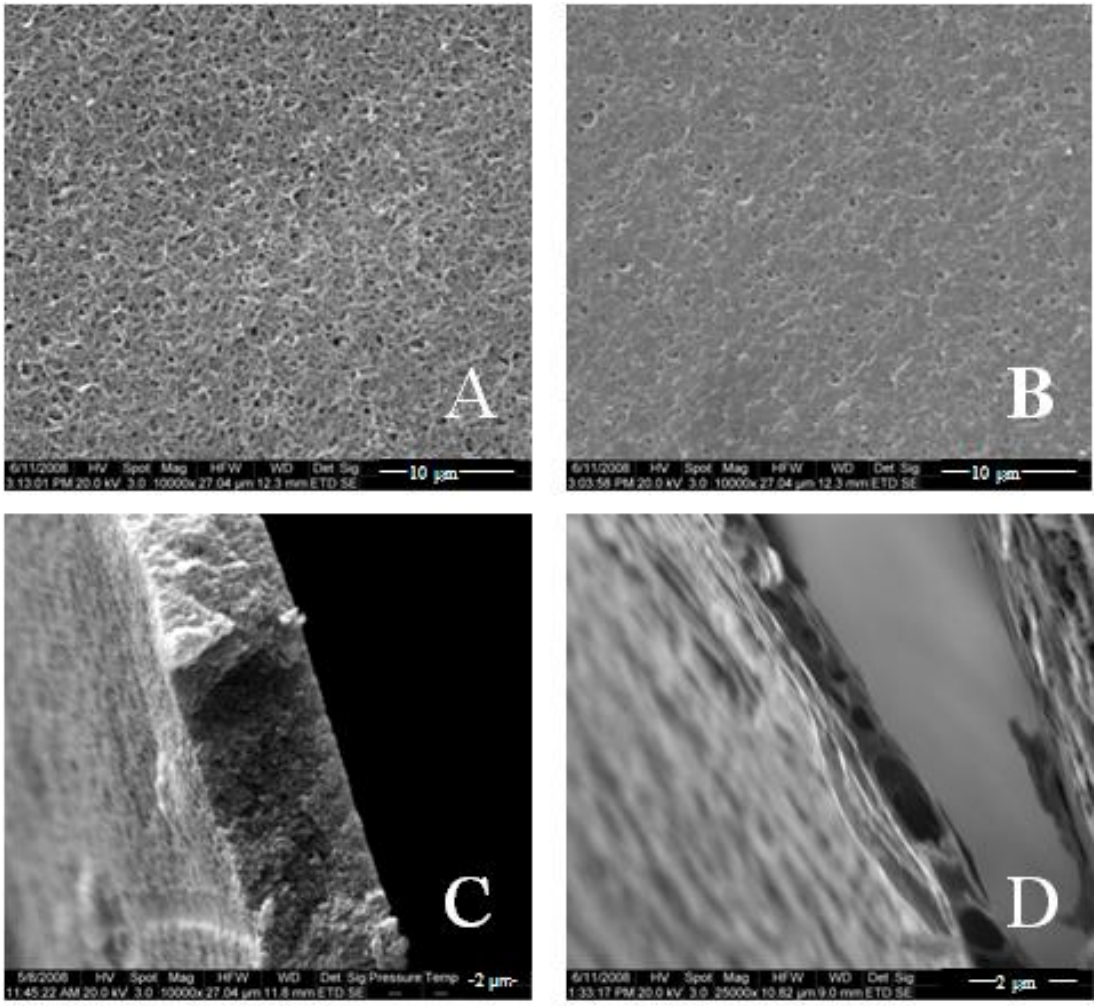

Figure 2.5: SEMs of some PANI films on polymer substrate with A), (before flash-welding) and B), (after flash-welding) as surface images. Cross-section images C, before flash-welding, and D, after flash-welding.

These results suggested that glass was acting as a heat sink. To overcome this limitation polymer substrates were evaluated based on their well known lower specific heat capacities [179]. Flash-welding PANI films on polyimide sheets resulted in flash-welding through the entire PANI film for films with thicknesses ranging from 3.6 to 14.4 μm, a significant improvement over the flash-welding process on glass. SEM images of surface and cross-sections of the non-flash-welded and flash-welded PANI films on polyimide substrates are given in Figure 2.5. The physical appearances of the PANI films before and after flash-welding were consistent with SEM images reported previously [150, 151], showing a mat of continuous nano-fibres before flash-welding and a much smoother film after flash-welding.

2.4.1.1Conductivity Analysis

Conductivities of the flash-welded and non-flash-welded regions of the PANI films on polyimide were measured using a four point probe. The regions of the films that had been flash-welded were outside the range of measurement for the four point probe and it is estimated that these areas have resistivity greater than 10^8 Ω sq^{-1}, indicating complete penetration of the welding through the film. The resistivities of the regions of PANI masked from the flash-welding light remained in the order of 1-10 Ω sq^{-1} which is within the range of semi-conductors.

2.4.1.2Raman Analysis

Raman spectroscopy is a suitable technique to measure the chemical changes in PANI following flash welding, particularly through mapping the first polaron peak at 1215 cm^{-1} and the quinoid ring stretching peaks at 1471 cm^{-1} ($C=N^+$) and 1588 cm^{-1} (C=C) [102, 119] [176, 177]. The peak at 1471 cm^{-1}, due to the $C=N^+$ stretching/bending, becomes more intense when there is more electron movement through this bond, or when there is full conjugation along the polymer. The peak

at 1588 cm^{-1}, due to C=C stretching/bending, is slightly more intense in the PANI-EB because the electron movement is more highly retained in the bonds of the (C=C ↔ C–C) benzene rings along the chain.

The spectra of non-conducting, flash-welded PANI-EB contain less intense peaks at 1215 cm^{-1} and 1471 cm^{-1} while the reduced intensity of the peak at 1588 cm^{-1} (C=C) can be assigned to a reduction of conjugation caused by broken bonds along the polymer chain [119]. The ratio of the intensities between the peaks at 1471 cm^{-1} and 1588 cm^{-1} are expected to be reflected in the conductivities of the films [102, 175]. Figure 2.6 shows an overlay of two Raman spectra taken from the non conductive PANI-EB form and from the conductive PANI-ES form where the differences between the main conductivity indicator peaks can be easily observed.

Figure 2.7 includes an overlay of the intensity profile map constructed from intensity differences between all three main conductivity indicators in Raman spectroscopy (peak intensities at 1215 cm^{-1}, 1471 cm^{-1} and 1588 cm^{-1}) on a photo of the masked-welded interface for a 5.5 μm thick PANI-ES film. The darker, cooler coloured regions indicate the conducting PANI-ES while the lighter, hotter coloured regions reflect the insulating, welded PANI. The interface is quite sharp, indicating that the masking is very effective and very little attenuation of the welding takes place in the masked areas. The interface is less than 15 μm wide, and the precision of this measurement is limited by the 6 μm focal point width of the laser beam used for the measurements. This indicated that flash-welding may indeed be applicable for producing fine conductive patterns from PANI films.

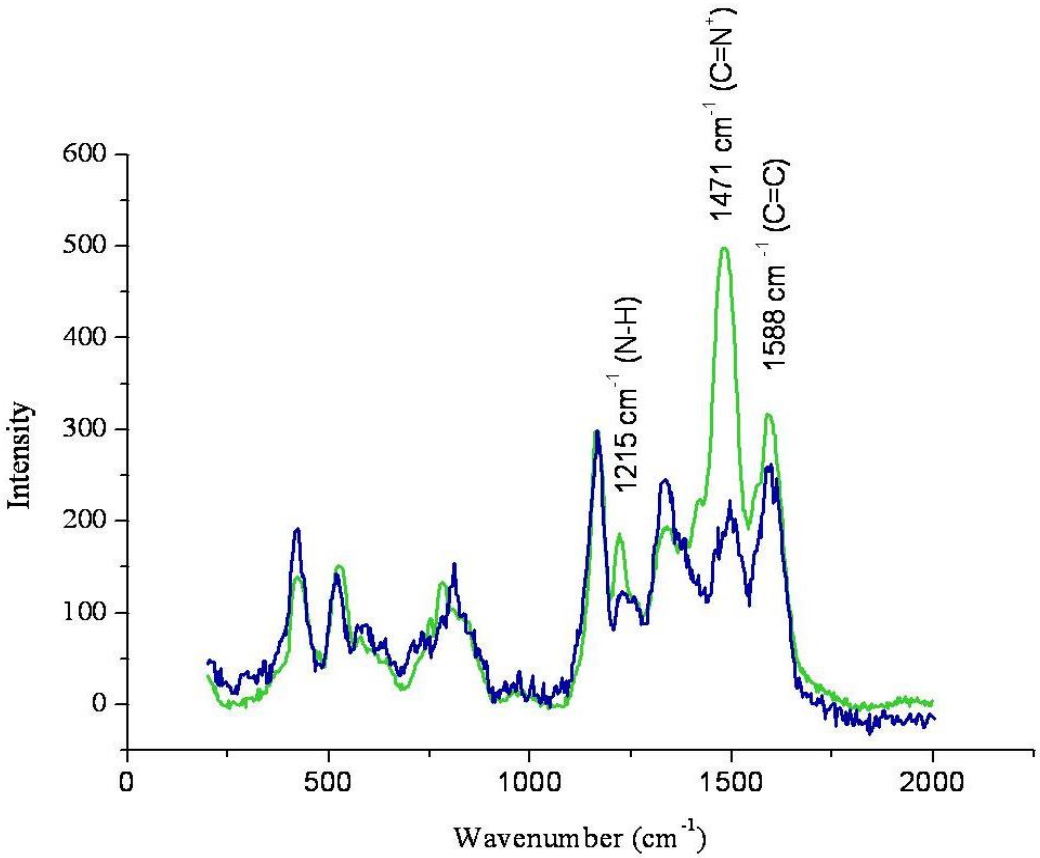

Figure 2.6: Raman spectra of conducting PANI-ES (green trace) and non-conducting PANI-EB (blue trace). These clearly show increased intensity of the first polaron band at 1215 cm^{-1} and the second polaron band at 1471 cm^{-1} in the conducting form.

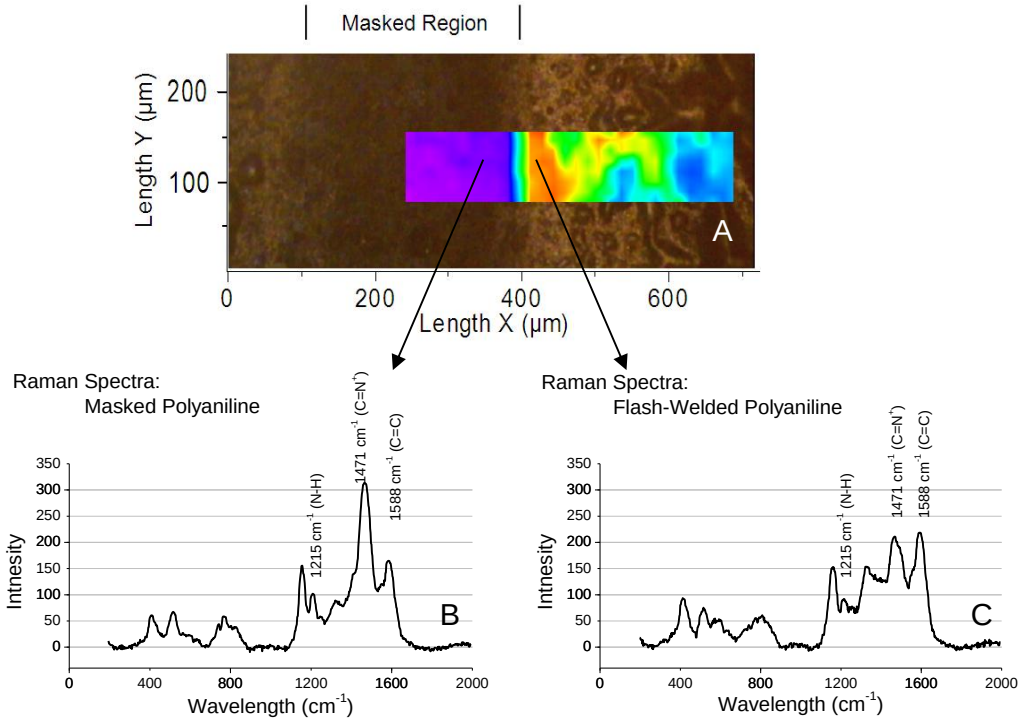

Figure 2.7: A); Raman map super-imposed over an image of a polyaniline film that has been processed by flash-lithography using masking to retain a conductive region. B) Raman spectra of the masked region taken at length X = 387.24 µm. C) Raman spectra of the unmasked region taken at length X = 402.24 µm.

More detail of the individual Raman spectra of the flashed and non-flashed (masked) regions of a PANI-ES film are given in Figure 2.7 (B) and 2.7 (C). The spectrum of PANI-ES (Figure 2.7 B) that was masked contains the high intensity peaks at 1215 cm^{-1} and 1471 cm^{-1} which are characteristic for conducting PANI-ES [175, 177]. The spectrum of the flashed region (Figure 2.7 C) shows less intense peaks at 1215 cm^{-1} and 1471 cm^{-1}, typical non-conducting welded PANI-EB. The peak at 1588 cm^{-1} (C=C) is also reduced. The ratio of the intensities between the peaks at 1471 cm^{-1} and 1588 cm^{-1}, the indicator for the conductivity of the PANI, dropped from almost 3:1 for non-flash-welded PANI-ES to 1:1 for the flash-welded ES confirming the large difference in the conductivity measured using the 4-point probe.

Mapping of films with thicknesses around 2.5 μm showed significant blurring of the boundaries caused by welding under the mask. This can be attributed to the lower number of fibres present in the film, leading to increased energy levels during the flash-welding and consequently attenuation of the welding under the mask. This attenuation is also expected to be enhanced by the thinner layer of PANI being less able to absorb the heat such that it dissipates more through the film. Even with this effect the resolution of the interface between the flash-welded and non-flash-welded regions was around 15 μm. This can be seen as the green region between the conductive blue centre of the Raman map in Figure 2.8 and yellow non-conducting region of the surrounding flash-welded region.

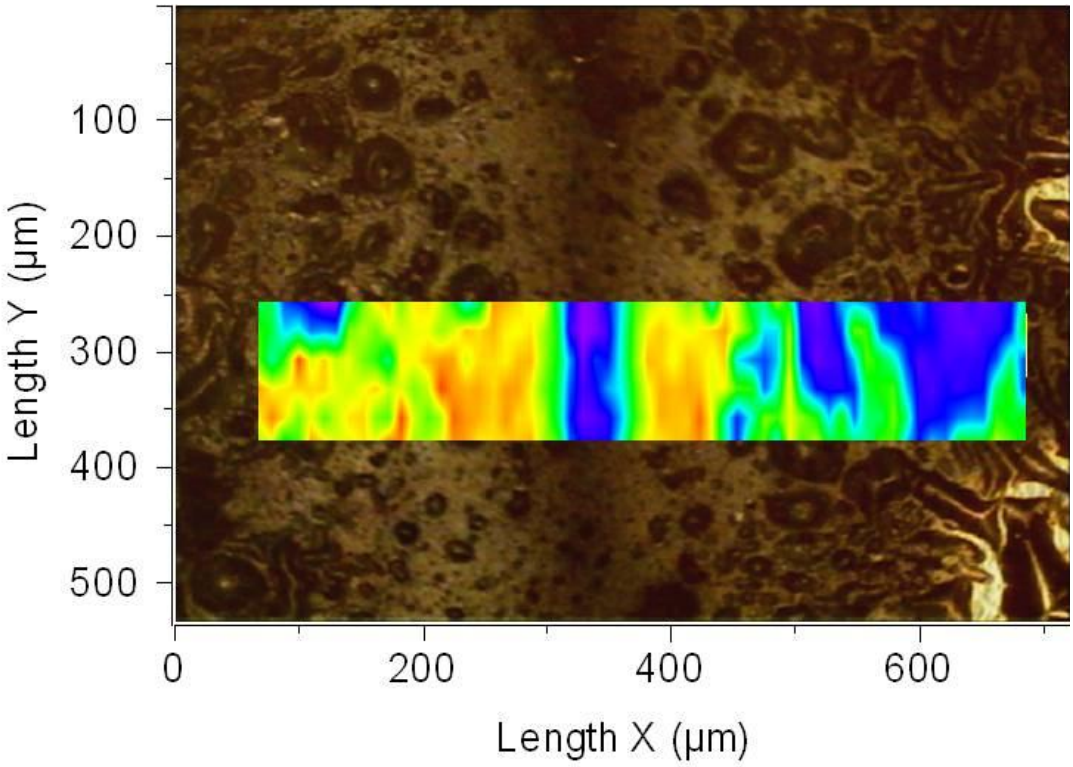

Figure 2.8: Raman map across an electrode wire patterned from a 2.5 µm thick film via flash-welding through a 100 µm mask. The conducting region can be seen to be reduced to 40 µm in width.

2.4.1.3 Wavelength Analysis

Up to this point, welding of polyaniline has only been performed using a broad spectrum light source. To provide a better insight into the flash-welding process, band pass filters transmitting in the wavelength regions of 400-480, 480-570, 560-600, 600-650 and 650-720 nm were placed between the flash and the PANI film leaving a 2 mm gap between the film and the filter during flash-welding. Effective flash-welding was only observed with filters transmitting light above of 570 nm. However, the most effective flash-welding was observed for filters transmitting light above 600 nm. Figure 2.9 shows the results of the flash-welding through the band pass filters with SEMs shown for films flash-welded through 400-480 nm (E) and 600-650 nm (F) filters. It can be seen that the 400-480 and 480-570 nm filters blocked the wavelength of light required for flash-welding and that welding occurred partially through the 560-600 nm filter and fully through the 600-650 filter. This coincides with the absorbance spectra of PANI given in Figure 2.10, where conducting PANI-ES absorbs strongly in the red to infra red regions above 570 nm, which is associated with the polaronic charge carrier ($C=N^{+}$)

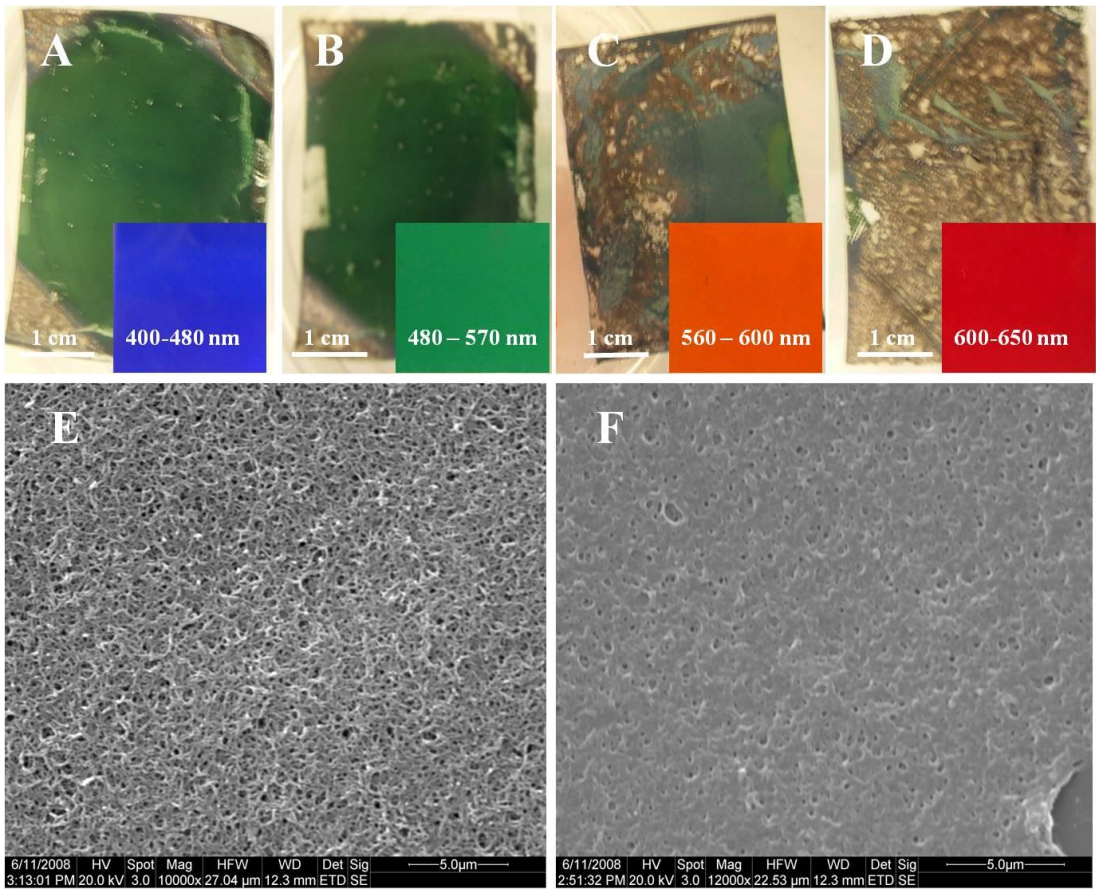

Figure 2.9: Photographs of PANI coated polyacetate flash-welded through band pass filters transmitting at A) 400-480 nm, B) 480-570 nm, C) 560 – 600 nm and D) 600-650 nm. SEMs of PANI after being flash-welded through E) 400-480 nm filter and F) 600 – 650 nm filter.

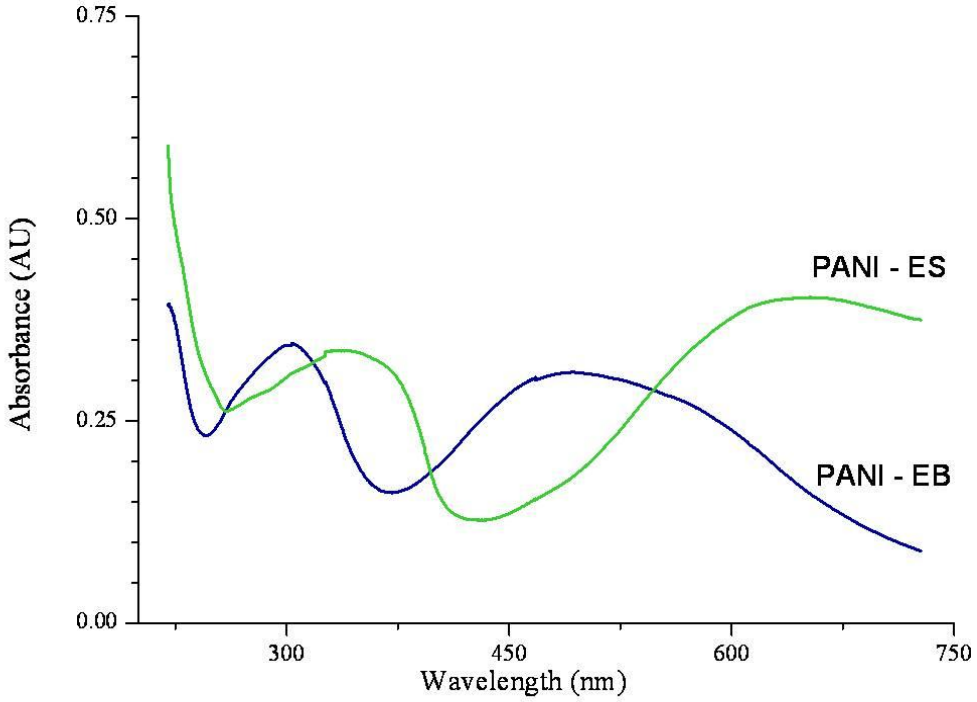

Figure 2.10: Polyaniline absorbance spectra. Green Trace for conducting PANI-ES and blue trace for the non-conducting PANI-EB.

2.4.2 Laser-Welding

2.4.2.1Manual Laser-Welding

The above results indicate that it should be possible to pattern the PANI using a high intensity light source with an output wavelength > 570 nm. To examine this a 4 mW red diode laser (635 nm, laser diode VLM2™, Coherent Laser Division, USA) was focused through a Mitutoyo 50 x Microscope Objective (Japan) onto a PANI coated substrate mounted in a microchip holder attached to a manual xyz stage allowing the PANI film to be moved through the focused laser. Optical microscope (a) and SEM (b-d) images of laser-welding of a 5 μm thick PANI film are given in Figure 2.11. From Figure 2.11 (a) it can be clearly seen that the laser had welded the PANI-ES film. This success led to the development of laser-welding as a replacement for flash-welding with masks.

LED light sources were trialled (Jaycar 100-3319 and 114-1082) as low power alternatives to the 4 mW Laser but were not sufficiently powerful to weld the polyaniline fibres. This led to a return to the 4 mW red laser discussed above for further work.

Laser-welding was initially used to weld a line in the PANI film and its useability examined by forming some basic shapes by manually moving the PANI film through the beam by hand. When the PANI film was moved at a velocity below 100 μm s^{-1}, the film was incinerated at the focal point of the laser in the center of the welded region. Movement of the film at around 100 μm s^{-1} allowed the welding of 10 μm wide lines. This ability to pattern PANI using finely focused light from a 635 nm laser allowed the creation of much finer features with the smallest non-conductive region that can be made being 10 μm in width. This contrasts to the results above using the flash as a light source in which the interface alone was 15 μm wide.

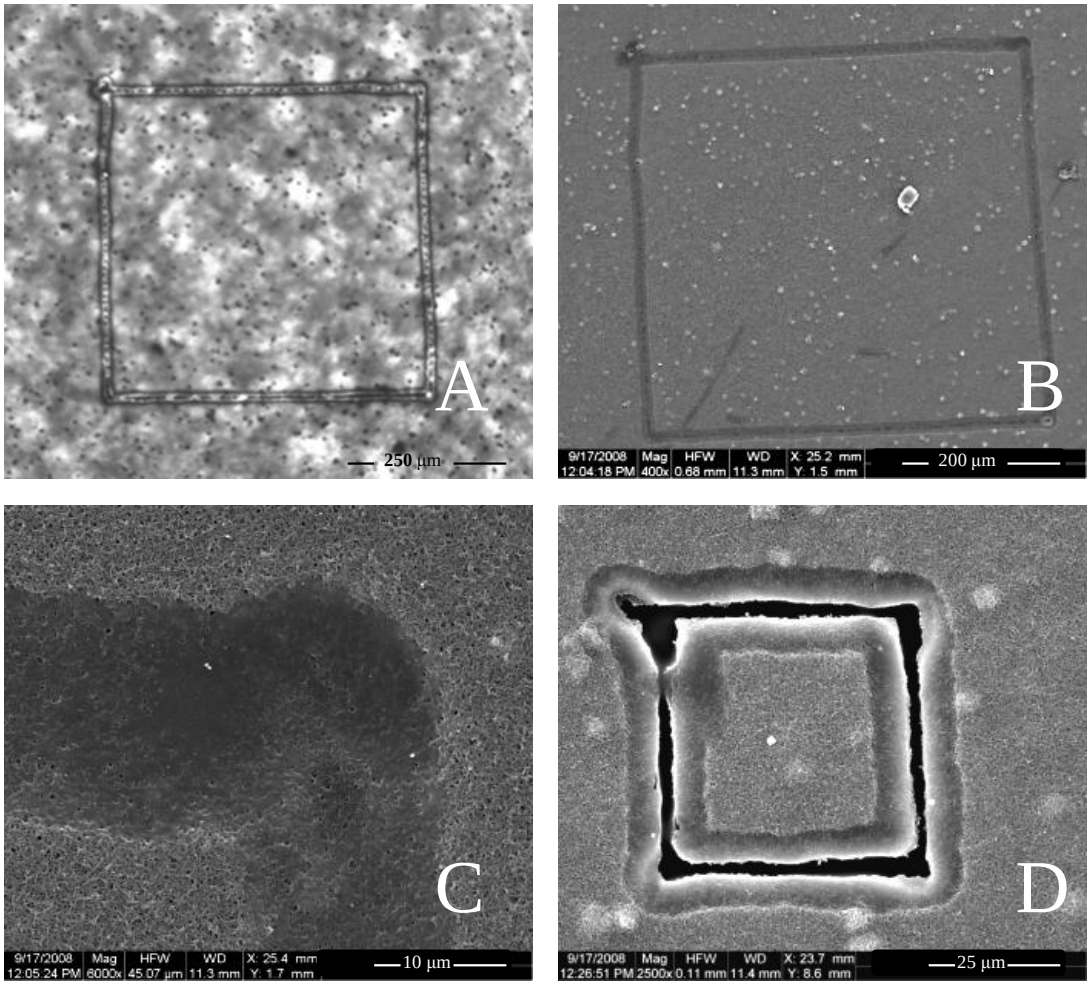

Figure 2.11: Light microscope 100 x magnification (A) and SEM (B, C, D) images of a PANI film that has been manually laser-welded with a 4 mW laser.

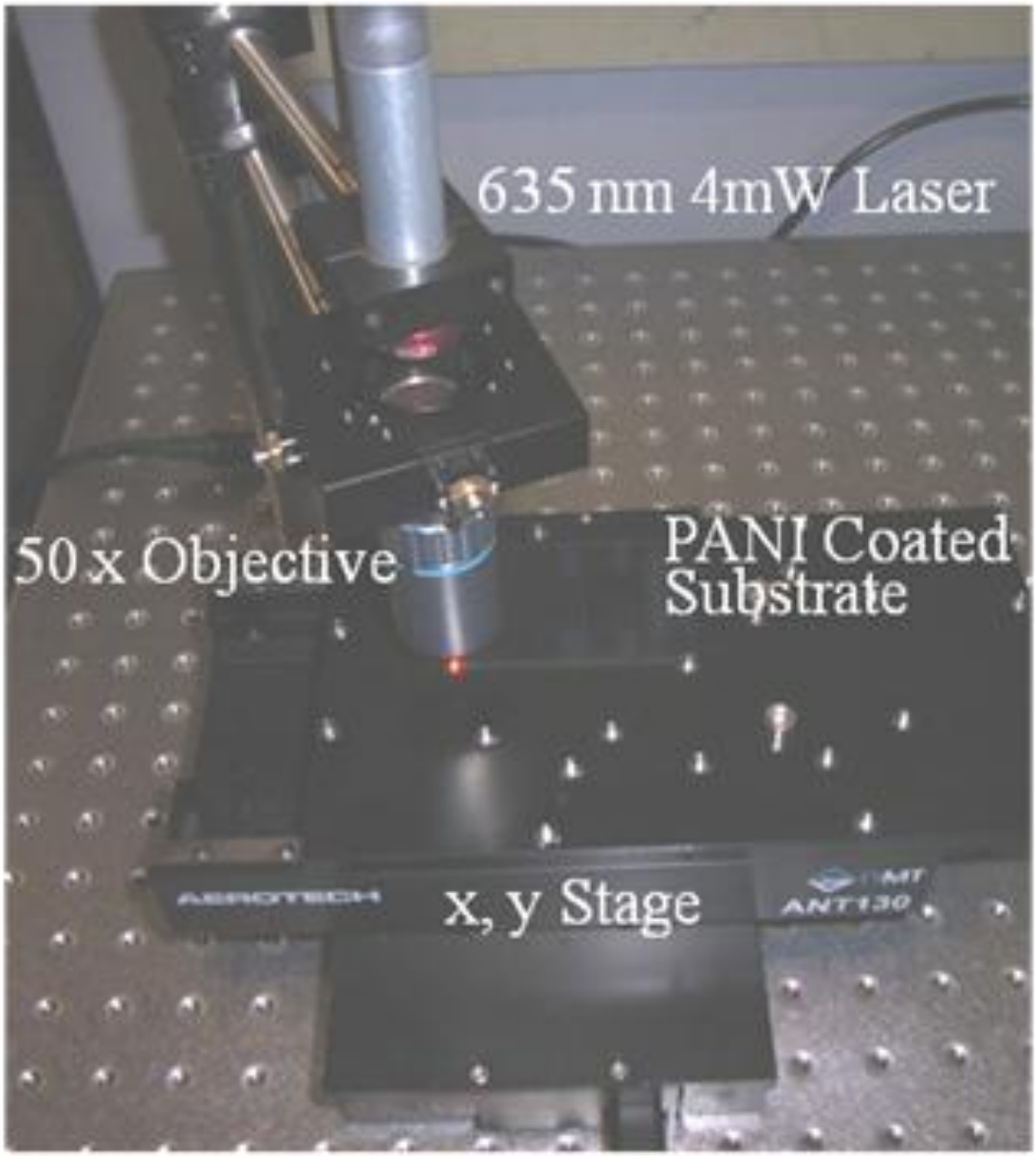

Figure 2.12: The experimental set up of the automated laser welding process.

2.4.2.2Automated Laser Welding

To make more complex patterns, the laser was mounted above a high precision computer-controlled stage (Aerotech ANT130). This setup is shown in Figure 2.12. The stage notionally allows for the creation of much finer conducting regions than 10 μm because of the 2 nm step size and ± 15 nm mm^{-1} repeatability of the stage. Substrates were moved under the focused laser using the stage at speeds from 1 mm s^{-1} to 20 mm s^{-1}. The stage could be programmed to operate for up to 24 h.

To optimise the laser welding process a range of speeds at which the PANI film moved under the focused laser were trialled, with the optimum speed being the fastest operating speed that the laser is able to weld through the entire thickness of the film. This was evaluated by checking for conductivity decreases across the welded lines with those lines not penetrating the entire film having no or very little reduction in the conductivity measured. Figure 2.13 shows a SEM of the laser-welded lines produced whilst increasing speed from 0.5 mm s^{-1} (bottom line) in 0.5 mm s^{-1} intervals. The optimal speed was found to be 5 mm s^{-1} since at speeds greater than this the welding became unreliable in fully welding the PANI film. However, speeds of 4 mm s^{-1} or slower were just as effective at producing the same width of 10 μm the centre of those welded regions were fully burnt away by the laser as described and shown above.

The disadvantage of this approach is the time required to fully pattern a device. It would take 20 h to fully weld a single 5 x 7.5 cm substrate when laser-welding at 5 mm s^{-1}. In an attempt to increase the width of the lines welded, the laser was defocused slightly to give a wider diameter spot on the PANI film. However, this resulted in the welding not penetrating the entire PANI film and no increase in the width of the welded regions.

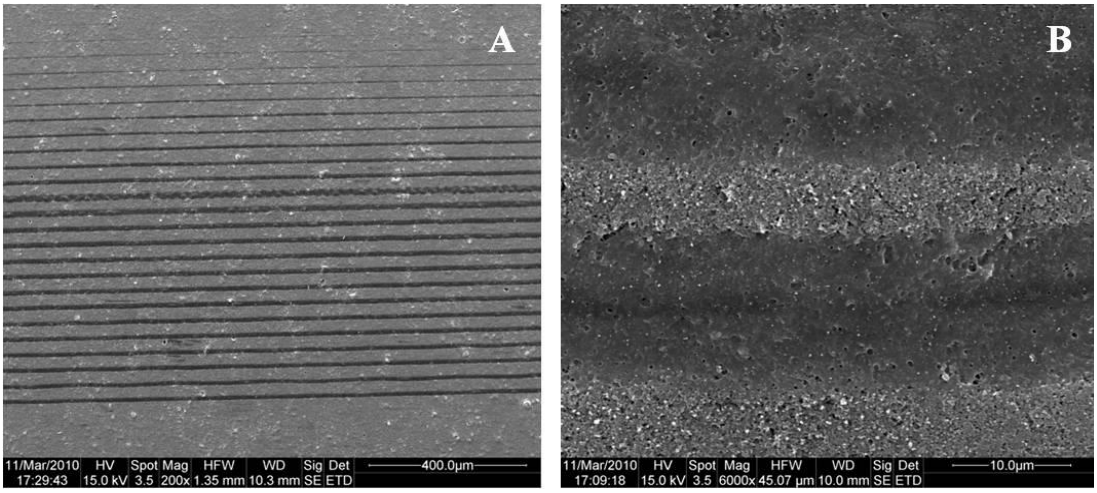

Figure 2.13: A) SEM of lines-welded with increasing speed, starting at 0.5 mm s^{-1} (bottom line) and increasing by 0.5 mm s^{-1} with each new line B) SEM of two laser-welded lines with centres 15 µm apart leaving a 5 µm non-welded region.

Because of the possibility of producing conducting regions less than 10 μm in width it was necessary to determine how narrow a conducting strip could be left without significant loss of conductivity. To determine this a 2 mm wide conductive strip of 3.6 μm thick PANI was continually narrowed by 10 μm using laser-welding and the resistivity monitored in real time to generate a plot of resistance against un-welded line width. Since resistance should have a linear inverse relationship with line width Figure 2.14 shows the plot of resistance against the inverse of the line width.

It can be seen from the plot that there is an inverse relationship between resistivity and line width of the PANI region with the resistivity increasing dramatically once the line width was reduced to below 500 μm. Once the line width had been reduced to below 100 μm the resistivity had increased above 10 MΩ cm^{-1} and into the insulating region of conductivities. This showed that there is a significant limitation of line width to conductivity and hence all the following work was done using laser-welded patterns with line widths of 500 μm or higher to maintain a reasonable level of conductivity. It is likely that thicker films of PANI would overcome this limitation, but this was not examined.

2.5 Polymer Printing

Direct printing of PANI onto a suitable substrate was trialled as an alternative to laser-welding for the production of large numbers of patterned PANI films. Printing was done using a syringe with a 200 μm diameter tip that was positioned within 50 μm of the substrate and filled with polymer solutions. The substrate was mounted on an automated xyz stage that was moved at 6 mm s^{-1} once the syringe was in place.

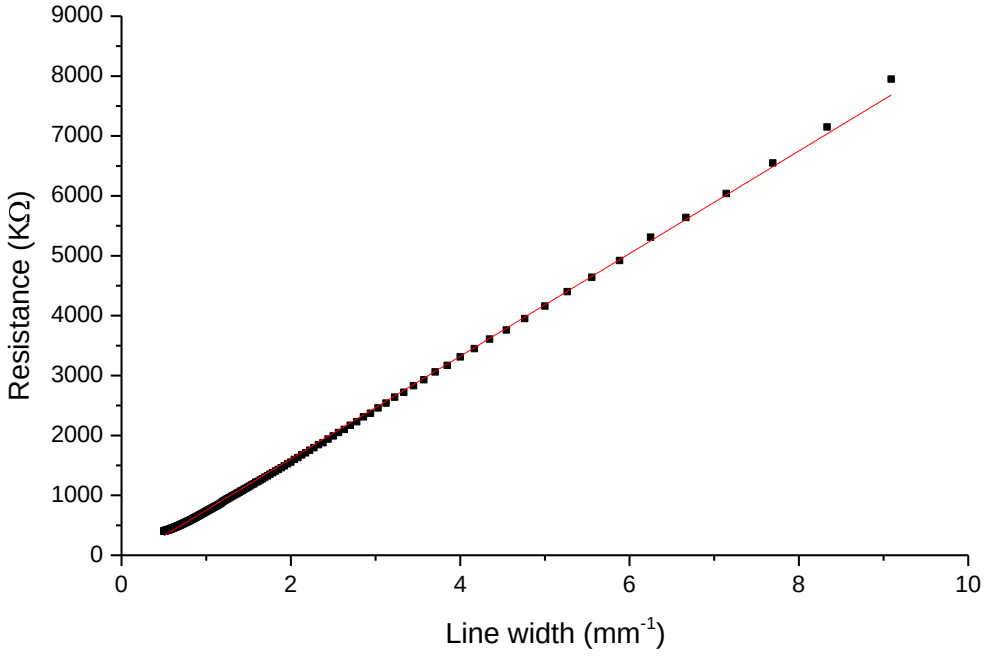

Figure 2.14: A plot showing the increasing resistance with line width^{-1} of a 5 cm long conducting PANI line. An $R^2 = 0.998$ shows a good linear fit.

2.5.1 Extrusion Printing

Extrusion printing was the first type of printing examined. The syringe contained concentrated 10 g L^{-1} solutions of either PANI or an alternative conducting polymer, poly(3,4-dioctyloxythiophene)/poly(4-styrenesulfonate) PDOT/PSS. A pressure of 4 psi was applied whilst the stage was moving to force the polymer solution out of the syringe and onto substrates of either glass or PVC. Figure 2.15 shows the resultant lines of PANI and PDOT/PSS, respectively. From the figure it can be seen that there is widening at the end of the lines forming a bulge that reduces the resolution. This bulge was unavoidable using this method of printing because stopping lateral stage movement and lowering of the substrate could not be done simultaneously, leading to a larger actual time period of printing at the ends of the lines. The maximum resolution that could be consistently achieved had a 500 μm gap between the lines of extruded polymer. Images of the PANI also clearly show severe cracking caused by the agglomeration of the fibres in such high concentration while drying. This was similar to observations when casting larger concentration suspensions of the polymer.

2.5.2 Capillary Force Printing

Capillary Force printing was similar to extrusion printing with the syringe close to the substrate but, in this case, with no pressure applied to force the solution from the syringe. This required more dilute, less viscous solutions of 2 g L^{-1} polymer. In this case the bulge at the end of the syringe tip would make contact with the substrate surface, and as the substrate moved the polymer suspension would be dragged out of the tip forming a line. Figure 2.16 shows the results of capillary force printing PANI and the conducting polymer, poly-2-methoxyaniline-5-sulfonic acid (PMAS), on PVC and photo paper. This was also attempted on glass but the surfaces of the glass microscope slides were not

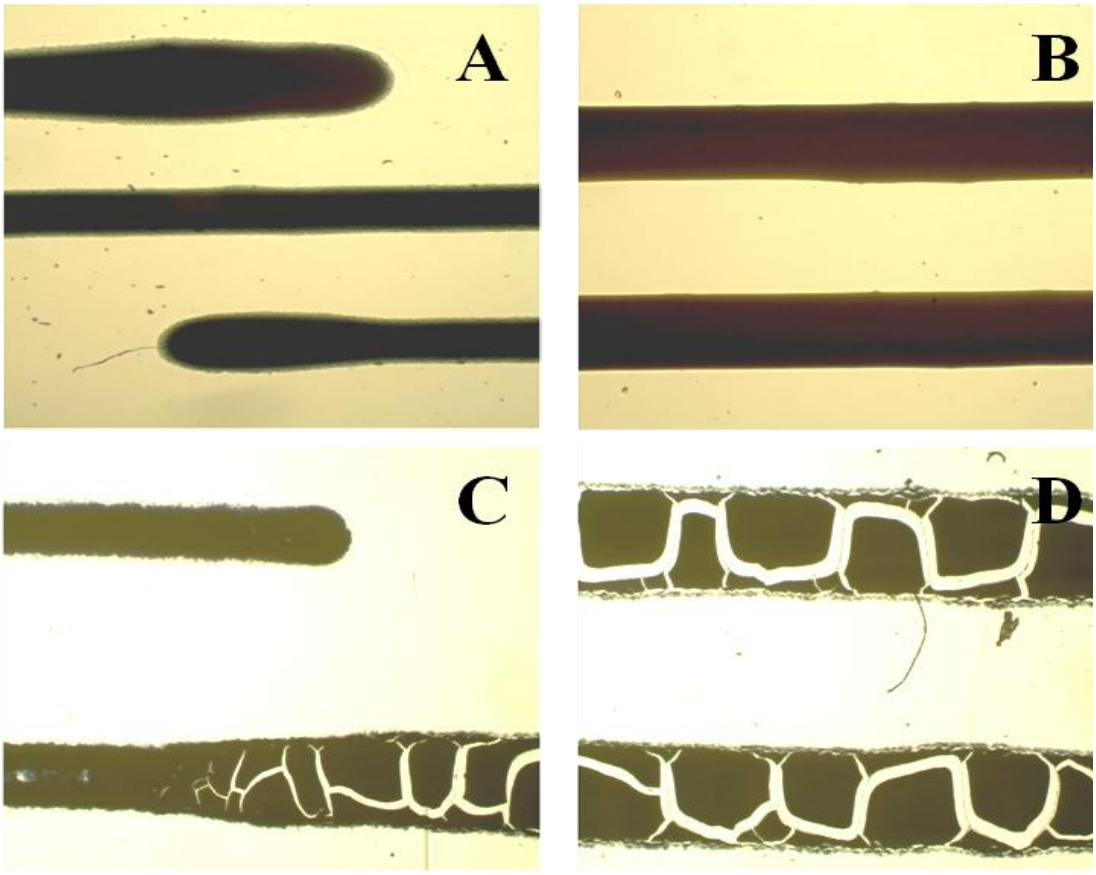

Figure 2.15: Microscope images of extruded A, B) PDOT/PSS and C, D) PANI.

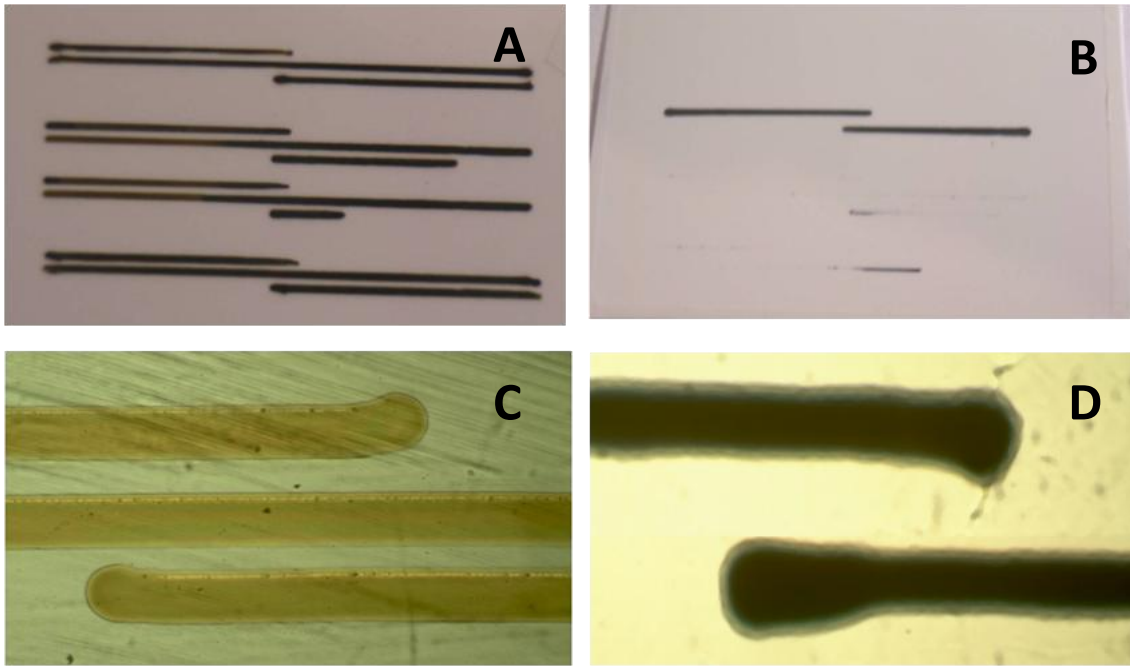

Figure 2.16: Photographs of capillary force printed PMAS (A) and PANI (B) onto photo paper. Microscope images of PMAS (C) and PANI (D) onto polycarbonate.

sufficiently flat so the syringe would often catch or scratch the glass, or move too far away from the surface for the capillary forces to withdraw the solution from the needle. When using more flexible substrates, such as PVC, the syringe could push down a little into the substrate without catching. Although this is not optimal, straight lines could still be formed. It can be seen in figure 2.16 that the results were similar to extrusion printing in that the ends of the lines of the printed polymers broadened, again reducing the resolution.

Although straight lines could be formed using both extrusion and capillary force printing the resolution was limited to hundreds of µm, far greater than that of laser-welding.

2.6 Conclusions

The drop casting method for producing PANI films was shown to reliably produce consistent films of 1.8 µm - 14.4 µm in thickness, dependent on the number of coats applied. These were then used for studying flash-welding as a photolithographic processing technique for PANI. The efficiency of the flash-welding process was enhanced through the use of polymeric substrates, enabling flash-welding of PANI films with thicknesses ranging from 3.6 to 14.4 µm. Partial masking of the PANI films during flash-welding enabled the formation of adjacent conducting and insulating regions, since the welding changes the electrical properties of the film.

Raman spectroscopy was used to determine the sharpness of the masked edges and the interface between the flash-welded and masked regions of the PANI films patterned by flash-welding, with an interface region of less than 15 µm wide observed. Although the interface regions for PANI films patterned by flash-welding the technique was shown to be relatively crude and destructive.

Through a study of the wavelength of light required for performing flash-welding, wavelengths above 570 nm were found to be largely responsible for the welding process, fitting well with the absorbance spectra of PANI-ES. This eliminated the necessity of a broad spectrum output such as a studio flash for flash-welding. A 635 nm laser diode was used for welding PANI, introducing welding of PANI using narrow wavelength light-sources. With the use a precision xy stage, laser-welding was shown to be able to accurately produce insulating regions and conducting regions each down to 10 μm in width.

Other patterning techniques of extrusion printing and capillary force printing were also examined with neither producing the same level of precision or reproducibility as laser-welding, although these techniques could be useful for patterning other conductive polymers.

Laser-welding has been shown to be an effective technique for producing simple electrode patterns within PANI films. However, it is the discovery of laser-welding as a platform to produce fine and complex electrode patterns in PANI films that could lead to a wide range of applications similar to those of conventional metal circuitry.

3. Microfluidic Electrophoresis Devices

3.1 Introduction

In recent times, there has been a strong trend towards developing more highly integrated microfluidic devices for a range of LOC applications [1, 180, 181]. The most significant applications are in the biomedical and life sciences area where there is a strong demand for portable and/or disposable microchips compatible with miniaturised analytical instrumentation for field analysis and POC diagnostics [182-184]. For these applications, LOC devices must be sufficiently cheap for single use, which eliminates most microchips made using expensive manufacturing processes and/or using expensive substrates like glass and quartz. This has led to significant research in the realm of materials science where polymers have become very popular because of their low cost and compatibility with mass replication manufacturing techniques, such as injection moulding and embossing. Although polymer microfluidic devices themselves may be made for a fraction of a cent, the integration of more components during their construction and the incorporation of electrodes often adds significantly to the duration and cost of the production process [35, 181].

Metal electrodes are typically deposited using physical vapour deposition techniques like sputtering and evaporation or by electroplating and are patterned by etching or by using a lift-off process. Many methods to develop cheaper electrodes for integrating into microfluidic devices have been, and are, continue to be explored and developed. These methods include the use of semiconducting films such as indium tin oxide to produce micro scale electrode structures [185]. Recently, an inexpensive process to integrate ion chromatography with microfluidic systems based on standard PCB technology was proposed [186].

Even these techniques produce disposable LOC devices that are still ten to a hundred times the cost required for a truly disposable device.

Conducting polymers have been shown to be a cheap alternative material to metals and other semiconductors [87]. The integration of polymer electrodes into microfluidic devices has the potential to significantly reduce the costs of integrated devices if the processing costs are kept low. Processing techniques used for the deposition of polymer electrodes include ink-jet and screen printing. Despite the capability of producing basic conducting structures, these printing techniques are slow and require highly specialised instrumentation [187, 188].

In Chapter 2 it was shown that PANI may be a suitable cheap alternative material that is easily patterned and may be suitable for use as high voltage electrodes. PANI has not previously been used for high voltage applications, but only as an alternative to metals for electrochemical detection in various analytical systems [181]. The use of PANI as high voltage electrodes to apply the potentials required for electrophoretic separation requires the conducting polymer to carry a significant current under application of several hundred to thousands of volts.

This chapter describes the development of a fully polymeric microchip with integrated PANI electrodes suitable for performing microchip electrophoresis. The polymer electrodes were fabricated in thin films of PANI patterned by flash lithography as described in Chapter 2. Highly efficient separations comparable to those achieved in similar microchips using platinum electrodes confirm the potential of PANI as a new material suitable for high voltage electrodes in LOC devices.

3.2 Manufacturing

Microfluidic devices were manufactured in two parts. The top half of the microchip contained the channels and reservoirs in a standard cross geometry

required for performing an electrophoretic separation in a microchip. The bottom base contained the integrated PANI electrodes.

3.2.1 Development of PDMS Microfluidic Channels

Microfluidic structures with depth and width of 50 μm in a simple cross design were made by casting polydimethysiloxane (PDMS, Sylgard 183, Dow Corning, USA) on a SU-8 template. Three channels were 20 mm ± 2 mm long from their reservoirs to the cross and one channel was 40 mm ± 2 mm long from reservoir to cross. This approach closely followed the standard methods described previously [19, 58], however, this section describes the specific approach used in this work.

3.2.2 SU-8 2010 Masters

SU-8 masters were created as moulds for casting PDMS microchips. The procedure for the development of SU-8 2100 (SU-8 2100, Michrochem, USA) masters was adapted from the SU-8 2000 manufacture process guidelines and previous research. The fabrication of the masters was conducted in a Class 1000 clean room to prevent dust and other small airborne particles from affecting this micro-engineering process.

3.2.3 Spin Coating

The photoresist, SU-8 2100 was spin coated onto silicon wafers (100 mm diameter, 525 +/- 25 μm thickness, single side polished, test grade, SWI Semiconductor Wafer Inc, Taiwan). This was done using an 8'' Portable Precision Spin Coater (Model P-6204, Cookson Electronics Equipment, IN, USA). The wafers were centred, polished side up, on the spin coater's vacuum chuck and held in place via vacuum suction. 10-20 ml of SU-8 was poured onto the centre of the wafers and spin coated for 25 s at 500 rpm followed by 25 s at 6000 rpm.

3.2.4 Pre-exposure Bake

Directly after spin coating, the wafers were baked on an ECHOtherm™ HS40 programmable hot plate (Torrey Pines Scientific, San Marcos, CA, USA) for 50 min at 110ºC with a 10 min ramp from 50ºC to 110ºC. The wafers were left on the hot plate to cool slowly to room temperature before the photolithography process.

3.2.5 Photolithography

The SU-8 coated wafers were taken from the hot plate, covered with a negative mask (Kodak Polychrome Image-setting film Pagi-Set, 4400 dpi, Pagination Design Services, Geelong, Australia) and placed in the exposure system. The apparatus used for the exposure of the wafers was a deep UV (DUV) lamp (OAI deep UV illumination system, Model LS30/5, San Jose, CA, USA), fitted with a 500 W HgXe-lamp (Ushio, Model UXM-501MA, Japan). Exposures were carried out at a constant intensity of 20.0 mW/cm^2. Three 5 min exposures were carried out with 10 min rest time between each exposure. The wafers were exposed to 400 mJ/cm^2 of 260 nm UV light.

3.2.6 Post Exposure Bake

After exposure the SU-8 was baked at 110ºC for 13 minutes on the hot plate with a 2 min ramp from 50ºC to 110ºC. The wafers were then allowed to cool slowly to room temperature on the hot plate.

3.2.7 Development of the Master

The unexposed SU-8 was dissolved by placing the wafers into a bath of developer solution (SU-8 Developer, Microchem, USA) for 5-10 min. This bath was on a gyro-rocker (Stuart® Scientific Gyro rocker, Model STR9, Bibby Sterlin Ltd.,

Staffordshire, United Kingdom) set at 20 rpm. The wafers were then rinsed by pipette with clean developer solution for 1 min. The developed wafer was then rinsed with isopropanol and dried under a stream of nitrogen.

3.2.8 Hard Bake

The SU-8 was cured by heating for 30 min at 200ºC on the hot plate and was ready for use as a master after being allowed to cool to room temperature on the hot plate.

3.2.9 Casting PDMS

Microchips were fabricated from poly(dimethylsiloxane) (PDMS). For a single chip, 50 g of the elastomer and 5 g of curing agent (Sylgard 184 elastomer kit, Dow Corning, Michigan, USA) were thoroughly mixed in a beaker. The beaker was then placed in a vacuum desiccator for 2 h to degas the PDMS. With the air bubbles removed, the PDMS was poured over the silicon or quartz master in a plastic petri dish (150 × 20 mm, Sarstedt Australia Pty. Ltd, Technology Park, South Australia). The PDMS was cured by placing it in an oven at 80ºC for 60 min. The master was then cut from the dish with a scalpel and the PDMS chip was cut out and peeled off the master.

3.3 Integrating Polyaniline into the Microfluidic Devices

While PANI has been used for many years in electrochemistry, particularly as detection electrodes, no report could be found on its ability to function as an electrode material for use in electrophoresis. To manufacture PANI high voltage carrying electrodes 5 µm thick films of PANI were made on 2 mm thick acrylic substrates. These films were then doped by dipping into 1M HCl to convert the PANI from the non-conducting PANI – EB to the conducting PANI – ES form and left to dry overnight. A small area of the PANI film was then removed by

scraping with a scalpel to create a window for optical detection. The remaining film was patterned using Flash Lithography.

3.3.1 High Voltage Capabilities

Studies of the PANI electrodes were undertaken to determine whether they could effectively handle the current that would be required in electrophoresis. To do this, a number of PANI "wires" were constructed and the ends were directly connected to the high voltage power supply. In these experiments, there was no microfluidic chip on the electrodes and the conducting regions of the PANI film provided the only conductive pathway for the current to flow. Application of 150 V producing an initial field strength of 50 V cm^{-1} resulted in currents greater than 300 μA. This slowly decreased by approximately 30% during the first minute of usage.

The same trend was observed when applying higher voltages of 450 V and 750 V (field strengths of 150 and 250 V cm^{-1}) although higher currents were recorded. After the initial decrease in conductivity of the PANI strips the currents remained stable for a minimum of 10 min as shown in Figure 3.1. The initial decrease in current could be attributed to the initial loss of moisture from the PANI electrodes as they heated up with the current flow. It is important to note that the currents obtained here are about ten times higher than those realistically expected to be used for microchip electrophoresis and these results support the concept of PANI high voltage electrodes.

3.3.2 High Voltage Electrodes

Although the Raman analysis, described in Chapter 2 showed good resolution of the flash-welding process, this was carried out over a restricted area much smaller than a whole 5 cm x 7.5 cm substrate. When applied to the whole substrate the

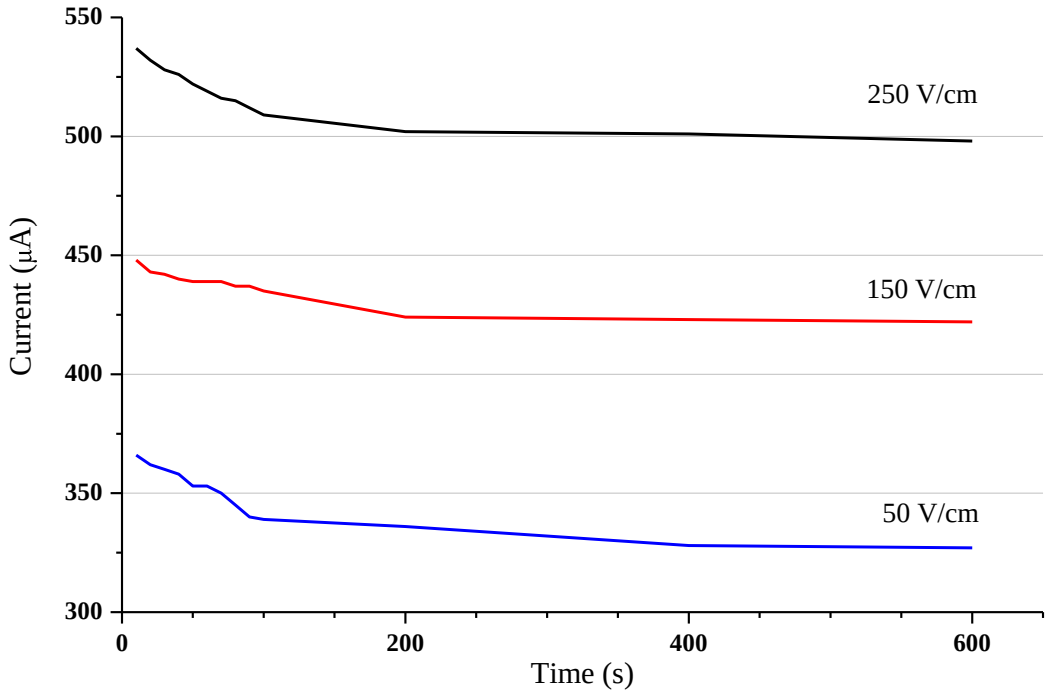

Figure 3.1: Currents recorded over time with high voltage applied to wires of PANI. The PANI wires were 500 μm wide, 4 μm thick and 3 cm long.

process of flash-welding was quite crude, with the exposed areas often burning or causing some of the PANI film to explode off the surface of the substrate. The crudeness of the technique was accentuated by multiple flashes being required to fully pattern an entire 5 cm x 7.5 cm film of PANI. Furthermore flash-welding was found to also deliver uneven levels of welding and destruction across the film for each flash. To pattern the high voltage electrodes, a mask was developed using black electrical tape on polyacetate that was then cut into the desired electrode shape. A total of 5 flashes were required to fully pattern the PANI films, moving the masked film 1 cm at a time under the flash. During flash welding the PANI fibres fused to the acrylic substrate, while the non-exposed, conducting regions that form the electrodes remained relatively fragile and weakly bound to the substrate.

3.3.3 Laminating with Dry Film Resist

In initial experiments to form the microchips with integrated PANI electrodes, the PDMS microchannels were placed directly on the lithographically patterned PANI films. However, as the PANI film consists of a network of interwoven nanofibers, it is porous and leakage was observed along the microchip once the microchannels were filled with BGE. PANI fibres from the conducting region were also pulled off the acrylic substrate when removing the PDMS from the electrode plate, destroying the PANI electrodes.

To overcome these limitations a 30 μm layer of dry film photoresist (DFR) Ordyl SY330 (Elga Europe, Italy) was used to cover the patterned PANI. The DFR was applied by lamination at 40^0C. This covered the porous PANI, making a smooth surface forming the bottom of the channels in the microfluidic device. The DFR was chosen because it could then be lithographically patterned to allow direct contact between the electrolyte and sample solutions in the reservoirs with the PANI. This was done using a Shark exposure system through a transparency

mask [189]. The exposure time of the system was 3 min after which the DFR-covered-PANI-coated substrate was baked at 110^0C. The DFR was then developed in solution for 1 min to remove the DFR from where the PDMS reservoirs would be placed above the PANI electrodes. This patterning of the DFR facilitated the contact required between the electrolyte in the reservoirs and PANI electrodes.

3.3.4 Fully Polymeric Microfluidic Devices

The fully polymeric microfluidic devices were comprised of a PDMS layer containing the microfluidics in a standard cross design (three of the channels were 1.5 ± 0.2 cm long and the separation channel was 5.0 ± 0.2 cm long), as shown in Figure 3.2. Reservoirs were made in the PDMS using a hole punch and the PDMS substrate was placed channel facing down onto the DFR, aligning the reservoirs with the PANI electrodes.

The PDMS layer was cleaned thoroughly before being placed onto the DFR by sonication in 1 M NaOH for 30 min. This was followed by sonication in HCl for 30 min and finally in Milli Q water, before being dried in an air stream. A cross sectional schematic of the microchip is shown in Figure 3.2 B. The substrates were stored for up to one week in a petri dish before being used. A photograph of a fully assembled polymer microchip is shown in Figure 3.3. Alligator clips were used to connect the PANI electrodes to an in-house built high voltage power supply.

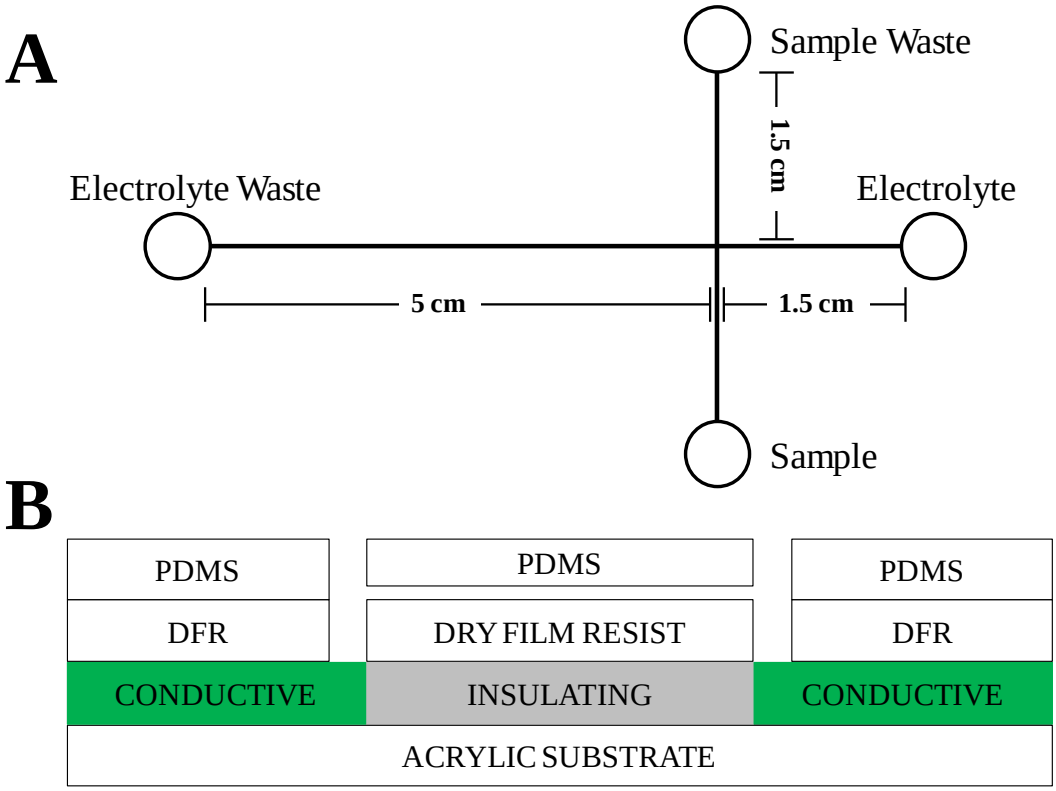

Figure 3.2: A) Schematic of the microfluidics contained within the device including channels and reservoirs. The reservoirs have been labelled in accordance with the solutions they will contain during microchip electrophoresis.

B) Schematic cross Section of the four layer microfluidic device (The figure is not to scale).The acrylic substrate was 1.5 mm thick, the PANI film 4 μm thick, the dry film resist 30 μm thick and a 50 μm high channel was incorporated in the 5 mm thick PDMS substrate:

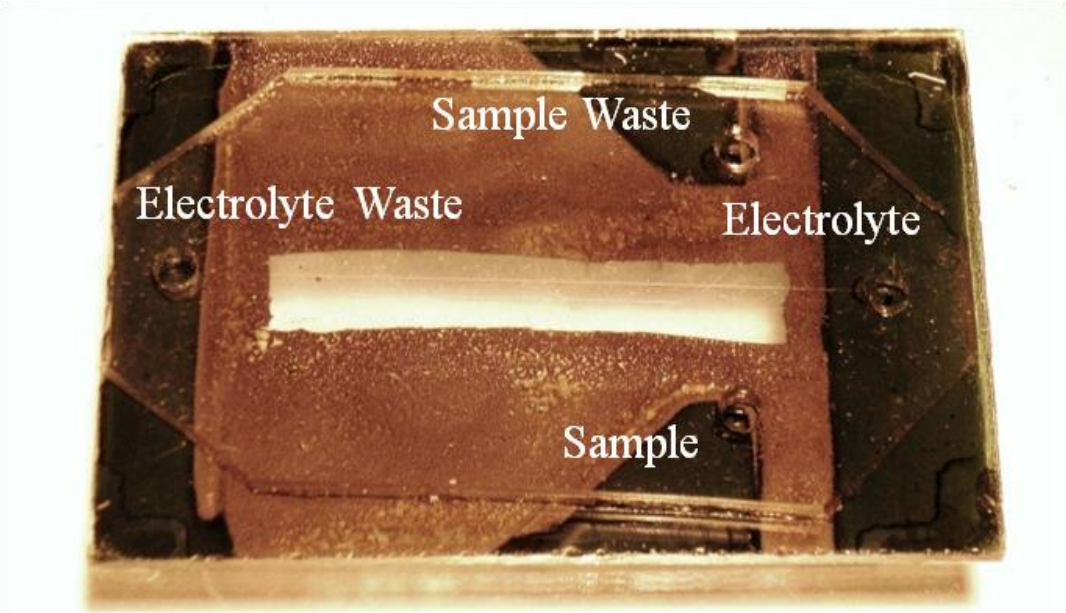

Figure 3.3: Photograph of a 7.5 cm x 5 cm x 0.5 cm full polymeric microfluidic device for electrophoresis with the reservoirs labelled. Electrolyte, Sample and Sample Waste reservoirs are 1.5 cm from the injection cross; Electrolyte Waste is 5 cm from the injection cross.

3.4 Microfluidic Electrophoresis

3.4.1 Experimental

The chemicals used for the preliminary analysis and application of the microfluidic electrophoresis devices developed in this chapter are given in Table 3.1

3.4.1.1 Preparing the Microfluidic Devices

The PDMS layer of the microfluidic devices used in this chapter was cleaned prior to use by sonication in a 1 M NaOH bath for 10 min followed by sonication in a 1M HCl bath for a further 10 min. The PDMS layer was then washed by sonication in a water bath for 10 min before being rinsed under running water and then dried under a stream of nitrogen.

Between runs the microfluidic channels were rinsed with 1 M HCl for 10 min via vacuum, generated using an empty syringe to suck to the Electrolyte Waste reservoir from the remaining reservoirs. This was followed with a 10 min water rinse using the same approach before the channels were filled with air for storage. Prior to use each device was rinsed with BGE for 10 min before the chip was filled with fresh BGE.

Before use each of the reservoirs was emptied by pipette and the Electrolyte, Electrolyte Waste and Sample Waste reservoirs were refilled with 35 µL of BGE. The Sample reservoir was filled with 33 µL of sample solution.

3.4.1.2 Optical Detection System

Optical detection was chosen as the detection method used to determine the performance of the electrophoresis chips because of the flexibility and frequent use of this technique with the microfluidic devices.

Table 3.1: The chemicals used during microchip electrophoresis.

Chemical	Abbreviation/Formula	Purity	Manufacturer
8-aminopyrene-1,3,6-trisulfonic acid	APTS		Sigma-Aldrich, USA
camphorsulfonic acid	CSA	98+%	Fluka (Switzerland)
glucose		99+%	Sigma-Aldrich, USA
hexa-dimethrine bromide	HDMB	99+%	Sigma-Aldrich, USA
hydrochloric acid	HCl	AR	Ajax Chemicals, AU
hydroxy propyl cellulose	HPC	98+%	Sigma-Aldrich, USA
lactose		99+%	Sigma-Aldrich, USA
maleic acid		99+%	Fluka, USA
maltose		99+%	Sigma-Aldrich, USA
sodium fluorescein			
sodium hydroxide	NaOH	98+%	BDH Chemicals

Optical detection was performed using a LED induced fluorescence detection system described previously [58]. A schematic of the experimental optical detection setup is shown in Figure 3.4.

The chip was mounted in a chip-holder that could be manoeuvred in the x, y and z planes to allow focusing of the LED beam on any part of the microfluidic device. The device was connected to a programmable 4-channel in-house built HV power supply using alligator clips. Refocusing was required every time the device was remounted, including for flushing between runs and for full cleaning of the PDMS.

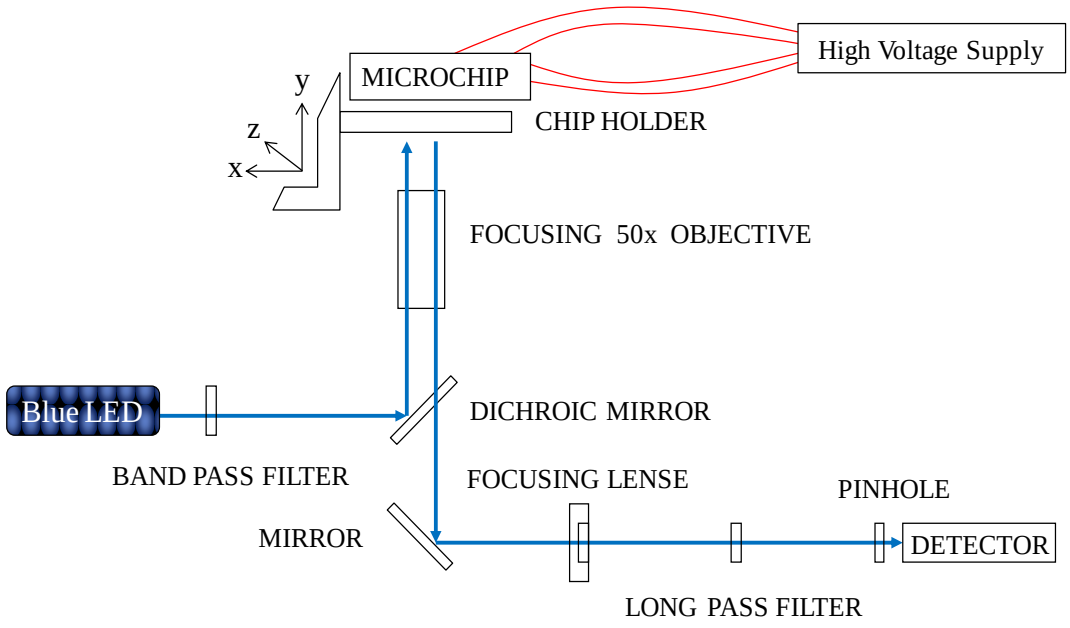

Figure 3.4: Schematic of the optical detection system showing microfluidic chip with integrated high voltage electrodes connected to the power supply and mounted above the optics.

3.5 Preliminary Analysis

The next stage involved using the PANI electrodes in the microfluidic device to confirm their suitability to apply high voltages as required for electrophoresis. The main limitation of using PANI as an alternative to metal electrodes is that it must remain in the acid doped conducting PANI – ES form. Ideally, the BGE should be at a pH of between 1 and 3, but this would significantly reduce the practical use of PANI electrodes for electrophoresis. A number of BGE studies were undertaken at different pHs, ranging from pH 4.5 to pH 7.5. The microchannels were filled with BGE and 1000 V was applied for 10 min. For buffer pH levels > 6 the currents decreased continually throughout the experiment, corresponding to de-doping of the PANI at the wells most likely cause by the movement of hydrogen ions away from the PANI fibres into the surrounding buffer and towards the negative electrode. Colour changes from green to purple were observed in the PANI electrodes after the experiment, confirming the de-doping of PANI at the wells. It was found that a pH < 6 did not rapidly de-dope the PANI due to the higher concentration of hydrogen ions and could therefore be used for electrophoresis. The buffer chosen for undertaking the initial experiments was 50 mm malic acid (pH 5.5).

In the initial experiments, only one analyte was used (fluorescein). The first experiment was to verify the sample loading step by the detection of fluorescein at the injection cross of the microfluidic device. Within 1 min an increase in the signal confirmed the migration of fluorescein through the microchannels. In the next stage the cross injection was verified by focusing the detection system on the separation channel. The HV power supply was programmed to run a sequence of sample loading (with pinching) and injection. Table 3.5 shows the voltages applied on each channel and the current recorded during loading and migration of the test analyte (fluorescein).

Initially, broad irregular peaks, caused by longitudinal diffusion resulting from differing EOF at the surfaces of PDMS and DFR in the microchannels, were detected. To overcome this, 0.75% hexa-dimethrine bromide (HDMB) was added to the separation BGE. This coated the channel walls to achieve a

Table 3.5: Loading, separation voltages and currents recorded during runs of the test analyte fluorescein

	Electrolyte	**Sample**	**Electrolyte Waste**	**Sample Waste**
Loading Voltage V	-400	-800	-600	800
Loading Current µA	-2	-8	-3	14
Separation Voltage V	-600	300	300	1000
Separation Current µA	-5	-7	-6	18

constant EOF throughout the device. A representative electropherogram is shown in Figure 3.6. The currents in the DFR-PDMS microchannels when using the PANI electrodes were comparable with those obtained in PDMS-glass microchannels of the same geometry using platinum electrodes. During electrophoresis differences of 1-2 µA were observed between different PANI films and between PANI electrodes on the same film, indicating a leak of up to 10% of the total current through the PANI films during electrophoresis. As shown in Figure 3.6, this did not have any adverse impact upon the ability of these electrodes to function in electrophoresis.

3.5.1 Microfluidic Electrophoresis Chip Performance

To better analyse the performance of these microfluidic devices a multiple analyte separation was attempted. APTS has been shown to be a very effective fluorescent label that can be used where the BGE pH is within the range of 3-6 [190]. A separation of sugars was considered the most appropriate for analysing the performance of the microfluidic devices since very robust procedures for labelling sugars with APTS are already known [191]. Using the fully polymeric

microfluidic chips a separation of three APTS-labelled sugars was performed, giving the electropherogram shown in Figure 3.7. The buffer used was 20 mM sodium hydrogen maleate pH 5.5 with 0.5% Hydroxypropyl cellulose (HPC) added to eliminate any EOF within the system. The microfluidic devices were initially flushed with BGE for 5 min before samples were loaded for separation. Under these conditions currents remained stable for up to 20 separations.

The total separation time, including loading, was under 30 s which is typical for microfluidic electrophoresis chips. The ratios between the voltages and currents recorded between channels during the separation, given the voltages applied were somewhat higher than expected with conventional platinum electrodes; however, these slight discrepancies did not prevent a good separation from being achieved.

After continued intermittent use over 1 h, with high voltages applied for roughly half of this time, the PANI electrodes began to show signs of deterioration. This was observed through a decrease in the currents recorded during the application of voltage and two distinct colour changes. At the electrode that was held at a negative potential for the entire separation cycle (loading and separation) there was a distinct purple colour formed in the PANI film. This suggests that the film was reduced over time, transforming the conductive PANI-ES to the non-conductive PANI-EB form of the polymer. It is likely that the change in current observed with prolonged use is a result of de-doping of the PANI film due to the pH not being sufficiently acidic to maintain the film in the emeraldine salt form.

This was supported by the fact that the colour change could be quickly reversed either through re-doping by placing a strong acid such as 1 M HCl in the well, or by reversing the polarity of the electrode and applying 500 V at that well with the remaining wells grounded for 1 min. At the electrode that remained positive for the entire separation cycle there was a transformation of the PANI around the

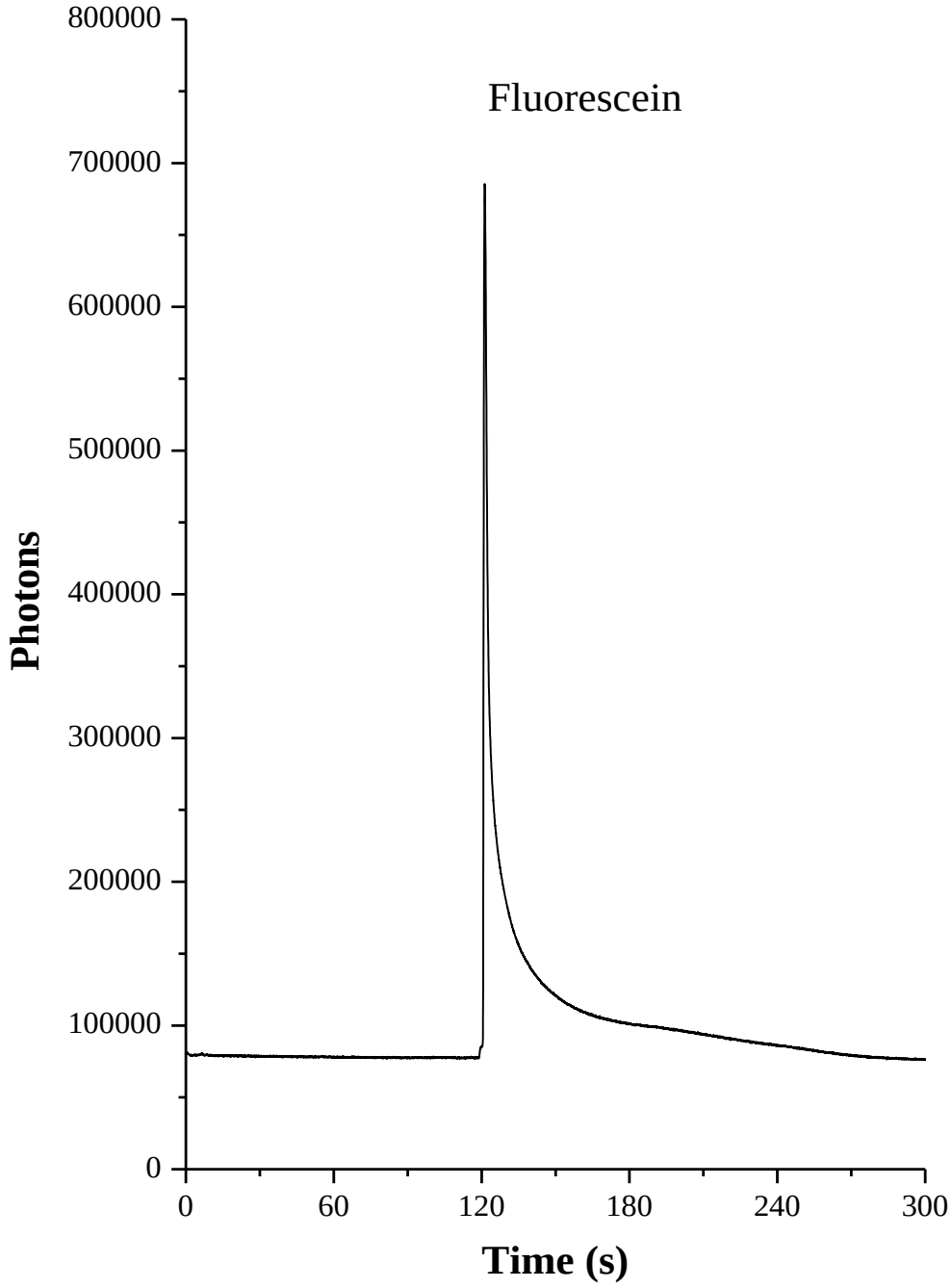

Figure 3.6: Separation of 10 µM fluorescein; Load time of 100 s; Separation time of 100 s; detection was at 2 cm from the injection cross via LED-induced fluorescence using a blue LED. Voltages applied at wells for loading: Electrolyte -400 V, Sample -800 V, Sample Waste +800 V, and Electrolyte Waste -600 V. Voltages applied at wells for Separation: Electrolyte -600 V, Sample +300 V, Sample Waste +300 V, and Electrolyte Waste +1000 V.

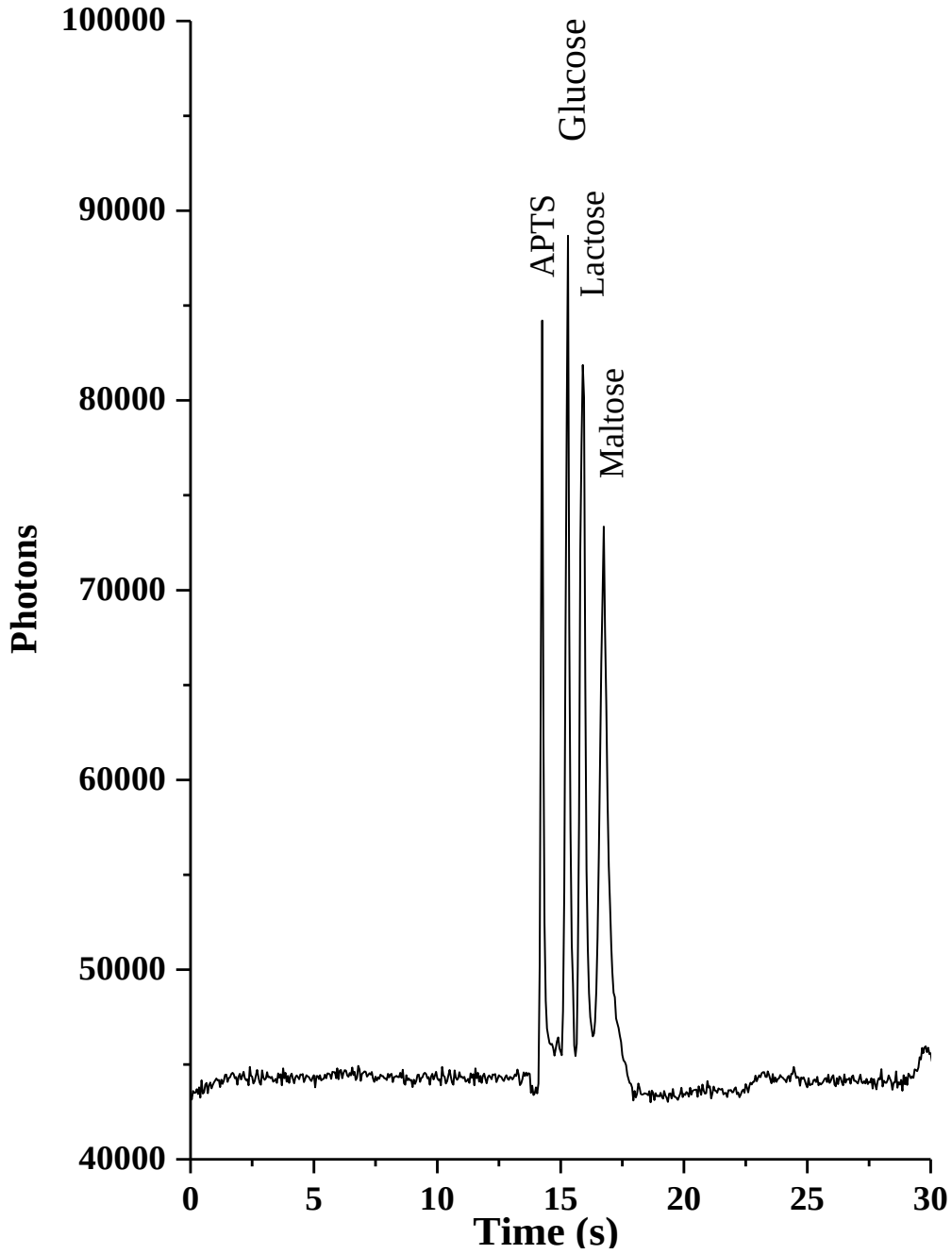

Figure 3.7: Separation of APTS labelled glucose, lactose and maltose. Load time of 20 s, Separation time of 20 s, detection was at 1.5 cm from the injection cross via LED-induced fluorescence using a blue LED. Voltages applied at wells for loading: Electrolyte -400 V, Sample -1000 V, Sample Waste +1200 V, and Electrolyte Waste -1000 V. Voltages applied at wells for Separation: Electrolyte -600 V, Sample +300 V, Sample Waste +300 V, and Electrolyte Waste +1800 V.

electrode from the conducting green emeraldine salt to an orange form, suggesting that the PANI may have become over-oxidised. The current at this electrode decreased until there was no current observed after 30 min of use with the applied voltage remaining constant. This reduced the lifetime of these chips to 30 min as this was an irreversible loss of conductivity under high voltage in the electrolyte systems used in this study. Despite this limited lifetime, 30 min of separation time is more than sufficient for a large number of microfluidic applications, as separations can often be completed in less than 10 s. The separation shown in Figure 3.7 clearly demonstrates that PANI electrodes are suitable for electrophoresis and, because of their low cost and easy manufacturing, they may have application in disposable microchips.

3.6 Conclusions

Flash-welding of PANI is the fastest way to produce simple electrode patterns with PANI [150, 151]. The use of patterned PANI as an alternate electrode material capable of supporting the high voltages necessary for electrophoresis is of particular significance as it would allow the development of a truly disposable, totally polymeric CE device in a cheap and simple manner.

The devices were constructed using a bottom-up approach. First the electrodes were patterned in a PANI film on an acrylic substrate. The PANI film was covered with a layer of DFR lithography, structured to enable direct contact between the electrodes and the electrolyte. A PDMS slab containing the microfluidics positioned on top of this film sealed the device, forming an integrated microfluidic device.

A successful separation of glucose, lactose and maltose was achieved making this the first use of PANI electrodes for driving electrophoresis, and with this the first

completely polymeric microchip with integrated electrodes capable of performing electrophoresis.

This chapter has shown that due to the low cost of fabrication and the potential for easy scale-up lithographically patterned PANI electrodes may be a viable approach for the mass production of low-cost, disposable LOC devices.

4. Development and Integration of Polyaniline Electrodes for Capacitively Coupled Contactless Conductivity Detection

4.1 Introduction

This chapter describes the development of PANI as an electrode material in a LOC device for integrated C^4D. Conductivity detection has been regarded as a simple and universal method of detection that is appealing for miniaturised analytical systems as sensitivity is not lost when downscaling, as occurs for optical detection methods**.** Conductivity detection can be performed either in the contact mode, with the electrode material directly in contact with the solution, or in a contactless fashion such as C^4D, where the electrode is separated from the liquid by insulating material. C^4D offers one major advantage for electrophoresis over the contact method, in that it is easy to decouple the high electric field required for separation from the detection electrode and electronics. An additional benefit is that the electrode surface does not become fouled. As such, C^4D has become a popular form of detection for microfluidic devices.

There are a number of ways that electrodes can be used for C^4D in microchips, as discussed in a number of recent reviews providing an excellent overview by Kuban *et al.* [61, 62, 192]. The easiest and most cost-effective approach is to have reusable, external electrodes that are not an integral part of the microchip itself [72]. Kuban and Hauser elegantly demonstrated the potential of this approach by using electrodes designed on a flexible printed circuit board and pressing this against a PMMA microchip. The downside of this approach is that, due to the thicker insulation layer of microchip material between the electrode and the solution in the micro-channel, detection is often not as sensitive as when the electrodes are integrated directly into the microchip.

The traditional approach for integrating electrodes into microfluidic devices uses lithography, with metal deposition in a lift-off process that has been demonstrated previously [193, 194]. Microchips made in this manner are commercially available in both glass and plastic, with a single plastic microchip including an integrated C^4D currently selling for € 125.00 [195]. By comparison, plastic chips without the integrated electrodes can be purchased in bulk at a cost of € 9.98 each. Hence, the costs of these devices are prohibitive and there is still need to develop cheaper methods for integrating electrodes.

The approach of using printed circuit boards has also been used to create integrated electrodes. Using a similar strategy Guijt *et al.* [58] demonstrated integrated electrodes within dry film microchip devices in which there was only a single 17 μm layer of dry film resist between the electrodes and the micro-channel. The use of semi-conducting films, such as indium tin oxide (ITO), to produce micro scale electrodes has also been popular [185, 196].

As shown in Chapter 3 PANI electrodes were capable of sustaining the high voltages required for microchip electrophoresis. However, the process of flash lithography was not able to reliably produce fine, sub mm patterns due to the high energy required to expose a large area. The destructive nature of flash lithography and exposure creep in which a small region of non-exposed PANI is welded due to thermal dissipation laterally through the PANI film were further drawbacks to this approach.

In this chapter, the use of PANI as a cost-effective alternative for the fabrication of C^4D in LOC devices is examined. Using the more controllable lithographic processing of laser-welding over flash-welding, fine electrode patterns could be produced from PANI films [197]. This chapter shows that the processing of PANI films for the integration of C^4D by laser-welding is an efficient and relatively

simple alternative to produce C^{4}D detectors that are comparable in performance to published manufacturing technologies.

4.2 Integrating Electrodes

In this chapter, two geometrically different C^{4}D designs were developed and integrated into microfluidic devices The first consisted of line electrodes that were produced using either direct printing or laser welding techniques. The second design was a more complex pad design developed in PANI using the laser welding technique. This design was too complex for replication with direct printing. Both designs were manufactured with Cu electrodes using the PCB technique for further comparison in order to benchmark the performance of the PANI detection electrodes.

Flash-welding had been found to be incapable of producing consistently sized patterns on the sub mm scale, as the high energy required could not be effectively masked during the process. The requirement for multiple flashes to expose the entire microchip led to considerable distortion of the desired patterns. Hence, only extrusion printing and laser welding were used for producing C^{4}D in PANI films.

Once the electrode designs had been produced within the PANI films or on the PCB, each substrate and detector was covered with a 17 μm dry film photoresist insulating layer that would also act as bottom wall of the microfluidic channel. This was done using the process described in chapter 3. A 5 mm area down both sides of each chip was not covered with the DFR in order to leave the electrodes exposed down the sides of the device, thereby allowing for connection to a TraceDec™ C^{4}D electronics system. Conection was made using copper wires that were glued with Wire Glue™ (Anders Products MA. USA) to the exposed ends of the PANI electrodes and connected to the TraceDec system.

PDMS was used for the remainder of the chip, forming the sides and top of the 50 x 50 µm separation channel and the sample and buffer reservoirs. The PDMS sections of the device were developed using standard moulding methods as described in chapter 4.

4.2.1 Straight line C4D Manufacturing and Integration

4.2.1.1Direct Printing

Straight line PANI electrodes were first produced using the capillary force printing technique as described in chapter 2 with electrode gaps of 500 µm +/- 100 µm. Because of the variance between the size of the detector gaps in this method each C^4D was individually measured under a light microscope before being used. Once the printed C^4D had been made, the 17 µm DFR layer was laminated over the surface as the insulator. Finally, the PDMS was carefully placed onto the surface making sure that the separation channel was aligned across the C^4D, thereby completing the microfluidic device.

4.2.1.2Laser Welding

The inability of extrusion printing to pattern features less than 500 µm as well as the shortcomings of other known techniques for developing PANI patterns, such as inkjet and screen-printing (minimum size 200 µm) [84], reinforced the reasoning behind developing the laser-welding technique. This approach clearly showed the potential to produce the highest resolution of any the PANI patterning techniques. For producing PANI C^4D by laser-welding, the automated system described in chapter 2 was used. PANI films with a thickness of 5 µm on an acrylic substrate were patterned with a laser speed of 5 mm s^{-1} with a laser focal point of 10 µm in width.

The best resolution that was achieved for the laser welded straight line C^4D was 10 µm, the width of the laser-welded area for one line of welding. However,

initially a 100 µm insulating gap between the electrodes at the detection head was developed and used in the following straight-line laser-welded C^4D. Figure 4.1 shows a photograph of the laser welded C^4D on an acrylic substrate with close up microscope images of two C^4Ds, one having a 100 µm detection gap and the other a 20 µm detection gap.

The distinction between laser welded insulating PANI and conducting PANI is also clearly shown in Figure 4.1. Each transverse of the laser used to weld the PANI can also be seen where there is not complete overlap. Once the C^4D patterns were produced, the microfluidic devices were completed in the same way as the directly printed C^4D devices. DFR was laminated over the laser welded C^4D forming the 17 µm insulating layer with PDMS containing the channels being placed on top, reversibly binding to the DFR. Figure 4.2 shows a schematic of the fully integrated, laser welded PANI C^4D microfluidic device.

4.2.2 C^4D Electrode Design

Laser-welding gave the ability to pattern sharp corners and other shapes with high resolution and accurate movement profiles of the x, y stage. It became possible to develop more highly resolved insulating patterns in PANI films and hence, more sophisticated C^4D electrode patterns. A pad design that had been successfully used in microfluidics [72], with lead lines attached to 2 x 2 mm pads with a 100 µm gap between them forming the detection region was developed. This design was shown to produce better Limits of Detection (LOD) and hence to be a more effective design than that of the straight line electrodes [72]. The pad design was chosen as an alternative to the simple straight-line design to show the beginnings of what could be possible with the laser-welding technique. A photograph of a substrate that has been patterned to contain 6 detectors with this design is shown in Figure 4.3.

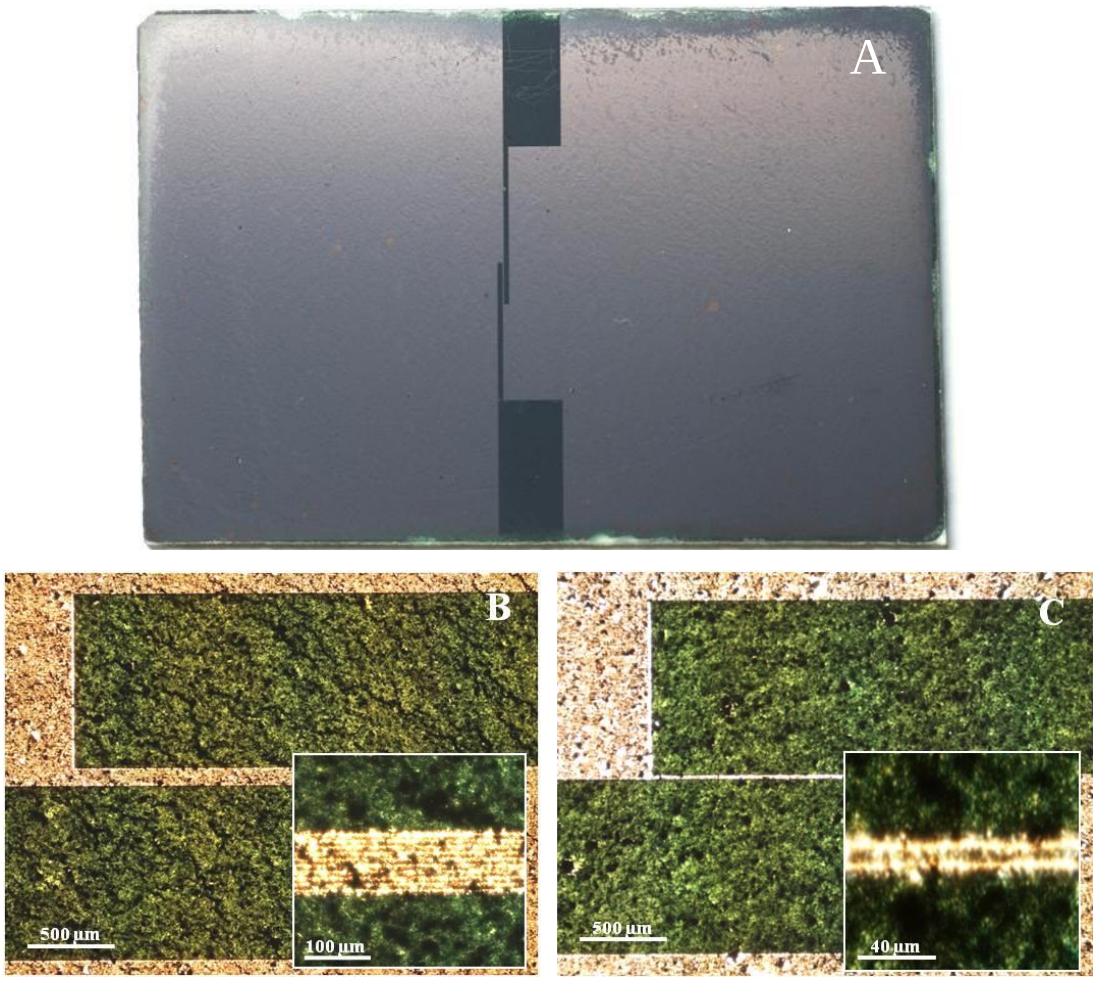

Figure 4.1: A) Photograph of the C^{4}D patterned PANI film, B,C) Light microscope image of laser-welded PANI leaving two conducting regions separated by B) 100 µm and C) 20 µm of welded PANI.

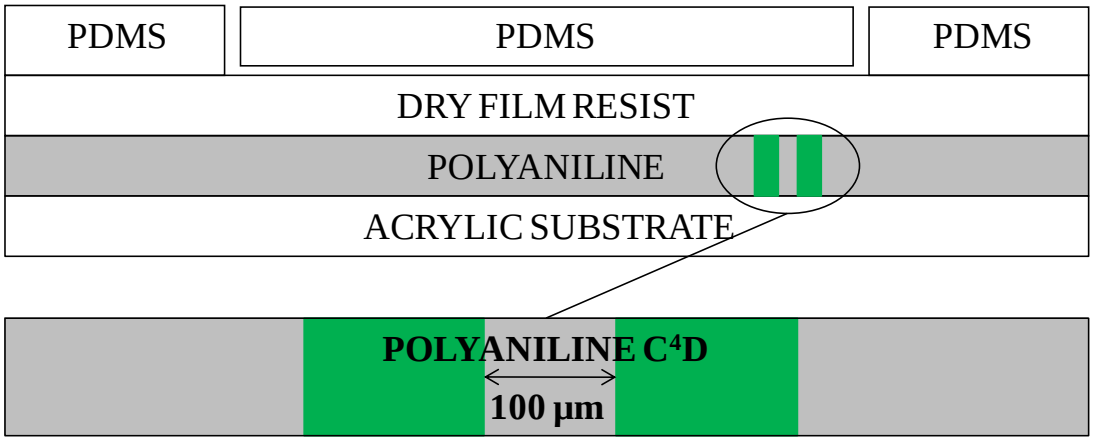

Figure 4.2: A schematic cross section of the microfluidic device incorporating a PANI C⁴D. The Figure is not to scale The acrylic substrate was 1.5 mm thick, the PANI film 4 µm thick, DFR 30 µm thick, conductive PANI detector lines 500 µm wide with 100 µm gap and a 50 µm high channel in PDMS.

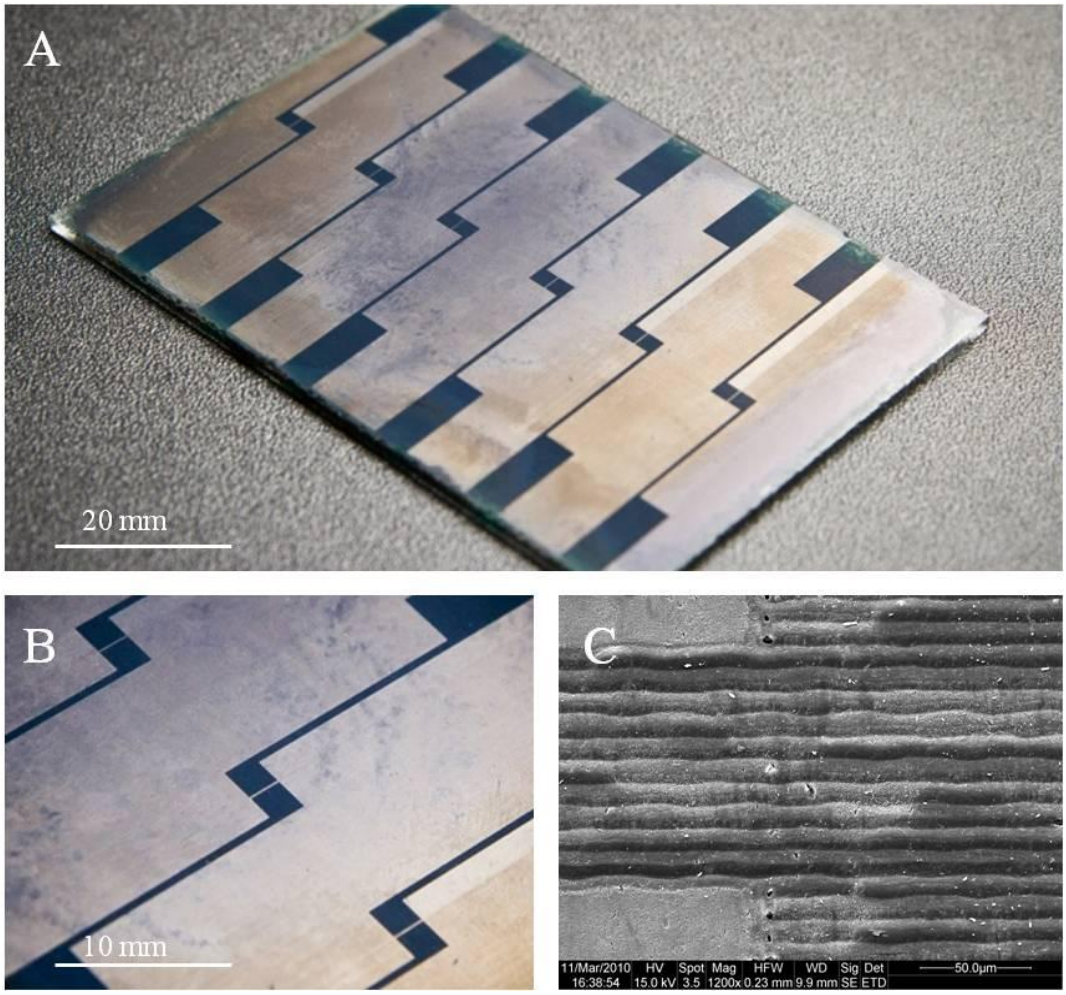

Figure 4.3: A) Photograph of a patterned PANI film on a 75 x 50 cm acrylic plate containing 6 C^{4}D, B) Close up image showing the good resolution around the detector pads. C) SEM of the electrode pad corners.

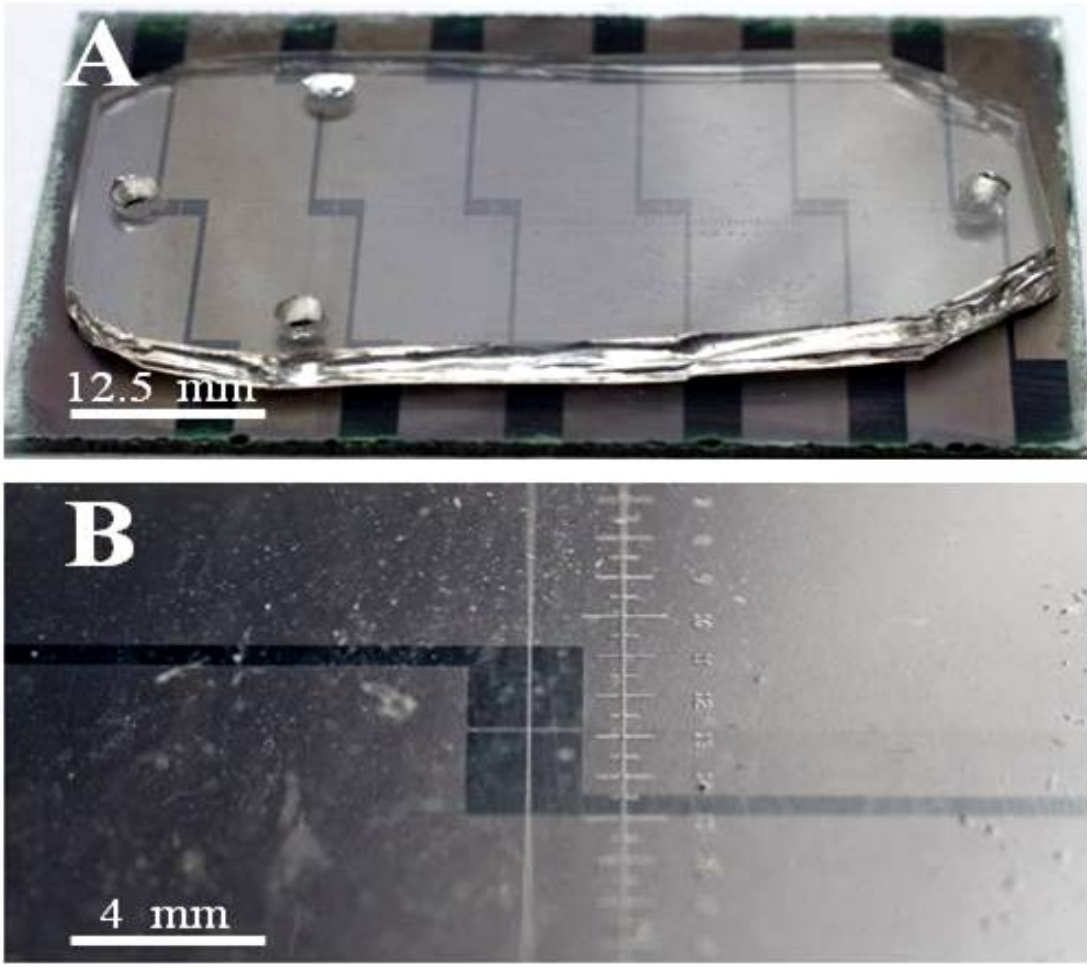

Figure 4.4: A) Photograph of full polymer C^{4}D chip with PDMS containing channels. B) Close up showing PDMS channel transversing the PANI C^{4}D detector head.

In Figure 4.3 the detector heads can be clearly determined, while Figure 4.3 (B) shows a closer view of a detector head where the 100 μm gap between the two leads can clearly be seen. An SEM of the area at the edge of a detector head is shown in Figure 4.3 (C).

The 10 lines made from the laser welding process to produce the detection gap are visible between the corners of each side of the detection head. Figure 4.4 shows the full microfluidic device containing the pad C^4Ds with the PDMS channels and wells in place ready for use. A close-up of the microfluidic channel passing over the detector is shown in Figure 4.4 (B).

4.2.3 Printed Circuit Board C^4D

Copper electrodes with identical widths and length to the PANI C^4D electrodes were produced using standard PCB manufacturing techniques in 30 μm thick copper films for comparison to the PANI devices. Figure 4.5 shows photographs of the copper-on-PCB electrodes developed for the comparison work.

4.3 Electrophoresis with Polymer C^4D

4.3.1 Experimental

To evaluate and benchmark the PANI C^4D detectors, simple microchip electrophoresis separations of the alkali metals lithium, sodium and potassium were performed. These analytes have been used extensively to develop and characterise C^4D in microchips, with detection limits in the low μM range being achieved. LOD values around 50 μM have been the most commonly reported [61]. The electrolyte chosen for the following experiments of the various PANI C^4D devices was a methanesulfonic acid (MES) – histidine (HIS) buffer used previously for the separation of these ions [198]. Table 4.6 shows the full list of chemicals used for the chip electrophoresis experiments.

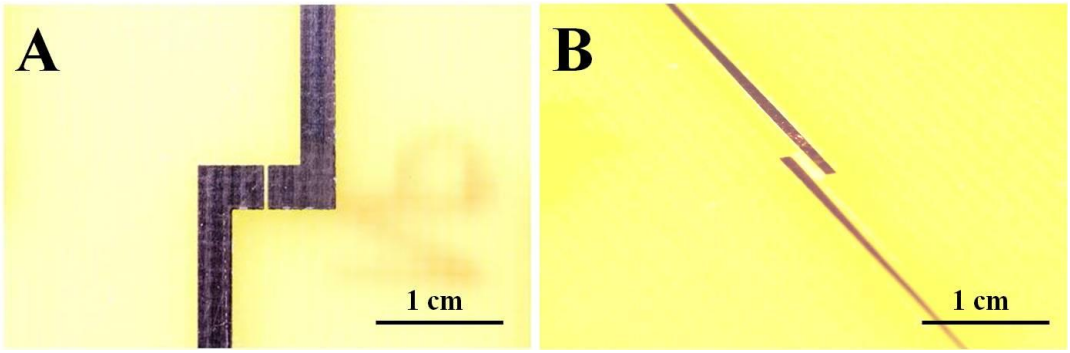

Figure 4.5: Photographs of copper printed circuit board C^{4}D detector designs used for comparison with PANI developed C^{4}D, A) Pad design with 100 µm gap and B) Straight design with 1 mm gap.

Table 4.6: Additional chemicals used during microchip C^4D.

Chemical	Abbreviation/Formula	Purity	Manufacturer
2-(N-Morpholino)ethane sulfonic acid	MES		Fluka, USA
histidine	HIS	98+%	Sigma-Aldrich, USA
lithium chloride	LiCl	99+%	Sigma-Aldrich, USA
sodium chloride	NaCl	99+%	Sigma-Aldrich, USA
potassium chloride	KCl	99+%	Sigma-Aldrich, USA
orthophosphoric acid	H_3PO_4	99+%	BDH Chemicals
sodium hydroxide	NaOH	98+%	BDH Chemicals

The high voltage power supply described in chapter 3 was used to apply voltages at each of the 4 wells in the microchips via a custom-made interface containing 4 platinum electrodes, as shown in Figure 4.7 (John Davis, Peter Dove, Central Science Laboratory, University of Tasmania).

4.3.1.1 Preparing the Microfluidic Devices

To perform initial separations the microfluidic device was flushed with electrolyte solution for 10 min. The initial electrolyte solution was a 50 mM MES-HIS pH 6.0 buffer previously used during the successful separation of all the chosen analytes. Once the channels had been flushed, all reservoirs were emptied using a pipette and refilled with 33 µL of electrolyte, except for the sample reservoir which was filled with 33 µL 100 ppm Li^+, Na^+ and K^+ in electrolyte solution. Once each well was filled, the microfluidic device was housed in a Faraday cage along with the exposed connections between the device and the Trace Dec™ conductivity detection system. Voltages were then applied to the device through the HV interface.

Figure 4.7: Electrode Interface with Platinum Electrodes for Applying High Voltages to Microchips

Table 4.7: Trace Dec™ conductivity detection, system settings, with maximum frequency and voltage

Voltage	Frequency	Gain	Offset
-30 dB	3 x High	50 %	50

The microfluidic device C^4D that was used in the initial studies was the straight line laser welded design with 1 mm wide leads with 2 mm overlap and 100 µm gap between them at the detection head, as shown in Figure 4.1. The Trace Dec™ detection system software was initially set at maximum levels for voltage and frequency for the detection of the three analytes, these settings are shown in Table 4.7.

The optimum voltages that produced the most stable baseline separated peaks were determined and are shown in Table 4.8.

The pinching voltage applied at the electrolyte waste during loading was higher than the electrolyte and sample voltages because that is the reservoir at the end of the longer separation channel. Lower pinching voltages led to insufficient pinching at the injection cross with analytes moving into the separation channel during loading which increased the width of the injection plug, leading to only one broad peak observed for the three analytes.

Once a successful separation had been achieved, differing electrolyte concentrations were trialled from 10 mM to 100 mM MES-HIS to identify the best ionic strength for the separation. As reported in the literature for similar systems the optimal concentration was 50 mM MES – 50 mM HIS pH 6.2.

Table 4.8: Voltages recorded for optimal microfluidic device performance.

	Electrolyte	Sample	Electrolyte Waste	Sample Waste
Loading Voltage (V)	200	200	300	-200
Separation Voltage (V)	200	GND	-600	GND

4.3.2 Straight Line Detector Results

These optimised conditions were then used for separations using the above microfluidic electrophoresis devices with integrated C^4D. Electropherograms for the separations of the three cations conducted under the same conditions are shown in Figure 4.9 using the direct printed PANI, laser welded PANI and Cu straight line C^4D. The analytes were easily separated in all devices, confirming them as suitable model analytes for determining the quality of the various C^4Ds. However, there is evidence of significant dispersion in the system leading to considerable band broadening in the peaks.

Figure 4.9 allows comparison of the separation of K^+, Na^+ and Li^+ on the three types of devices under consideration. Figure 4.9 (A) is the output using the Cu C^4D straight line configuration with an electrode width of 1 mm, an overlap of 2 mm and a detection gap of 100 µm. It can be seen that there was very little difference in LOD between the copper and the laser welded PANI C^4D (Figure 4.9 (B)) with the limits of detection for Na^+ being 34.4 and 30.6 µM for Cu and LW-PANI detectors, respectively.

Table 4.10 shows the results for all three analytes on each device. It can be seen that the directly printed PANI detector Figure 4.9 (C) was considerably higher in its limits of detection than the other two, most likely due to the roughness and

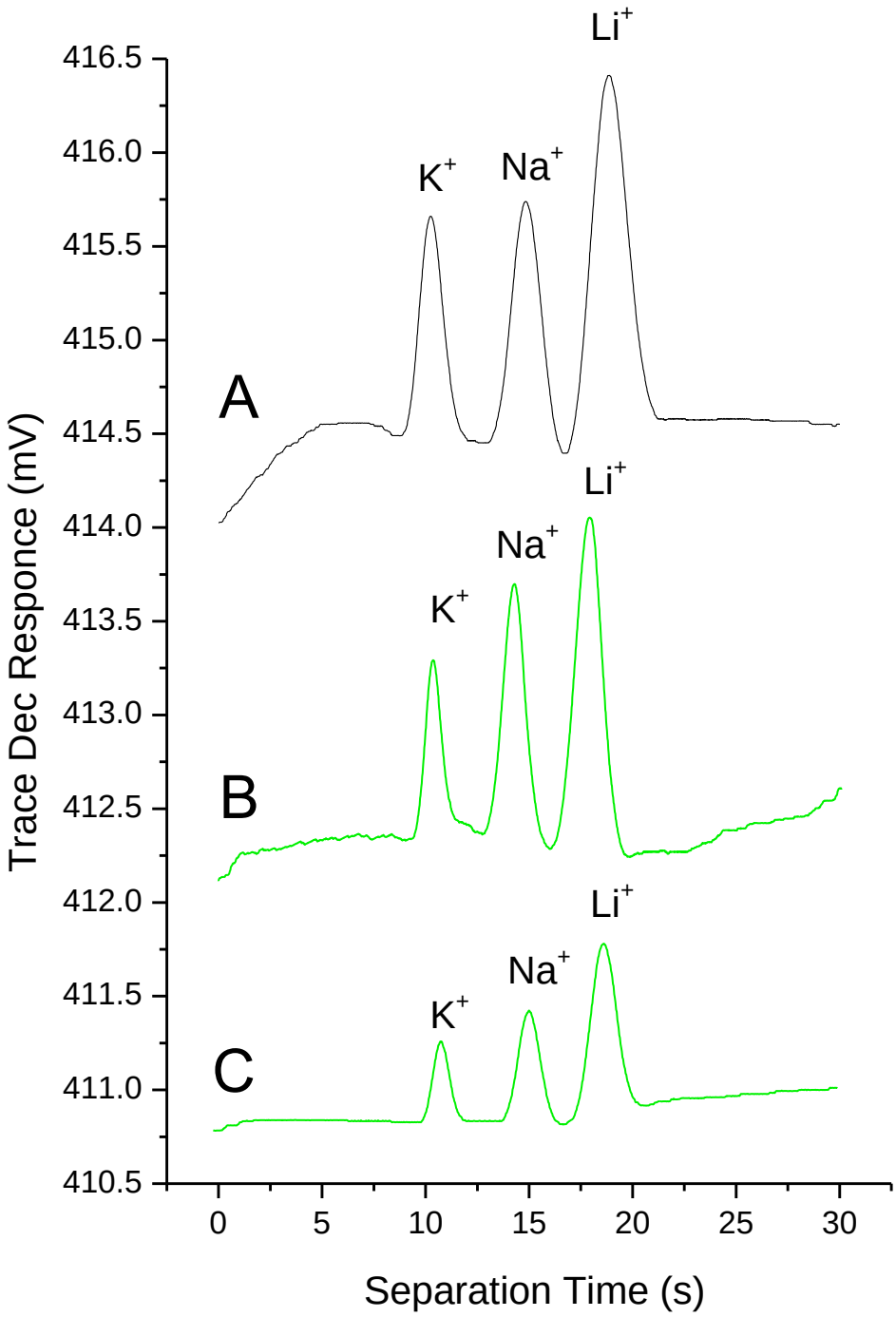

Figure 4.9: Separations of three cations (K^+, Na^+ and Li^+) performed using PDMS DFR composite microfluidic devices with straight line design C^{4}D; A) copper, B) laser welded PANI, C) extrusion printed PANI. Cu and Laser welded PANI dertectors had detection gaps of 100 µM with the direct printed PANI having a detection gap of 500 µM all electrodes were 1000 µm wide at the detector.

Table 4.10: Straight Line electrode Limits of Detection for each of the analytes

	LOD Li^+ (µM)	LOD Na^+ (µM)	LOD K^+ (µM)
Direct Printed PANI	156	79.1	45.9
Laser Welded PANI	81.9	34.4	22.2
Printed Circut Board Cu	74.7	30.6	26.4

cracked nature of the deposited PANI that occurred during the deposition and drying process.

4.3.3 Optimal Pad Detector Results

The same separation was performed using the pad electrode design for C^4D of the three cations. The voltages used to drive electrophoresis and the TraceDec™ settings were kept the same as for the straight-line detector separation, again the detection point was 13 mm down the separation channel from the injection cross of the microfluidic device. The resulting electropherograms are shown in Figure 4.11 with (A) the laser welded PANI Pad C^4D and (B) the Cu PCB Pad C^4D. This electrode design could not be fabricated by the direct printing methods. The separation detection limits when using the pad design electrodes were lower than the detection limits achieved with the straight line C^4D for both the Cu and PANI. The limits of detection as calculated from three times signal to noise are given in Table 4.12 for each of the analytes with a LOD of 18.9 µM for Na^+ found for both the Cu and PANI pad design C^4D. The minimal difference in the performance between the PANI and the Cu electrodes shows that using PANI as an electrode material has no disadvantages when it comes to detection sensitivity in this system. A comparisons with results reported in the literature is given in Table 4.13. The LODs obtained in this study are comparable to literature values, although not as low as some external microfluidic C^4D systems.

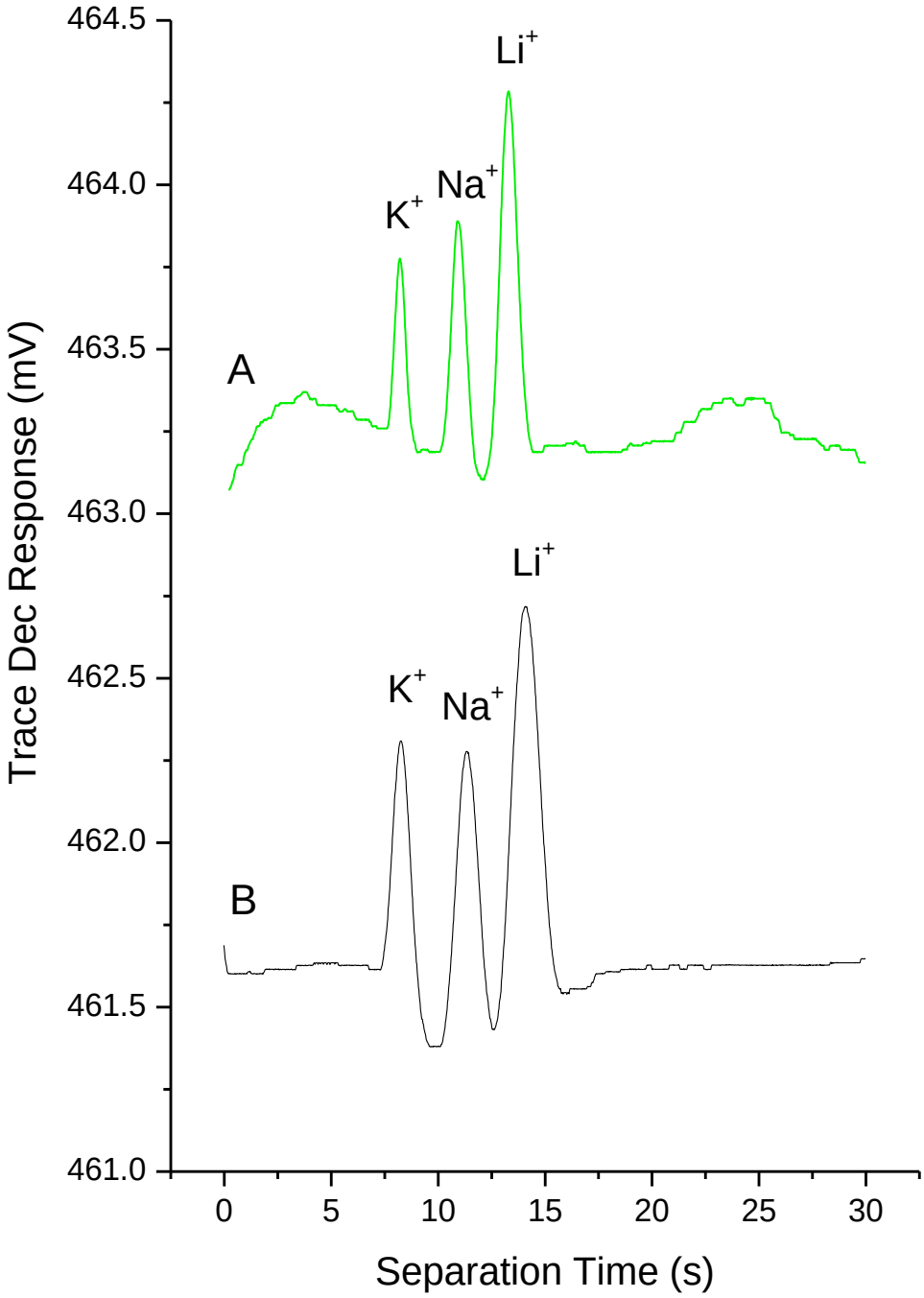

Figure 4.11: Separations of cations performed using Pad design C^{4}D with A) PANI and B) Cu C^{4}D. Each with a 100 µm detection gap and 2 x 2 mm pad area.

Table 4.12: Pad electrode Limits of Detection for each of the analytes

	LOD Li^+	LOD Na^+ (µM)	LOD K^+ (µM)
Laser Welded PANI	48	18.9	16.2
Printed Circut Board Cu	43.2	18.9	14.4

These systems have reported detection capabilities down to 0.1 µM for Na^+ [76]. However, the lowest LOD for Na^+ reported for simple integrated C^4D separations has been 17 µM using screen printed electrodes on ceramics with field amplified stacking used to increase sensitivity [199]. A more complex multiple detector arrangement using a novel data acquisition system has allowed for these limits to be improved to 1.5 µM in an integrated system [79]. Other straight-line PCB detectors have been shown to give similar LODs for Na^+ and similar designs made with metals using the lift-off process in their manufacturing have shown to have slightly lower LOD's, down to 4.3 µM for Na^+[200, 201].

Smaller detection gaps down to 20 µm were produced and tested in the PANI films but could not be directly compared to the copper device because the smallest electrode gap which could be produced in the copper using the PCB technique was 100 µm. However, predominantly due to dispersion within the separation system leading to significant band broadening, it was not surprising that the LODs were not significantly different from the separations achieved with 100 µm detection gaps.

4.4 Conclusions

This chapter shows that the use of polyaniline as an alternative material to metal for C^4D applications within LOC devices is not only a cheap alternative but is also capable of retaining the same level of performance as metal-based devices.

Table 4.13: Microfluidic C^4D Comparisons

Detector Construct	Device Construct	Detector Insulation	BGE	Limits of Detection µM	Ref
Integrated Direct Printed PANI	PDMS / DFR	17 µm DFR	50 mM MES 50 mM HIS pH 6.1	K^+ 45.9, Na^+ 79.1, Li^+ 156.	
Integrated Straight Line LW PANI	PDMS / DFR	17 µm DFR	50 mM MES 50 mM HIS pH 6.1	K^+ 22.2, Na^+ 34.4, Li^+ 81.9.	
Integrated Straight line Cu PCB	PDMS / DFR	17 µm DFR	50 mM MES 50 mM HIS pH 6.1	K^+ 26.4, Na^+ 30.6, Li^+ 74.4.	
Integrated Pad LW PANI	PDMS / DFR	17 µm DFR	50 mM MES 50 mM HIS pH 6.1	K^+ 16.2, Na^+ 18.9, Li^+ 48.0.	
Integrated Pad Cu PCB	PDMS / DFR	17 µm DFR	50 mM MES 50 mM HIS pH 6.1	K^+ 14.4 Na^+ 18.9, Li^+ 43.2.	
Non Integrated Pad Cu PCB	PMMA	175 µm PMMA	15 mM Arg 10.75 mM malic acid, 1.5 mM 18-crown-6, pH 5.9	K^+ 1.5, Na^+ 3.0, Li^+ 7.5.	[72]
Non Integrated Cu	GLASS	100 µm GLASS	10 mM MES 10 mM HIS pH 6.0	K^+ 0.6, Na^+ 0.4.	[76]
Integrated Pad Cu PCB	PDMS / GLASS	100 µm PDMA	20 mM MES 20 mM HIS pH 6.0	K^+ 11.6, Na^+ 12.5.	[200]
Integrated Straight line Al Lift Off	Polyester	100 µm Polyester	20 mM MES 20 mM HIS pH 6.0	K^+ 3.1, Na^+ 4.3, Li^+ 7.2.	[201]
Integrated Straight line Screen Printed Ag	Ceramic	100 µm Ceramic	11 mM MES 10 mM HIS pH 5.8	K^+ 10.0, Na^+ 17.0, Li^+ 21.0.	[199]

Through further development of the photolithographic process of laser welding, fine microscale patterns required for detector electrodes could be produced with insulating regions down to 10 μm in width. With the use of 17 μm thick DFR as an insulating layer, these PANI electrodes were closer to the separation medium than any contactless detectors previously reported, with the closest reported to date being 80 μm [202]. Integrated devices made using these electrodes were successfully used as detectors during the separations of Li^+, Na^+ and K^+, with LODs down to 16.4 μM.

5. Fully Integrated Polymer Microfluidic Device using Polyaniline as High Voltage and Capacitivily Coupled Contactless Conductivity Detection Electrodes

5.1 Introduction

Replication techniques allow for low-cost manufacturing of large numbers of plastic devices capable of performing a range of functionalities. Complex tasks, however, often require the integration of electrodes, significantly increasing the costs per device when integrating metal electrodes.

Previously in this thesis the use of flash-welded PANI as a high voltage electrode in chip-based electrophoresis devices [203, 204] has been discussed. Refinement of the welding process from a flash to a laser has enabled further enhancements of the PANI processing for the development of electrode patterns, with electrodes as small as 9 µm wide, with a resolution tolerance of 1 µm. However, for microfluidic devices to be considered more appropriately as LOC devices a higher level of integration should be incorporated into each individual device. Although there has been few publications of electrophoresis devices that have incorporated multiple functions, these should be such that the device is capable of performing two or more operations on the one platform.

In this chapter laser-welding is further extended by combining the manufacturing of both PANI HV electrodes and PANI electrodes for C^4D into the one microfluidic device. This new technology has enabled the creation of the first metal-free LOC device for capillary electrophoresis with an integrated detector, using PANI electrodes to carry the DC voltages required for fluid handling and electrophoretic separation as well as to apply AC voltages required for

conductivity detection. For comparisons with previous results and the literature these devices were used for the electrophoretic separation of Li^+, Na^+ and K^+.

5.2 Manufacturing

In this chapter, laser welding as described in chapter 4 was used to develop a fully polymeric chip with containing PANI electrodes for both high voltage application and C^4D within the one device.

Photographs of a PANI-covered acrylic substrate after welding are given in Figure 5.1. The figure shows the whole substrate, containing four 5 mm wide high voltage electrodes and two 200 µm wide electrodes for contactless conductivity detection. To prevent cross-talk between the detection electrodes other than through the channel, the electrodes were positioned in an anti-parallel configuration allowing 2 mm overlap in the sensing area [205]. Figure 5.1 B shows a close up of the detection electrodes, showing the 100 µm wide gap between the electrodes. The sharp edges illustrate the high accuracy that can be obtained using laser welding.

Once patterned, each substrate was covered with a 17 µm thick film of DFR using an office laminator. Four holes with a diameter of 3 mm were punched from the DFR prior to lamination to enable contact between the HV electrodes and the microchannels. Whilst photolithographic removal of the DFR is also feasible as described in chapter 3, the hole punch was found to be faster and sufficiently accurate. The DFR was cut slightly smaller than the PANI-coated substrate to leave the outer 5 mm of the PANI film accessible for connecting to the high voltage supply and detection electronics. The four HV electrodes were connected to the custom HV power supply using alligator clips and the TraceDec™ system was connected to the device as described in chapter 4. A microfluidic structure cast in PDMS was reversibly sealed to the DFR layer with the reservoirs aligned

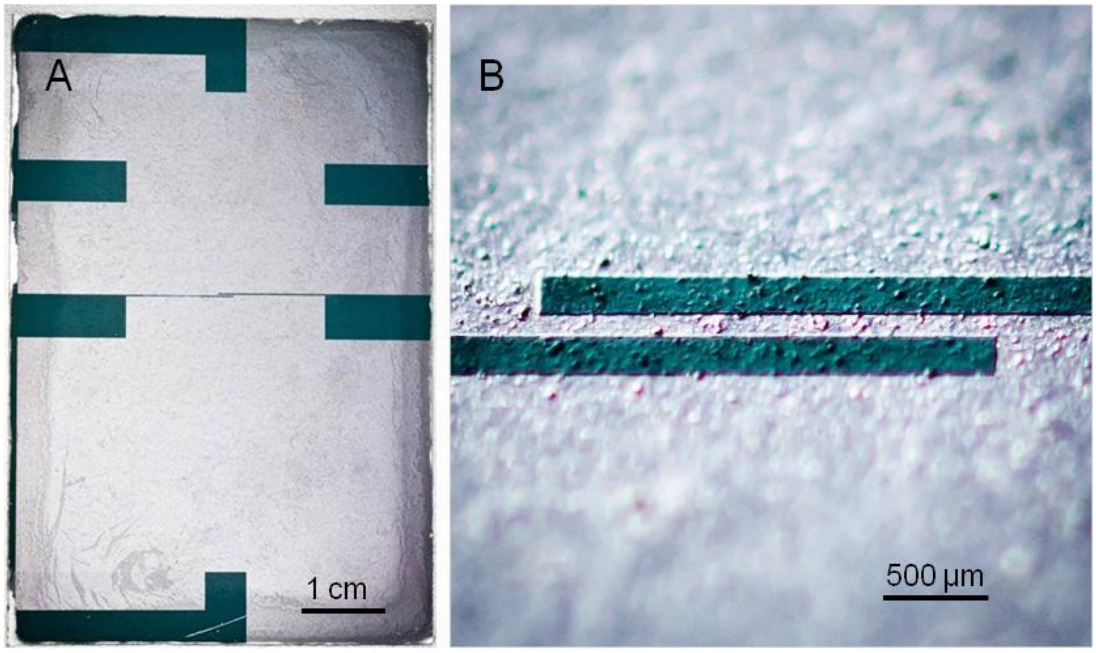

Figure 5.1: Photographs of the laser welded PANI on acrylic plastic with HV carrying electrodes for separation and C^4D electrodes. A), the entire substrate and B), close up of the detection electrodes at the detection area.

with the HV electrodes through the holes in the DFR. The layout was a standard cross design as described in chapter 3. The separation channel was positioned crossing the detector at 13 mm from the injection cross. A photograph of a device ready for attachment to the HV and detection electronics is shown in Figure 5.2.

5.3 Experimental

The chemicals used during the ananlysis of these microfluidic devices were the same as described in chapter 4 and are shown in table 4.6. The standards and sample preparation procedures remained the same, as described in chapter 4 along with the Trace Dec™ and HV power supply configurations. The BGE used was a 45 mM MES – 55 mM HIS pH 5.9. The optimum voltages that produced the most stable baseline-separated peaks were used, as describe in chapter 4 (Table 4.8).

5.4 Fully Polymeric Microfluidic Chip Performance

The fully-integrated fully-polymer microchip was used for the electrophoretic separation of a mixture of Li^+, Na^+ and K^+ in a background electrolyte containing 45 mM MES and 55 mM HIS (pH of 5.9). Initially a 50 mM MES – 50 mM HIS BGE was used; however, at the pH of 6.2 signs of PANI de-doping where the HV electrodes contacted the BGE occurred before any separation was attempted. By changing the buffer composition to 45 mM MES – 55 mM His, pH 5.9, visible PANI de-doping at the HV electrode BGE contact areas was eliminated. Separations were performed using pinching and pullback techniques that are well described within the field. Voltages of up to 600 V were applied on the PANI electrodes, but it is important to note that the application of the voltages was not limited by the PANI, but by the risk of destruction of the detection electronics following dielectric breakdown of the 17 um thin insulating film. A 100 ppm sample was successfully separated in 30 s with an efficiency of 22,419 plates m^{-1}, as illustrated in Figure 5.3.

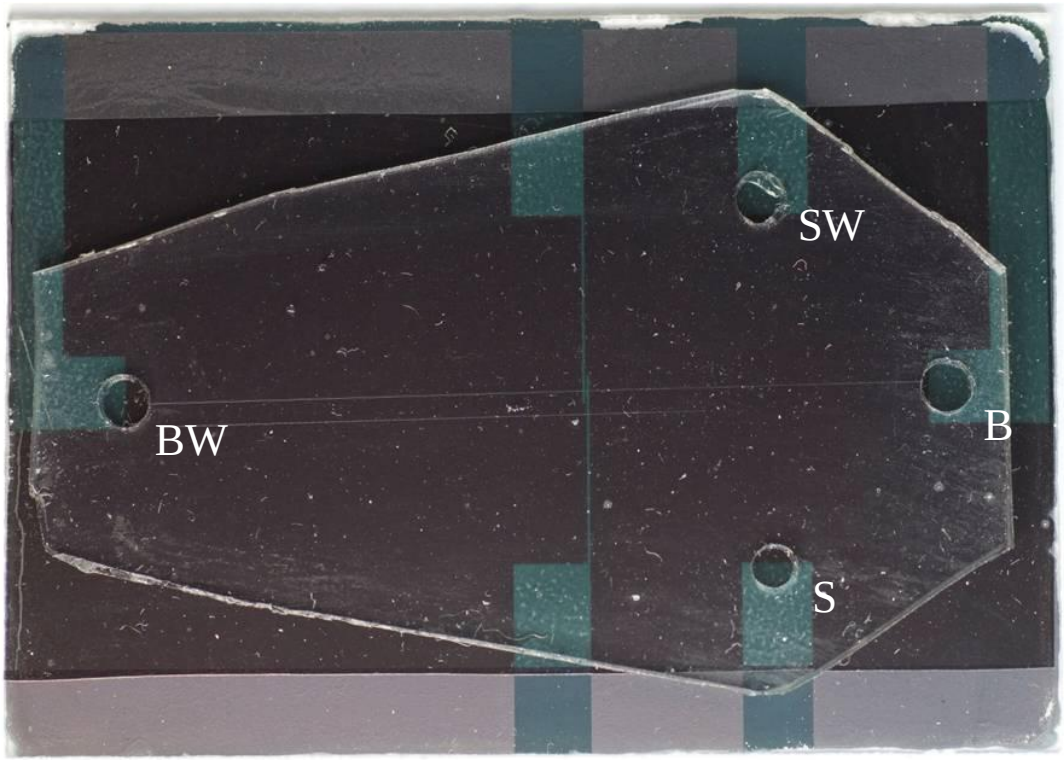

Figure 5.2: Photograph of the fully integrated microfluidic Chip with PANI HV and C^4D electrodes.

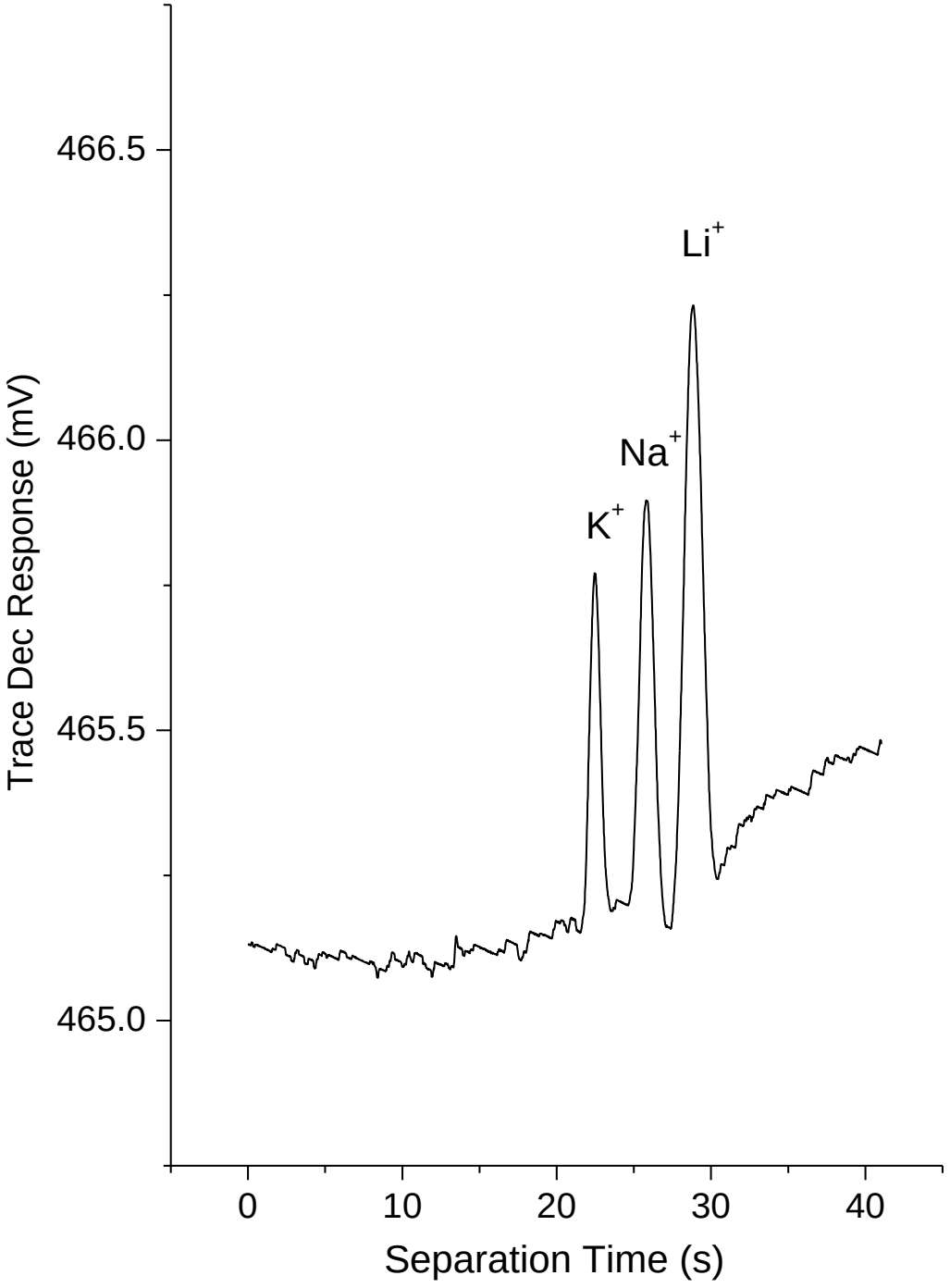

Figure 5.3: Separation of cations using PANI electrodes for HV application and C^4D

Table 5.4: Straight Line electrode Limits of Detection for each of the analytes

	LOD Li^+ (μM)	LOD Na^+ (μM)	LOD K^+ (μM)
PANI HV and C^4D	72.7	29.3	26.2

The limits of detection (LOD) as calculated at 3 x noise for each of the ions is shown in Table 5.4. With the exception of a recent report on LODs down to 0.15 μM using a more complex detection electrode geometry [73], LODs of around 30 μM have been most commonly reported with integrated C^4D without sample stacking [206]. The microfluidic chip and detection hardware used here are most comparable with those of Ding and Rogers [207], who reported LODs of 3-4 ppm for warfare degradation products using TraceDec™ electronics and metal detection electrodes 50 μm away from the separation channel, demonstrating the excellent performance of the all-polymer device.

5.5 Conclusions

In this chapter it has been shown that polyaniline (PANI) is a highly suitable material for the complex electrode structures required for producing highly integrated LOC devices. Three of the most important LOC processers, namely fluid handling, separation and detection, were integrated into a single all-polymer device. Laser-patterned PANI electrodes were integrated in a polymer microchip to carry the DC voltages required for fluid handling and electrophoretic separation as well as to apply the AC voltages required for detection. The analytical performance of the device, used for the electrophoretic separation of Li^+, Na^+ and K^+ with a detection limit down to 25 μM and an efficiency of 22,000 theoretical plates m^{-1}, is in the same range as the performance of devices employing metal electrodes. With no loss in performance, the low cost and the increased compatibility with bulk manufacturing of polymer devices, the use of

polymer electrodes may facilitate the production of more affordable complex LOC devices and therefore stimulate an increased uptake of LOC technology.

6. Concluding Remarks

The uptake of LOC technology for routine applications is strongly correlated to the price of the devices. Simple devices can be made for low cost using replication techniques, but the price per device increases sharply when integrated electrodes are required due to the costs of metal and metal deposition processes. The total cost of producing one conducting layer or one set of electrode of PANI being approximately $0.07 AU compared to a similar layer of metal costing around $2.00 AU for gold or platinum and $0.40 Au for Cu PCB. Conducting polymers offer a cheaper way to integrate electrodes in polymer microchips for a range of applications.

Polyaniline was identified as a suitable ICP material for use in LOC devices for both HV and as detection applications because films of PANI can be lithograpically processed into conductive circuitry suitable for integrating into such devices. Other advantageous properties of PANI include the good stability and conductivity of the PANI-ES form and low cost compared to other conducting polymers.

In this thesis, the first fully polymeric LOC device with integrated electrodes for capillary electrophoresis was developed with the use of PANI patterned by flash-welding. A more highly integrated device was then developed with integrated electrodes for application of the HV and for contactless conductivity detection.

Two significant advances improving the potential of PANI-ES to produce fine conducting circuitry were developed. The efficiency of the flash-welding process was enhanced through the use of a high power light source and polymeric substrates, enabling the flash welding of PANI films with a thickness ranging from 5 to 15 μm. Partial masking of the PANI films during flash welding enabled

the formation of conducting and insulating regions on single substrates. Raman spectroscopy was used to determine the sharpness of the masked edges and the interface between the flash-welded and masked regions of the PANI films was typically less than 15 µm wide.

Furthermore, light with a wavelength above 570 nm was found to be responsible for the welding process, matching the absorbance spectra of PANI-ES. This eliminated the necessity of a broad-spectrum output such as a studio flash for flash-welding. A 635 nm laser diode was used for welding PANI, introducing welding of PANI using narrow wavelength light sources. When used for direct writing lithography, the laser diode was able to weld 10 µm wide lines in a PANI film.

The flash welded HV PANI electrode devices were used for separations of APTS-derivatised sugars and these chips showed similar performance to that obtained with platinum electrodes, confirming the successful use of PANI for high voltage electrodes in electrophoresis. These devices did degrade over time and the conductivity was reduced after multiple uses, suggesting that PANI would only be suitable for single-use disposable devices.

The laser-patterned PANI electrodes that were integrated in a polymer microchip showed much better patterning control and reproducibility than the flash-welded electrodes. These electrodes were used to carry the DC voltages required for fluid handling and electrophoretic separation as well as to apply AC voltages required for detection. The analytical performance of these devices, used for the electrophoretic separation of Li^+, Na^+ and K^+ with a detection limit down to 25 µM and an efficiency of 22,000 plates m^{-1}, is in the same range as the performance of devices employing metal electrodes.

The processing technique of laser welding for the development PANI electrode patterns developed in this thesis has the potential to scale-up into a mass production batch process. With the potential for the development of low cost disposable devices on a large scale, the use of PANI as an electrode material could be enough to drive an increase in the uptake of LOC technology.

6.1 Future Prospects: Polyaniline in Microfluidics

From this thesis the future of PANI as an alternative electrode material within LOC devices is bright as PANI has been shown to be effective for both applications here. There are a number of key areas of research that could be undertaken for extending the use of PANI and ICPs in LOC, devices as outlined below.

1. The further development of different C^4D for microfluidics is also a possiblilty with success found in this area and although PANI lends itself to low cost disposables, the C^4D produced in this work showed no signs of performance loss with prolonged use.

2. The laser-welding technique developed here is extremely accurate and efficient way to produce fine conductive circutry in PANI films and this approach could easily be extended to producing more complicated conductive patterns than were shown in this work. The main limitation of the laser-welding process was the time taken to pattern a single film (up to 24 h). This could easily be improved by using a more powerful laser for which a faster patterning speed could be achieved. A wider focal point of a laser could also be used to increase the area patterned with each transvers of the laser.

3. Although PANI has been shown to be an appropriate ICP for the uses shown in this thesis, other ICPs could be explored for their applicability. One example would be PEDOT which also shows good stability in a range of conditions [208]. However, the patterning of any other conducting polymers via current techniques, such as screen printing or direct writing, will not preduce the same resolution as laser-welded PANI.

4. For PANI to be used in a fully disposable system, its compatibility with the processes of hot embossing and injection moulding will need to be examined. Currently PANI is considered to be stable at temperatures up to 100 ^{o}C. However, it is known that its conductivity is reduced by more than 100 fold when moisture is completely removed [121].

5. One other area for whiich PANI could be explored as an electrode material is that of paper-based microfluidics [209, 210]. PANI could be printed onto paper in direct paterns or as a film patterned by laser-welding. Paper devices have become very attractive in microfluidics because of the extremely low cost of the base substrate (paper). However, there are significant challenges involved in generating insulating regions with paper as the substrate, given that paper is a fibrous material and shows significant uptake of water, even in low humidity environments.

7. References

1. Verpoorte, E., *Microfluidic chips for clinical and forensic analysis.* Electrophoresis, 2002. **23**(5): p. 677-712.
2. Zeng, Y., H. Chen, D.W. Pang, Z.L. Wang, and J.K. Cheng, *Microchip capillary electrophoresis with electrochemical detection.* Analytical Chemistry, 2002. **74**(10): p. 2441-2445.
3. Chen, S.H., Y.H. Lin, L.Y. Wang, C.C. Lin, and G.B. Lee, *Flow-through sampling for electrophoresis-based microchips and their applications for protein analysis.* Analytical Chemistry, 2002. **74**(19): p. 5146-5153.
4. Marle, L. and G.M. Greenway, *Microfluidic devices for environmental monitoring.* Trac-Trends in Analytical Chemistry, 2005. **24**(9): p. 795-802.
5. Wang, J., *Microchip devices for detecting terrorist weapons.* Analytica Chimica Acta, 2004. **507**(1): p. 3-10.
6. Mark, D., S. Haeberle, G. Roth, F. von Stetten, and R. Zengerle, *Microfluidic lab-on-a-chip platforms: requirements, characteristics and applications.* Chemical Society Reviews, 2010. **39**(3): p. 1153-1182.
7. Kraly, J.R., R.E. Holcomb, Q. Guan, and C.S. Henry, *Review: Microfluidic applications in metabolomics and metabolic profiling.* Analytica Chimica Acta, 2009. **653**(1): p. 23-35.
8. Harris, D.C., *Quantitative Chemical Analysis*. Seventh ed, ed. J. Fiorillo. 2007, New York: W. H. Freeman and Company. 663.
9. Manz, A., N. Graber, and H.M. Widmer, *Miniaturized total chemical analysis systems - a novel concept for chemical sensing.* Sensors and Actuators B-Chemical, 1990. **1**(1-6): p. 244-248.
10. Wlodkowic, D. and J.M. Cooper, *Tumors on chips: oncology meets microfluidics.* Current Opinion in Chemical Biology, 2010. **14**(5): p. 556-567.
11. Trietsch, S.J., T. Hankemeier, and H.J. van der Linden, *Lab-on-a-chip technologies for massive parallel data generation in the life sciences: A review.* Chemometrics and Intelligent Laboratory Systems, 2011. **108**(1): p. 64-75.
12. Webster, A., J. Greenman, and S.J. Haswell, *Development of microfluidic devices for biomedical and clinical application.* Journal of Chemical Technology and Biotechnology, 2010. **86**(1): p. 10-17.
13. Chin, C.D., T. Laksanasopin, Y.K. Cheung, D. Steinmiller, V. Linder, H. Parsa, J. Wang, H. Moore, R. Rouse, G. Umviligihozo, E. Karita, L. Mwambarangwe, S.L. Braunstein, J. van de Wijgert, R. Sahabo, J.E. Justman, W. El-Sadr, and S.K. Sia, *Microfluidics-based diagnostics of infectious diseases in the developing world.* Nature Medicine, 2011. **17**(8): p. 1015-U138.
14. Becker, H., *Chips, money, industry, education and the "killer application".* Lab on a Chip, 2009. **9**(12): p. 1659-1660.
15. Terry, S.J., J. H.;Angell, J. B., IEEE Transactions on Electron Devices, 1979. **ED**(26): p. 1880-1886.
16. Manz, A., E. Verpoorte, C.S. Effenhauser, N. Burggraf, D.E. Raymond, and H.M. Widmer, *Planar Chip Technology for Capillary Electrophoresis.* Fresenius Journal of Analytical Chemistry, 1994. **348**(8-9): p. 567-571.

17. Manz, A., D.J. Harrison, E.M.J. Verpoorte, J.C. Fettinger, A. Paulus, H. Ludi, and H.M. Widmer, *Planar Chips Technology for Miniaturization and Integration of Separation Techniques into Monitoring Systems - Capillary Electrophoresis on a Chip.* Journal of Chromatography, 1992. **593**(1-2): p. 253-258.
18. Pu, Q.S., R. Luttge, H. Gardeniers, and A. van den Berg, *Comparison of capillary zone electrophoresis performance of powder-blasted and hydrogen fluoride-etched microchannels in glass.* Electrophoresis, 2003. **24**(1-2): p. 162-171.
19. Duffy, D.C., J.C. McDonald, O.J.A. Schueller, and G.M. Whitesides, *Rapid prototyping of microfluidic systems in poly(dimethylsiloxane).* Analytical Chemistry, 1998. **70**(23): p. 4974-4984.
20. McCreedy, T., *Rapid prototyping of glass and PDMS microstructures for micro total analytical systems and micro chemical reactors by microfabrication in the general laboratory.* Analytica Chimica Acta, 2001. **427**(1): p. 39-43.
21. Lacher, N.A., N.F. de Rooij, E. Verpoorte, and S.M. Lunte, *Comparison of the performance characteristics of poly(dimethylsiloxane) and Pyrex microchip electrophoresis devices for peptide separations.* Journal of Chromatography A, 2003. **1004**(1-2): p. 225-235.
22. Ng, J.M.K., I. Gitlin, A.D. Stroock, and G.M. Whitesides, *Components for integrated poly(dimethylsiloxane) microfluidic systems.* Electrophoresis, 2002. **23**(20): p. 3461-3473.
23. Microchem. *Nano SU-8 2000 - Negative tone photoresist formulations 2002-2025*. 2004 [cited 2005 1/11]; Available from: http://www.microchem.com/products/pdf/SU8_2002-2025.pdf.
24. Becker, H. and L.E. Locascio, *Polymer microfluidic devices.* Talanta, 2002. **56**(2): p. 267-287.
25. Whitesides, G.M. and A.D. Stroock, *Flexible methods for microfluidics.* Physics Today, 2001. **54**(6): p. 42-48.
26. Yu, H., O. Balogun, B. Li, T.W. Murray, and X. Zhang, *Fabrication of three-dimensional microstructures based on singled-layered SU-8 for lab-on-chip applications.* Sensors and Actuators, A: Physical, 2006. **A127**(2): p. 228-234.
27. McDonald, J.C., D.C. Duffy, J.R. Anderson, D.T. Chiu, H.K. Wu, O.J.A. Schueller, and G.M. Whitesides, *Fabrication of microfluidic systems in poly(dimethylsiloxane).* Electrophoresis, 2000. **21**(1): p. 27-40.
28. Satyanarayana, S., R.N. Karnik, and A. Majumdar, *Stamp-and-stick room-temperature bonding technique for microdevices.* Microelectromechanical Systems, Journal of, 2005. **14**(2): p. 392-399.
29. Katzenberg, F., *Plasma-bonding of poly(dimethylsiloxane) to glass.* E-Polymers, 2005.
30. Hui, A.Y.N., G. Wang, B.C. Lin, and W.T. Chan, *Microwave plasma treatment of polymer surface for irreversible sealing of microfluidic devices.* Lab on a Chip, 2005. **5**(10): p. 1173-1177.
31. Lim, Y.C., A.Z. Kouzani, and W. Duan, *Lab-on-a-chip: a component view.* Microsystem Technologies-Micro-and Nanosystems-Information Storage and Processing Systems, 2010. **16**(12): p. 1995-2015.
32. Illa, X., O. Ordeig, D. Snakenborg, A. Romano-Rodriguez, R.G. Compton, and J.P. Kutter, *A cyclo olefin polymer microfluidic chip with integrated gold*

microelectrodes for aqueous and non-aqueous electrochemistry. Lab on a Chip, 2010. **10**(10): p. 1254-1261.
33. Zhan, W., J. Alvarez, and R.M. Crooks, *Electrochemical sensing in microfluldic systems using electrogenerated chemiluminescence as a photonic reporter of redox reactions.* Journal of the American Chemical Society, 2002. **124**(44): p. 13265-13270.
34. MicrofluidicChipShop, *Lab-on-a-Chip Catalogue* 2010.
35. Santiago, J.G. and C.H. Chen, *Special issue on fundamental principles and techniques in microfluidics.* Lab on a Chip, 2009. **9**(17): p. 2423-2424.
36. Wang, Z.Y., O. Hansen, P.K. Petersen, A. Rogeberg, J.P. Kutter, D.D. Bang, and A. Wolff, *Dielectrophoresis microsystem with integrated flow cytometers for on-line monitoring of sorting efficiency.* Electrophoresis, 2006. **27**(24): p. 5081-5092.
37. Liu, R.H., J.N. Yang, R. Lenigk, J. Bonanno, and P. Grodzinski, *Self-contained, fully integrated biochip for sample preparation, polymerase chain reaction amplification, and DNA microarray detection.* Analytical Chemistry, 2004. **76**(7): p. 1824-1831.
38. Fair, R.B., *Digital microfluidics: is a true lab-on-a-chip possible?* Microfluidics and Nanofluidics, 2007. **3**(3): p. 245-281.
39. Cho, S.K., H.J. Moon, and C.J. Kim, *Creating, transporting, cutting, and merging liquid droplets by electrowetting-based actuation for digital microfluidic circuits.* Journal of Microelectromechanical Systems, 2003. **12**(1): p. 70-80.
40. Liu, C.C. and D.F. Cui, *Design and fabrication of poly(dimethylsiloxane) electrophoresis microchip with integrated electrodes.* Microsystem Technologies-Micro-and Nanosystems-Information Storage and Processing Systems, 2005. **11**(12): p. 1262-1266.
41. Johnson, A.S., A. Selimovic, and R.S. Martin, *Integration of microchip electrophoresis with electrochemical detection using an epoxy-based molding method to embed multiple electrode materials.* Electrophoresis, 2011. **32**(22): p. 3121-3128.
42. Deyl, Z., I. Miksik, and A. Eckhardt, *Comparison of standard capillary and chip separations of sodium dodecylsulfate-protein complexes.* Journal of Chromatography A, 2003. **990**(1-2): p. 153-158.
43. Erickson, D. and D.Q. Li, *Integrated microfluidic devices.* Analytica Chimica Acta, 2004. **507**(1): p. 11-26.
44. Gao, Y., Z. Shen, H. Wang, Z.P. Dai, and B.C. Lin, *Chiral separations on multichannel microfluidic chips.* Electrophoresis, 2005. **26**(24): p. 4774-4779.
45. Lee, J.N., C. Park, and G.M. Whitesides, *Solvent compatibility of poly(dimethylsiloxane)-based microfluidic devices.* Analytical Chemistry, 2003. **75**(23): p. 6544-6554.
46. Sato, K., A. Hibara, M. Tokeshi, H. Hisamoto, and T. Kitamori, *Microchip-based chemical and biochemical analysis systems.* Advanced Drug Delivery Reviews, 2003. **55**(3): p. 379-391.
47. Ghosal, S., *Fluid mechanics of electroosmotic flow and its effect on band broadening in capillary electrophoresis.* Electrophoresis, 2004. **25**(2): p. 214-228.

48. Ghosal, S., *Electrokinetic flow and dispersion in capillary electrophoresis.* Annual Review of Fluid Mechanics, 2006. **38**: p. 309-338.
49. Harrison, D.J., A. Manz, Z.H. Fan, H. Ludi, and H.M. Widmer, *Capillary electrophoresis and sample injection systems integrated on a planar glass chip.* Analytical Chemistry, 1992. **64**(17): p. 1926-1932.
50. vonHeeren, F., E. Verpoorte, A. Manz, and W. Thormann, *Micellar electrokinetic chromatography separations and analyses of biological samples on a cyclic planar microstructure.* Analytical Chemistry, 1996. **68**(13): p. 2044-2053.
51. Jacobson, S.C., R. Hergenroder, L.B. Koutny, R.J. Warmack, and J.M. Ramsey, *Effects of injection schemes and column geometry on the performance of microchip electrophoresis devices.* Analytical Chemistry, 1994. **66**(7): p. 1107-1113.
52. Chabinyc, M.L., D.T. Chiu, J.C. McDonald, A.D. Stroock, J.F. Christian, A.M. Karger, and G.M. Whitesides, *An integrated fluorescence detection system in poly(dimethylsiloxane) for microfluidic applications.* Analytical Chemistry, 2001. **73**(18): p. 4491-4498.
53. Effenhauser, C.S., A. Manz, and H.M. Widmer, *Glass chips for high-speed capillary electrophoresis separations with submicrometer plate heights .* Analytical Chemistry, 1993. **65**(19): p. 2637-2642.
54. Li, H.F., J.M. Lin, R.G. Su, K. Uchiyama, and T. Hobo, *A compactly integrated laser-induced fluorescence detector for microchip electrophoresis.* Electrophoresis, 2004. **25**(12): p. 1907-1915.
55. Lin, Y.W., T.C. Chiu, and H.T. Chang, *Laser-induced fluorescence technique for DNA and proteins separated by capillary electrophoresis.* Journal of Chromatography B-Analytical Technologies in the Biomedical and Life Sciences, 2003. **793**(1): p. 37-48.
56. Dang, F., L. Zhang, H. Hagiwara, Y. Mishina, and Y. Baba, *Ultrafast analysis of oligosaccharides on microchip with light-emitting diode confocal fluorescence detection.* Electrophoresis, 2003. **24**(4): p. 714-721.
57. Suzuki, S. and S. Honda, *Miniaturization in carbohydrate analysis.* Electrophoresis, 2003. **24**(21): p. 3577-3582.
58. Guijt, R.M., E. Candish, and M.C. Breadmore, *Dry film microchips for miniaturised separations.* Electrophoresis, 2009. **30**(24): p. 4219-4224.
59. Renaud, L., P. Kleimann, O. Dispagne, L. Denoroy, P. Pittet, R. Ferigno, and P. Morin, *PDMS microfluidic systems with integrated fluorescence detection application to amino acids separation.* Houille Blanche-Revue Internationale De L Eau, 2006(4): p. 45-50.
60. Lichtenberg, J., N.F. de Rooij, and E. Verpoorte, *A microchip electrophoresis system with integrated in-plane electrodes for contactless conductivity detection.* Electrophoresis, 2002. **23**(21): p. 3769-3780.
61. Kuban, P. and P.C. Hauser, *Capacitively coupled contactless conductivity detection for microseparation techniques - recent developments.* Electrophoresis, 2011. **32**(1): p. 30-42.
62. Kuban, P. and P.C. Hauser, *Fundamentals of electrochemical detection techniques for CE and MCE.* Electrophoresis, 2009. **30**(19): p. 3305-3314.

63. Guijt, R.M., C.J. Evenhuis, M. Macka, and P.R. Haddad, *Conductivity detection for conventional and miniaturised capillary electrophoresis systems.* Electrophoresis, 2004. **25**(23-24): p. 4032-4057.
64. Kuban, P. and P.C. Hauser, *Contactless conductivity detection in capillary electrophoresis: A review.* Electroanalysis, 2004. **16**(24): p. 2009-2021.
65. Gas, B., M. Demjanenko, and J. Vacik, *High-frequency contactless conductivity detection in isotachophoresis.* Journal of Chromatography, 1980. **192**(2): p. 253-257.
66. Zemann, A.J., E. Schnell, D. Volgger, and G.K. Bonn, *Contactless conductivity detection for capillary electrophoresis.* Analytical Chemistry, 1998. **70**(3): p. 563-567.
67. da Silva, J.A.F. and C.L. do Lago, *An oscillometric detector for capillary electrophoresis.* Analytical Chemistry, 1998. **70**(20): p. 4339-4343.
68. Pumera, M. and A. Escarpa, *Nanomaterials as electrochemical detectors in microfluidics and CE: Fundamentals, designs, and applications.* Electrophoresis, 2009. **30**(19): p. 3315-3323.
69. Brito-Neto, J.G.A., J.A.F. da Silva, L. Blanes, and C.L. do Lago, *Understanding capacitively coupled contactless conductivity detection in capillary and microchip electrophoresis. Part 1. Fundamentals.* Electroanalysis, 2005. **17**(13): p. 1198-1206.
70. Brito-Neto, J.G.A., J.A.F. da Silva, L. Blanes, and C.L. do Lago, *Understanding capacitively coupled contactless conductivity detection in capillary and microchip electrophoresis. Part 2. Peak shape, stray capacitance, noise, and actual electronics.* Electroanalysis, 2005. **17**(13): p. 1207-1214.
71. Kuban, P. and P.C. Hauser, *Effects of the cell geometry and operating parameters on the performance of an external contactless conductivity detector for microchip electrophoresis.* Lab on a Chip, 2005. **5**(4): p. 407-415.
72. Kuban, P. and P.C. Hauser, *Evaluation of microchip capillary electrophoresis with external contactless conductivity detection for the determination of major inorganic ions and lithium in serum and urine samples.* Lab on a Chip, 2008. **8**(11): p. 1829-1836.
73. Mahabadi, K.A., I. Rodriguez, C.Y. Lim, D.K. Maurya, P.C. Hauser, and N.F. de Rooij, *Capacitively coupled contactless conductivity detection with dual top-bottom cell configuration for microchip electrophoresis.* Electrophoresis, 2010. **31**(6): p. 1063-1070.
74. Fu, L.M., C.Y. Lee, M.H. Liao, and C.H. Lin, *Fabrication and testing of high-performance detection sensor for capillary electrophoresis microchips.* Biomedical Microdevices, 2008. **10**(1): p. 73-80.
75. Vazquez, M., C. Frankenfeld, W.K.T. Coltro, E. Carrilho, D. Diamond, and S.M. Lunte, *Dual contactless conductivity and amperometric detection on hybrid PDMS/glass electrophoresis microchips.* Analyst, 2010. **135**(1): p. 96-103.
76. Liu, C., Y.Y. Mo, Z.G. Chen, X. Li, O.L. Li, and X. Zhou, *Dual fluorescence/contactless conductivity detection for microfluidic chip.* Analytica Chimica Acta, 2008. **621**(2): p. 171-177.
77. Coltro, W.K.T., J.A.F. da Silva, and E. Carrilho, *Rapid prototyping of polymeric electrophoresis microchips with integrated copper electrodes for contactless conductivity detection.* Analytical Methods, 2010. **3**(1): p. 168-172.

78. Lui, J., J. Wang, Z. Chen, T. Yu, X. Yang, X. Zhang, Z. Xu, and C. Liu. *A three-layer PMMA electrophoresis Microchip with Pt microelectrodes insulated by a thin film for contactless conductivity detection*. LAb on a Chip [Technical Note] 2011 [cited 11 11]; 969-973].
79. Fercher, G., A. Haller, W. Smetana, and M.J. Vellekoopt, *End-to-End Differential Contact less Conductivity Sensor for Microchip Capillary Electrophoresis.* Analytical Chemistry, 2010. **82**(8): p. 3270-3275.
80. Nguyen, N.T., X.Y. Huang, and K.C. Toh, *Thermal flow sensor for ultra-low velocities based on printed circuit board technology.* Measurement Science & Technology, 2001. **12**(12): p. 2131-2136.
81. Guijt, R.M., J.P. Armstrong, E. Candish, V. Lefleur, W.J. Percey, S. Shabala, P.C. Hauser, and M.C. Breadmore, *Microfluidic chips for capillary electrophoresis with integrated electrodes for capacitively coupled conductivity detection based on printed circuit board technology.* Sensors and Actuators B-Chemical, 2011. **159**(1): p. 307-313.
82. Tsai, D.M., K.W. Lin, J.M. Zen, H.Y. Chen, and R.H. Hong, *A new fabrication process for a microchip electrophoresis device integrated with a three-electrode electrochemical detector.* Electrophoresis, 2005. **26**(15): p. 3007-3012.
83. Walker, C.E., Z. Xia, Z.S. Foster, B.J. Lutz, and Z.H. Fan, *Investigation of airbrushing for fabricating microelectrodes in microfluidic devices.* Electroanalysis, 2008. **20**(6): p. 663-670.
84. Fercher, G., A. Haller, W. Smetana, and M.J. Vellekoop, *Ceramic capillary electrophoresis chip for the measurement of inorganic ions in water samples.* Analyst, 2010. **135**(5): p. 965-970.
85. Siegel, A.C., D.A. Bruzewicz, D.B. Weibel, and G.M. Whitesides, *Microsolidics: Fabrication of three-dimensional metallic microstructures in poly(dimethylsiloxane).* Advanced Materials, 2007. **19**(5): p. 727-+.
86. Priest, C., P.J. Gruner, E.J. Szili, S.A. Al-Bataineh, J.W. Bradley, J. Ralston, D.A. Steele, and R.D. Short, *Microplasma patterning of bonded microchannels using high-precision "injected" electrodes.* Lab on a Chip, 2011. **11**(3): p. 541-544.
87. Jagur-Grodzinski, J., *Electronically conductive polymers.* Polymers for Advanced Technologies, 2002. **13**(9): p. 615-625.
88. Shirakawa, H., E.J. Louis, A.G. Macdiarmid, C.K. Chiang, and A.J. Heeger, *Synthesis of Electrically Conducting Organic Polymers - Halogen Derivatives of Polycetylene, (CH)x.* Journal of the Chemical Society-Chemical Communications, 1977(16): p. 578-580.
89. Rozlosnik, N., *New directions in medical biosensors employing poly(3,4-ethylenedioxy thiophene) derivative-based electrodes.* Analytical and Bioanalytical Chemistry, 2009. **395**(3): p. 637-645.
90. Erlandsson, P.G. and N.D. Robinson, *Electrolysis-reducing electrodes for electrokinetic devices.* Electrophoresis, 2010. **32**(6-7): p. 784-790.
91. Chun, H.G., T.D. Chung, and J.M. Ramsey, *High Yield Sample Preconcentration Using a Highly Ion-Conductive Charge-Selective Polymer.* Analytical Chemistry, 2010. **82**(14): p. 6287-6292.
92. Holmes, R.J., C. McDonagh, J.A.D. McLaughlin, S. Mohr, N.J. Goddard, and P.R. Fielden, *Microwave bonding of poly(methylmethacrylate) microfluidic*

devices using a conductive polymer. Journal of Physics and Chemistry of Solids, 2011. **72**(6): p. 626-629.

93. Conklin, J.A., S.C. Huang, S.M. Huang, T.L. Wen, and R.B. Kaner, *Thermal-Properties of Polyaniline and Poly(Aniline-Co-O-Ethylaniline).* Macromolecules, 1995. **28**(19): p. 6522-6527.
94. Huo, L.H., L.X. Cao, H.N. Cui, D.M. Wang, G.F. Zeng, and S.Q. Xi, *Preparation and characterization of DBSA doped polyaniline thin films.* Molecular Crystals and Liquid Crystals, 1999. **337**: p. 261-264.
95. Kumar, D. and R.C. Sharma, *Advances in conductive polymers.* European Polymer Journal, 1998. **34**(8): p. 1053-1060.
96. Riul, A., L.H.C. Mattoso, G.D. Telles, P.S.P. Herrmann, L.A. Colnago, N.A. Parizotto, V. Baranauskas, R.M. Faria, and O.N. Oliveira, *Characterization of Langmuir-Blodgett films of parent polyaniline.* Thin Solid Films, 1996. **285**: p. 177-180.
97. Syed, A.A. and M.K. Dinesan, *Polyaniline - a Novel Polymeric Material - Review.* Talanta, 1991. **38**(8): p. 815-837.
98. Negi, Y.S. and P.V. Adhyapak, *Development in polyaniline conducting polymers.* Journal of Macromolecular Science-Polymer Reviews, 2002. **C42**(1): p. 35-53.
99. Wessling, B., *Dispersion as the link between basic research and commercial applications of conductive polymers (polyaniline).* Synthetic Metals, 1998. **93**(2): p. 143-154.
100. Wu, A., E.C. Venancio, and A.G. MacDiarmid, *Polyaniline and polypyrrole oxygen reversible electrodes.* Synthetic Metals, 2007. **157**(6-7): p. 303-310.
101. Jeong, S.K., J.S. Suh, E.J. Oh, Y.W. Park, C.Y. Kim, and A.G. Macdiarmid, *Preparation of Polyaniline Free Standing Film by Controlled Processing and Its Transport Property.* Synthetic Metals, 1995. **69**(1-3): p. 171-172.
102. Baker, C.O., B. Shedd, P.C. Innis, P.G. Whitten, G.M. Spinks, G.G. Wallace, and R.B. Kaner, *Monolithic actuators from flash-welded polyaniline nanofibers.* Advanced Materials, 2008. **20**(1): p. 155-+.
103. Antonietti, M. and K. Tauer, *90 years of polymer latexes and heterophase polymerization: More vital than ever.* Macromolecular Chemistry and Physics, 2003. **204**(2): p. 207-219.
104. Kinlen, P.J., J. Liu, Y. Ding, C.R. Graham, and E.E. Remsen, *Emulsion polymerization process for organically soluble and electrically conducting polyaniline.* Macromolecules, 1998. **31**(6): p. 1735-1744.
105. Osterholm, J.E., Y. Cao, F. Klavetter, and P. Smith, *Emulsion Polymerization of Aniline.* Polymer, 1994. **35**(13): p. 2902-2906.
106. Marie, E., R. Rothe, M. Antonietti, and K. Landfester, *Synthesis of polyaniline particles via inverse and direct miniemulsion.* Macromolecules, 2003. **36**(11): p. 3967-3973.
107. Antonietti, M. and K. Landfester, *Polyreactions in miniemulsions.* Progress in Polymer Science, 2002. **27**(4): p. 689-757.
108. Bhadra, S., N.K. Singha, and D. Khastgir, *Polyaniline by new miniemulsion polymerization and the effect of reducing agent on conductivity.* Synthetic Metals, 2006. **156**(16-17): p. 1148-1154.

109. Diaz, A.F. and J.A. Logan, *Electroactive Polyaniline Films.* Journal of Electroanalytical Chemistry, 1980. **111**(1): p. 111-114.
110. Bhadra, S., S. Chattopadhyay, N.K. Singha, and D. Khastgir, *Improvement of conductivity of electrochemically synthesized polyaniline.* Journal of Applied Polymer Science, 2008. **108**(1): p. 57-64.
111. Choi, J., S.J. Kim, J. Lee, J.H. Lim, S.C. Lee, and K.J. Kim, *Controlled self-assembly of self-templating synthesis nanoporous alumina for the of polyaniline nanowires.* Electrochemistry Communications, 2007. **9**(5): p. 971-975.
112. Delvaux, M., J. Duchet, P.Y. Stavaux, R. Legras, and S. Demoustier-Champagne, *Chemical and electrochemical synthesis of polyaniline micro- and nano-tubules.* Synthetic Metals, 2000. **113**(3): p. 275-280.
113. Wei, Z.X., Z.M. Zhang, and M.X. Wan, *Formation mechanism of self-assembled polyaniline micro/nanotubes.* Langmuir, 2002. **18**(3): p. 917-921.
114. Wu, C.G. and T. Bein, *Conducting Polyaniline Filaments in a Mesoporous Channel Host.* Science, 1994. **264**(5166): p. 1757-1759.
115. Huang, J.X. and R.B. Kaner, *A general chemical route to polyaniline nanofibers.* Journal of the American Chemical Society, 2004. **126**(3): p. 851-855.
116. Chen, J.Y., D.M. Chao, X.F. Lu, and W.J. Zhang, *Novel interfacial polymerization for radially oriented polyaniline nanofibers.* Materials Letters, 2007. **61**(6): p. 1419-1423.
117. Huang, J.X. and R.B. Kaner, *Nanofiber formation in the chemical polymerization of aniline: A mechanistic study.* Angewandte Chemie-International Edition, 2004. **43**(43): p. 5817-5821.
118. Jing, X.L., Y.Y. Wang, D. Wu, L. She, and Y. Guo, *Polyaniline nanofibers prepared with ultrasonic irradiation.* Journal of Polymer Science Part a-Polymer Chemistry, 2006. **44**(2): p. 1014-1019.
119. Quillard, S., G. Louarn, S. Lefrant, and A.G. Macdiarmid, *Vibrational Analysis of Polyaniline - a Comparative-Study of Leucoemeraldine, Emeraldine, and Pernigraniline Bases.* Physical Review B, 1994. **50**(17): p. 12496-12508.
120. Zhang, D.H. and Y.Y. Wang, *Synthesis and applications of one-dimensional nano-structured polyaniline: An overview.* Materials Science and Engineering B-Solid State Materials for Advanced Technology, 2006. **134**(1): p. 9-19.
121. Focke, W.W., G.E. Wnek, and Y. Wei, *Influence of oxidation-state, pH, and counterion on the conductivity of polyaniline.* Journal of Physical Chemistry, 1987. **91**(22): p. 5813-5818.
122. Huang, W.S., B.D. Humphrey, and A.G. Macdiarmid, *Polyaniline, a novel conducting polymer - morphology and chemistry of its oxidation and reduction in aqueous-electrolytes.* Journal of the Chemical Society-Faraday Transactions I, 1986. **82**: p. 2385-&.
123. Bredas, J.L. and G.B. Street, *Polarons, bipolarons, and solutions in conducting polymers.* Accounts of Chemical Research, 1985. **18**(10): p. 309-315.
124. Brazovskii, S.A. and N.N. Kirova, *Excitons, polarons, and bipolarons in conducting-polymers.* Jetp Letters, 1981. **33**(1): p. 4-8.
125. Stafstrom, S., J.L. Bredas, A.J. Epstein, H.S. Woo, D.B. Tanner, W.S. Huang, and A.G. Macdiarmid, *Polaron lattice in highly conducting polyaniline - theoretical and optical studies.* Physical Review Letters, 1987. **59**(13): p. 1464-1467.

126. Wolter, A., P. Rannou, J.P. Travers, B. Gilles, and D. Djurado, *Model for aging in HCl-protonated polyaniline: Structure, conductivity, and composition studies.* Physical Review B, 1998. **58**(12): p. 7637-7647.
127. Ameen, S., V. Ali, M. Zulfequar, M.M. Haq, and M. Husain, *Preparation and measurements of electrical and spectroscopic properties of sodium thiosulphate doped polyaniline.* Current Applied Physics, 2009. **9**(2): p. 478-483.
128. Bhadra, S., D. Khastgir, N.K. Singha, and J.H. Lee, *Progress in preparation, processing and applications of polyaniline.* Progress in Polymer Science, 2009. **34**(8): p. 783-810.
129. Ramadin, Y., M. Ahmad, A. Zihlif, R. Al-Haddad, M. Makadsi, G. Ragosta, and E. Martuscelli, *Determination of the type of charge carriers in carbon fiber polymer composite.* Polymer Testing, 1998. **17**(4): p. 257-264.
130. Zhang, Z.M., Z.X. Wei, and M.X. Wan, *Nanostructures of polyaniline doped with inorganic acids.* Macromolecules, 2002. **35**(15): p. 5937-5942.
131. Hennig, C., K.H. Hallmeier, and R. Szargan, *XANES investigation of chemical states of nitrogen in polyaniline.* Synthetic Metals, 1998. **92**(2): p. 161-166.
132. Pouget, J.P., M.E. Jozefowicz, A.J. Epstein, X. Tang, and A.G. Macdiarmid, *X-ray structure of polyaniline.* Macromolecules, 1991. **24**(3): p. 779-789.
133. Zhang, H.M., J.L. Lu, X.H. Wang, J. Li, and F.S. Wang, *From amorphous to crystalline: Practical way to improve electrical conductivity of water-borne conducting polyaniline.* Polymer. **52**(14): p. 3059-3064.
134. Aleshin, A.N., *Polymer nanofibers and nanotubes: Charge transport and device applications.* Advanced Materials, 2006. **18**(1): p. 17-27.
135. Jeon, D., J. Kim, M.C. Gallagher, and R.F. Willis, *Scanning tunneling spectroscopic evidence for granular metallic conductivity in conducting polymeric polyaniline.* Science, 1992. **256**(5064): p. 1662-1664.
136. Zhang, L.X., L.J. Zhang, M.X. Wan, and Y. Wei, *Polyaniline micro/nanofibers doped with saturation fatty acids.* Synthetic Metals, 2006. **156**(5-6): p. 454-458.
137. Kulkarni, M.V., A.K. Viswanath, R. Marimuthu, and T. Seth, *Synthesis and characterization of polyaniline doped with organic acids.* Journal of Polymer Science Part a-Polymer Chemistry, 2004. **42**(8): p. 2043-2049.
138. Holland, E.R., S.J. Pomfret, P.N. Adams, and A.P. Monkman, *Conductivity studies of polyaniline doped with CSA.* Journal of Physics-Condensed Matter, 1996. **8**(17): p. 2991-3002.
139. Saraswathi, R., S. Kuwabata, and H. Yoneyama, *Influence of basicity of dopant anions on the conductivity of polyaniline* . Journal of Electroanalytical Chemistry, 1992. **335**(1-2): p. 223-231.
140. Tzou, K. and R.V. Gregory, *A Method to Prepare Soluble Polyaniline Salt-Solutions - Insitu Doping of Pani Base with Organic Dopants in Polar-Solvents.* Synthetic Metals, 1993. **53**(3): p. 365-377.
141. Nguyen, M.T., P. Kasai, J.L. Miller, and A.F. Diaz, *Synthesis and properties of novel water solubale conducting polyaniline copolymers.* Macromolecules, 1994. **27**(13): p. 3625-3631.
142. Inzelt, G., *Rise and rise of conducting polymers.* Journal of Solid State Electrochemistry, 2011. **15**(7-8): p. 1711-1718.

143. Ameen, S., M.S. Akhtar, and M. Husain, *Polyaniline and Its Nanocomposites: Synthesis, Processing, Electrical Properties and Applications.* Science of Advanced Materials, 2010. **2**(4): p. 441-462.
144. Yakuphanoglu, F., R. Mehrotra, A. Gupta, and M. Munoz, *Nanofiber Organic Semiconductors: The Effects of Nanosize on the Electrical Charge Transport and Optical Properties of Bulk Polyanilines.* Journal of Applied Polymer Science, 2009. **114**(2): p. 794-799.
145. Genies, E.M., A.A. Syed, and C. Tsintavis, *Electrochemical study of polyaniline in aqueous and organic medium -redox and kinetic-properties.* Molecular Crystals and Liquid Crystals, 1985. **121**(1-4): p. 181-186.
146. Liu, H.Q., J. Kameoka, D.A. Czaplewski, and H.G. Craighead, *Polymeric nanowire chemical sensor.* Nano Letters, 2004. **4**(4): p. 671-675.
147. Monkman, A.P. and P. Adams, *Optical and electronic -properties of stretch-oriented solution-cast polyaniline films.* Synthetic Metals, 1991. **40**(1): p. 87-96.
148. Noh, Y.Y., N. Zhao, M. Caironi, and H. Sirringhaus, *Downscaling of self-aligned, all-printed polymer thin-film transistors.* Nature Nanotechnology, 2007. **2**(12): p. 784-789.
149. Pede, D., G. Serra, and D. De Rossi, *Microfabrication of conducting polymer devices by ink-jet stereolithography.* Materials Science & Engineering C-Biomimetic Materials Sensors and Systems, 1998. **5**(3-4): p. 289-291.
150. Huang, J.X. and R.B. Kaner, *Flash welding of conducting polymer nanofibres.* Nature Materials, 2004. **3**(11): p. 783-786.
151. Li, D. and Y.N. Xia, *Nanomaterials - Welding and patterning in a flash.* Nature Materials, 2004. **3**(11): p. 753-754.
152. Elizalde-Torres, J., H.L. Hu, and A. Garcia-Valenzuela, *NO(2)-induced optical absorbance changes in semiconductor polyaniline thin films.* Sensors and Actuators B-Chemical, 2004. **98**(2-3): p. 218-226.
153. Virji, S., R.B. Kaner, and B.H. Weiller, *Hydrogen sensors based on conductivity changes in polyaniline nanofibers.* Journal of Physical Chemistry B, 2006. **110**(44): p. 22266-22270.
154. Mahanta, D., N. Munichandraiah, S. Radhakrishnan, G. Madras, and S. Patil, *Polyaniline modified electrodes for detection of dyes.* Synthetic Metals. **161**(9-10): p. 659-664.
155. Syed, A.A. and M.K. Dinesan, *Polyaniline - reaction stoichiometry and use as an ion - exchange polymer and acid - base indicator.* Synthetic Metals, 1990. **36**(2): p. 209-215.
156. Kim, J.S., S.O. Sohn, and J.S. Huh, *Fabrication and sensing behavior of PVF2 coated-polyaniline sensor for volatile organic compounds.* Sensors and Actuators B-Chemical, 2005. **108**(1-2): p. 409-413.
157. Hosseini, S.H. and A.A. Entezami, *Preparation and characterization of polyaniline blends with polyvinyl acetate, polystyrene and polyvinyl chloride for toxic gas sensors.* Polymers for Advanced Technologies, 2001. **12**(8): p. 482-493.
158. Spinks, G.A., S.R. Shin, G.G. Wallace, P.G. Whitten, I.Y. Kim, S.I. Kim, and S.J. Kim, *A novel "dual mode" actuation in chitosan/polyaniline/carbon nanotube fibers.* Sensors and Actuators B-Chemical, 2007. **121**(2): p. 616-621.

159. Spinks, G.M., B.B. Xi, V.T. Truong, and G.G. Wallace, *Actuation behaviour of layered composites of polyaniline, carbon nanotubes and polypyrrole.* Synthetic Metals, 2005. **151**(1): p. 85-91.
160. Otero, T.F., *Soft, wet, and reactive polymers. Sensing artificial muscles and conformational energy.* Journal of Materials Chemistry, 2009. **19**(6): p. 681-689.
161. Meng, C.Z., C.H. Liu, and S.S. Fan, *Flexible carbon nanotube/polyaniline paper-like films and their enhanced electrochemical properties.* Electrochemistry Communications, 2009. **11**(1): p. 186-189.
162. Tseng, R.J., J.X. Huang, J. Ouyang, R.B. Kaner, and Y. Yang, *Polyaniline nanofiber/gold nanoparticle nonvolatile memory.* Nano Letters, 2005. **5**(6): p. 1077-1080.
163. Qiao, Y., C.M. Li, S.J. Bao, and Q.L. Bao, *Carbon nanotube/polyaniline composite as anode material for microbial fuel cells.* Journal of Power Sources, 2007. **170**(1): p. 79-84.
164. Tan, S.X., J. Zhai, M.X. Wan, L. Jiang, and D.B. Zhu, *Polyaniline as a hole transport material to prepare solid solar cells.* Synthetic Metals, 2003. **137**(1-3): p. 1511-1512.
165. Ke, W.J., G.H. Lin, C.P. Hsu, C.M. Chen, Y.S. Cheng, T.H. Jen, and S.A. Chen, *Solution processable self-doped polyaniline as hole transport layer for inverted polymer solar cells.* Journal of Materials Chemistry. **21**(35): p. 13483-13489.
166. Tan, F.R., S.C. Qu, J. Wu, Z.J. Wang, L. Jin, Y. Bi, J. Cao, K. Liu, J.M. Zhang, and Z.G. Wang, *Electrodepostied polyaniline films decorated with nano-islands: Characterization and application as anode buffer layers in solar cells.* Solar Energy Materials and Solar Cells. **95**(2): p. 440-445.
167. Dodabalapur, A., *Organic light emitting diodes.* Solid State Communications, 1997. **102**(2-3): p. 259-267.
168. Ahmad, N. and A.G. MacDiarmid, *Inhibition of corrosion of steels with the exploitation of conducting polymers.* Synthetic Metals, 1996. **78**(2): p. 103-110.
169. Desvergne, S., A. Gasse, and A. Pron, *Electrical Characterization of Polyaniline-Based Adhesive Blends.* Journal of Applied Polymer Science, 2011. **120**(4): p. 1965-1973.
170. Sancaktar, E. and C.J. Liu, *Use of polymeric emeraldine salt for conductive adhesive applications.* Journal of Adhesion Science and Technology, 2003. **17**(9): p. 1265-1282.
171. Denneulin, A., J. Bras, A. Blayo, B. Khelifi, F. Roussel-Dherbey, and C. Neuman, *The influence of carbon nanotubes in inkjet printing of conductive polymer suspensions.* Nanotechnology, 2009. **20**(38).
172. Loffredo, F., A.D. Del Mauro, G. Burrasca, V. La Ferrara, L. Quercia, E. Massera, G. Di Francia, and D.D. Sala, *Ink-jet printing technique in polymer/carbon black sensing device fabrication.* Sensors and Actuators B-Chemical, 2009. **143**(1): p. 421-429.
173. Pauw, L.J.v.d., *A Metheod of Measuring Specific Resistivity and Hall Effect of Discs of Arbirary Shape.* Philips Research Reports, 1958. **13**(334): p. 1-9.
174. Folch, S., A. Gruger, A. Regis, and P. Colomban, *Optical and vibrational spectra of sols/solutions of polyaniline: Water as secondary dopant.* Synthetic Metals, 1996. **81**(2-3): p. 221-225.

175. Louarn, G., M. Lapkowski, S. Quillard, A. Pron, J.P. Buisson, and S. Lefrant, *Vibrational properties of polyaniline - Isotope effects.* Journal of Physical Chemistry, 1996. **100**(17): p. 6998-7006.
176. Boyer, M.I., S. Quillard, E. Rebourt, G. Louarn, J.P. Buisson, A. Monkman, and S. Lefrant, *Vibrational analysis of polyaniline: A model compound approach.* Journal of Physical Chemistry B, 1998. **102**(38): p. 7382-7392.
177. Cochet, M., G. Louarn, S. Quillard, M.I. Boyer, J.P. Buisson, and S. Lefrant, *Theoretical and experimental vibrational study of polyaniline in base forms: non-planar analysis. Part I.* Journal of Raman Spectroscopy, 2000. **31**(11): p. 1029-1039.
178. Mire, C.A., A. Agrawal, G.G. Wallace, P. Calvert, and M.I.H. Panhuis, *Inkjet and extrusion printing of conducting poly(3,4-ethylenedioxythiophene) tracks on and embedded in biopolymer materials.* Journal of Materials Chemistry, 2011. **21**(8): p. 2671-2678.
179. Wunderlich, B., *The Athas Database on heat - capacities of polymers.* Pure and Applied Chemistry, 1995. **67**(6): p. 1019-1026.
180. Haeberle, S. and R. Zengerle, *Microfluidic platforms for lab-on-a-chip applications.* Lab on a Chip, 2007. **7**(9): p. 1094-1110.
181. Zhang, X.L. and S.J. Haswell, *Materials matter in microfluidic devices.* Mrs Bulletin, 2006. **31**(2): p. 95-99.
182. Becker, H., *Hype, hope and hubris: the quest for the killer application in microfluidics.* Lab on a Chip, 2009. **9**(15): p. 2119-2122.
183. Gervais, L. and E. Delamarche, *Toward one-step point-of-care immunodiagnostics using capillary-driven microfluidics and PDMS substrates.* Lab on a Chip, 2009. **9**(23): p. 3330-3337.
184. Sia, S.K. and L.J. Kricka, *Microfluidics and point-of-care testing.* Lab on a Chip, 2008. **8**(12): p. 1982-1983.
185. Sista, R., Z.S. Hua, P. Thwar, A. Sudarsan, V. Srinivasan, A. Eckhardt, M. Pollack, and V. Pamula, *Development of a digital microfluidic platform for point of care testing.* Lab on a Chip, 2008. **8**(12): p. 2091-2104.
186. Wu, A., L. Wang, E. Jensen, R. Mathies, and B. Boser, *Modular integration of electronics and microfluidic systems using flexible printed circuit boards.* Lab on a Chip, 2010. **10**(4): p. 519-521.
187. Pede, D., G. Serra, and D. De Rossi, *Microfabrication of conducting polymer devices by ink-jet stereolithography.* Materials Science & Engineering C-Biomimetic and Supramolecular Systems, 1998. **5**(3-4): p. 289-291.
188. Noh, Y.Y., X.Y. Cheng, H. Sirringhaus, J.I. Sohn, M.E. Welland, and D.J. Kang, *Ink-jet printed ZnO nanowire field effect transistors.* Applied Physics Letters, 2007. **91**(4).
189. Guijt, R.M. and M.C. Breadmore, *Maskless photolithography using UV LEDs.* Lab on a Chip, 2008. **8**(8): p. 1402-1404.
190. Evangelista, R.A., A. Guttman, and F.T.A. Chen, *Acid-catalyzed reductive amination of aldoses with 8-aminopyrene-1,3,6-trisulfonate.* Electrophoresis, 1996. **17**(2): p. 347-351.
191. Evangelista, R.A., M.S. Liu, and F.T.A. Chen, *Characterization of 9-Aminopyrene-1,4,6-Trisulfonate-Derivatized Sugars by Capillary*

Electrophoresis with Laser-Induced Fluorescence Detection. Analytical Chemistry, 1995. **67**(13): p. 2239-2245.
192. Kuban, P. and P.C. Hauser, *Ten years of axial capacitively coupled contactless conductivity detection for CZE - a review.* Electrophoresis, 2009. **30**(1): p. 176-188.
193. Pumera, M., *Contactless conductivity detection for microfluidics: Designs and applications.* Talanta, 2007. **74**(3): p. 358-364.
194. Coltro, W.K.T., D.P. de Jesus, J.A.F. da Silva, C.L. do Lago, and E. Carrilho, *Toner and paper-based fabrication techniques for microfluidic applications.* Electrophoresis, 2010. **31**(15): p. 2487-2498.
195. ChipShop, M., *Lab-on-a-Chip Catologue*. 2011.
196. Matson, D.W., P.M. Martin, W.D. Bennett, J.W. Johnston, D.C. Stewart, and C.C. Bonham, *Sputtered coatings for microfluidic applications.* Journal of Vacuum Science & Technology a-Vacuum Surfaces and Films, 2000. **18**(4): p. 1998-2002.
197. Henderson, R.D., M.C. Breadmore, L. Dennany, R.M. Guijt, P.R. Haddad, E.F. Hilder, P.C. Innis, T.W. Lewis, and G.G. Wallace, *Photolithographic patterning of conducting polyaniline films via flash welding.* Synthetic Metals, 2010. **160**(13-14): p. 1405-1409.
198. Hutchinson, J.P., C. Johns, M.C. Breadmore, E.F. Hilder, R.M. Guijt, C. Lennard, G. Dicinoski, and P.R. Haddad, *Identification of inorganic ions in post-blast explosive residues using portable CE instrumentation and capacitively coupled contactless conductivity detection.* Electrophoresis, 2008. **29**(22): p. 4593-4602.
199. Fercher, G., W. Smetana, and M.J. Vellekoop, *Microchip electrophoresis in low-temperature co-fired ceramics technology with contactless conductivity measurement.* Electrophoresis, 2009. **30**(14): p. 2516-2522.
200. Li, O.A., Y.L. Tong, Z.G. Chen, C. Liu, S. Zhao, and J.Y. Mo, *A Glass/PDMS Hybrid Microfluidic Chip Embedded with Integrated Electrodes for Contactless Conductivity Detection.* Chromatographia, 2008. **68**(11-12): p. 1039-1044.
201. Coltro, W.K.T., J.A.F. da Silva, and E. Carrilho, *Fabrication and integration of planar electrodes for contactless conductivity detection on polyester-toner electrophoresis microchips.* Electrophoresis, 2008. **29**(11): p. 2260-2265.
202. Xu, Y., J. Liang, H.T. Liu, X.G. Hu, Z.Y. Wen, Y.J. Wu, and M.X. Cao, *Characterization of a capacitance-coupled contactless conductivity detection system with sidewall electrodes on a low-voltage-driven electrophoresis microchip.* Analytical and Bioanalytical Chemistry, 2010. **397**(4): p. 1583-1593.
203. Andresen, K.O., M. Hansen, M. Matschuk, S.T. Jepsen, H.S. Sorensen, P. Utko, D. Selmeczi, T.S. Hansen, N.B. Larsen, N. Rozlosnik, and R. Taboryski, *Injection molded chips with integrated conducting polymer electrodes for electroporation of cells.* Journal of Micromechanics and Microengineering, 2010. **20**(5): p. 9.
204. Henderson, R.D., R.M. Guijt, P.R. Haddad, E.F. Hilder, T.W. Lewis, and M.C. Breadmore, *Manufacturing and application of a fully polymeric electrophoresis chip with integrated polyaniline electrodes.* Lab on a Chip, 2010. **10**(14): p. 1869-1872.

205. Kubáň, P. and P.C. Hauser, *Effects of the cell geometry and operating parameters on the performance of an external contactless conductivity detector for microchip electrophoresis.* Lab on a Chip, 2005. **5**(4): p. 407-415.
206. Kubáň, P. and P.C. Hauser, *Capacitively coupled contactless conductivity detection for microseparation techniques – recent developments.* Electrophoresis, 2011. **32**(1): p. 30-42.
207. Ding, Y., C.D. Garcia, and K.R. Rogers, *Poly(dimethylsiloxane) Microchip Electrophoresis with Contactless Conductivity Detection for Measurement of Chemical Warfare Agent Degradation Products.* Analytical Letters, 2008. **41**(2): p. 335-350.
208. Kirchmeyer, S. and K. Reuter, *Scientific importance, properties and growing applications of poly(3,4-ethylenedioxythiophene).* Journal of Materials Chemistry, 2005. **15**(21): p. 2077-2088.
209. Martinez, A.W., S.T. Phillips, E. Carrilho, S.W. Thomas, H. Sindi, and G.M. Whitesides, *Simple telemedicine for developing regions: Camera phones and paper-based microfluidic devices for real-time, off-site diagnosis.* Analytical Chemistry, 2008. **80**(10): p. 3699-3707.
210. Martinez, A.W., S.T. Phillips, G.M. Whitesides, and E. Carrilho, *Diagnostics for the Developing World: Microfluidic Paper-Based Analytical Devices.* Analytical Chemistry, 2010. **82**(1): p. 3-10.